

STUDIA
UNIVERSITATIS BABEŞ-BOLYAI

CHEMIA

2

1987

CLUJ-NAPOCA

REDACTOR-ŞEF: Prof. A. NEGUCIOIU

REDACTORI-ŞEFI ADJUNCȚI: Prof. A. PAL, conf. N. EDROIU, conf. L. GHERGARI

**COMITETUL DE REDACȚIE CHIMIE: Prof. E. CHIFU, prof. I. HAIDUC,
prof. L. KÉKEDY, prof. GH. MARCU, prof. L. ONICIU (redactor responsabil),
conf. S. MAGER, conf. E. VARGHA (secretar de redacție)**

TEHNOREDACTOR: C. Tomoaia-COTIȘEL

STUDIA UNIVERSITATIS BABEŞ-BOLYAI

CHEMIA

2

Redacția: 3400 CLUJ-NAPOCA, str. M. Kogălniceanu, 1 • Telefon 16101

SUMAR — CONTENTS — SOMMAIRE — INHALT

M. JITARU, GH. MARCU, Biologically Active Metallic Chelates. II. Complexes of Hg^{2+} with Antiseptic-Disinfectant Action	3
M. JITARU, GH. MARCU, Biologically Active Metallic Chelates. III. Complexes of $Co(II)$ with Amino-Acids with Antitumour Activity	8
M.M. GIURGIU, A Spectrophotometric Kinetic Study of the Manganic Cysteinate Decomposition in Aqueous Solution	15
GH. MARCU, CS. VÁRHELYI, D. ITUL, B. SZALMA, Untersuchung Über die Tetrathiocyanato-Diamin-Chromate Einiger Amine und Phosphine • Study on the Tetrathiocyanato-Diamine-Chromates (III) of Some Amines and Phosphines	22
I. SIMINICEANU, I. TODEA, M. STANCA, A. POP, Katalytischer Umsatz des Methanolos mit Wasserdampf. I. Stöchiometrie, Gleichgewicht und Wärmebilanz des Vorganges • Catalytic Conversion of Methanol With Water Vapours. I. Stoichiometry, Equilibrium and Thermic Balance of the Process	27
I. SIMINICEANU, I. TODEA, M. STANCA, A. POP, A. GHÎTEA, Katalytischer Umsatz von Methanol und Wasserdampf. II. Kinetik des Vorganges • Catalytic Conversion of Methanol with Water Vapours. II. Kinetics of the Process	33
I. BĂLDEA, The Reaction Between Chromate and Thiols. III. The Oxidation of Thioglycolic Acid	42
F. MÁNOK, G. DÉNEZSI, CS. VÁRHELYI, A. BENKÓ, On the Dioximine Complexes of Transition Metals. LXIX. Kinetics and Mechanism of the Hydrolysis of Nyoxine in acidic medium	50
CS. VÁRHELYI, I. GĂNESCU, Neue Tetrachloro- und Tetrabromo-Platinite (II) der Kobalt (III) Aminen • New Tetrachloro- and Tetrabromo-Platinite (II) Type Cobalt (III) Amines	57
U. SHUKLA, B.B. PRASAD, Suitability of Graphite Electrodes for Combination with Platinum, in Biomperometric Indication	57
GH. MARCU, L. CRIVEI, N. PASCU, Distribution Coefficients and Cation Exchange Behaviour of $Cd(II)$ and $Zn(II)$ Ions in Water-Hydrochloric Acid and Acetone — Water-Hydrochloric Acid Media	61
D. DUMITRESCU, L. KÉKEDY, Classification of Mineral Waters by Pattern Recognition Processing of Chemical Composition Data	64
	68

I. OLTEANU, F. PAIU, V. FĂRCĂŞAN, TLC of Some Derivatives of Fluorene	74
GH. D. PASAT, C.I. ANGHEL, GH. MENCINICOPSCHI, V. D. ANGHEL, Particularités de l'agitation des systèmes gaz-liquide. Applications dans la construction des bioréacteurs • Specific Features of Mixing for Gas-Liquid Systems. Bindings for Designing of Biochemical Reactors	77
R.D. POP, A. ECNEA, V. CHIOREAN, V. FĂRCĂŞAN, The Biological Activity of Some Schiff's Bases of 4-Amino-Biphenyl and 2-Phenyl-4-(p-Aminophenyl) Thiazole	85
E. CHIFU, J. ZSAKÓ, M. TOMOAIA-COTIŞEL, M. SĂLĂJAN, I. DEMETER-VODNÁR, CS. VÁRHELYI, Adsorbed Films at the Benzene/Water Interface	90
Recenzii — Book Reviews — Comptes rendus — Buchbesprechungen	
Paul C. Hiemenz, „Principles of Colloid and Surface Chemistry” (E. CHIFU)	98
Liviu Oniciu et al., La corrosion des métaux. Aspects fondamentaux et protection anti-corrosive (C. POPESCU)	98
Liviu Literat, Transport Phenomena and Specific Equipment in Chemical Industry (Z. GROPSIAN)	99
L. Kékedy, Metalllic and Ion-selective Electrochemical Sensor (L. ONICIU)	100
Cronică — Chronicle — Chronique — Chronik	
Participări la manifestări științifice internaționale	102
Vizite în străinătate	102
Vizite din străinătate	102
Organizări de manifestări științifice în cadrul universității	102
Publicări de tratate, cărți și cursuri universitare	102
Lucrări științifice apărute în reviste de specialitate din țară și străinătate	103
Brevete	104
Susțineri de teze de doctorat	104

BIOLOGICALLY ACTIVE METALLIC CHELATES

II. Complexes of Hg^{2+} with Antiseptic-Disinfectant Action

MARIA JITARU* and GHEORGHE MARCU**

Received: October 10, 1985

To continue our study [1-3] regarding the synthesis, the structural characterization in solid state and in solution followed by the testing of the biological activity of some complex combinations, we isolated solid complexes of $Hg(II)$ with pyrazolonic ligands-antipyrine (Antp) and pyramidon (Pyr); with different amines-pyridine (Py) piperydine (Pip) and morpholin (Morf) and other ligands-urea (U) and tiourea (T). The result was salt-type complexes with protonate ligands, as well as neutral complexes under the form of HgL_2I_2 . The neutral complexes $HHgL_2I_2$ in which $L = Py$, Pip and Morf presented an antiseptic-disinfectant action much more important than the phenol and the sodium mercuritolate. We studied the formation of these complexes in solution and outlined the IR spectrum and their differential calorimetric analysis, obtaining the value of the corresponding thermodynamic parameters. The values of the activation energies — E_a — and of the decomposition enthalpies — ΔH — prove the tendency of these combinations to lose the ligand, forming HgI_2 . The bacteriostatic activity of these compounds is greater than that of the HgI_2 .

As concerns the possibility of coordinating the aminic ligands in water-alcohol, at Hg^{2+} in the presence of I^- anion we must remind that the donicity of the amines [4] is, generally, lower than the donicity OH^- and I^- . At these values of the donicity of the amines we must add, though, the possibility of forming some donor-acceptor bondings that increases the probability of coordinating the organic ligand. Out of the complex-forming potentiometric curves in the system $Hg-I-OH$ [5] we infer the equilibrium constant of the most stable species, $HgIOH$, $HgIOH \approx (8 \pm 2) \cdot 10^8$, which proves the great affinity of the $Hg(II)$ for I^- . Though it is not a typical complex-generator, previous studies [6-8] and more recent ones [9-10] take into consideration complex combinations of mercury with pyrazolonic and aminic ligands, obtained to determine their biological activity. The results of the tests done have not been published yet.

Preparation of the complexes. The salt-type complexes $[HgI_4] (HL)$ were prepared using the method described in the previous paper [3]. In order to obtain pure compounds of the form HgI_2L in which $L = Antp$, Pyr we revised Kumov's formula [11] in point of the ratio $Hg : L$. 20–25% mercuric salt in excess to the amount of ligand leads to some unitary compounds. We obtain yellowish crystals which decompose in components — HgI_2 and L — above 70–80°C. The HgI_2L_2 complexes in which $L = Py$, Pip, Morf were obtained using our own method in an alcoholic medium: the hot alcoholic solution — 80°C — of HgI_2 is refluxed for one hour with the stoichiometric quantity of ligand. The obtained solution is suddenly cooled and the result is microcrystals, pink-orange coloured, of the complex HgI_2L_2 .

* ICECHIM — Institute of Chemical and Biochemical Energetics, Cluj-Napoca Research Group 3400 Cluj-Napoca Romania

** University of Cluj-Napoca, Faculty of Chemical Technology, 3400 Cluj-Napoca, Romania

The obtaining output is lower with respect to the metal — 30–40% — but the compounds obtained are pure, as could be seen in Table 1. The neutral complexes of Hg^{2+} with U and T were prepared following directions in literature [12] from ethanolic solutions. We obtained combinations like HgI_nL in which $n = 2–4$. Out of the 9 complexes isolated in a solid state we are interested particularly in the combinations $HgPy_2I_2$, $HgMorf_2I_2$, $HgPip_2I_2$ and $HgPyrI_2$ which have proved an antiseptic-disinfectant action. The results of the determination of the composition of these combinations are presented in Table 1.

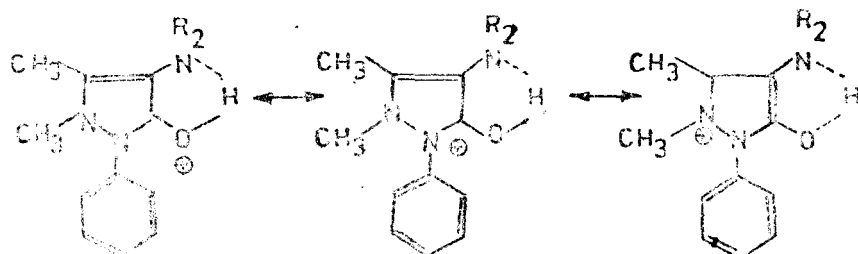
Table 1

The composition of the complexes $Hg(I)$ with Py, Pip and Morf

Compound	% Hg		% I		% N		decomp. T °C
	calc	found	calc.	found	calc.	found	
$HgPy_2I_2 \cdot H_2O$	31.79	31.87	40.25	40.47	4.24	4.14	88
		31.82		40.22		4.18	
$HgMorf_2I_2$	37.60	37.55	46.80	46.71	5.17	5.19	67
		37.65		46.75		5.20	
$HgPip_2I_2$	38.21	38.33	46.00	45.92	5.07	5.14	72
		38.22		46.21		5.12	

IR Spectrum of the Synthesized Combinations. To confirm the structure of the combinations obtained, the IR spectrums were drawn, using a PERKIN-ELMER 457 spectrophotometer in the $250–4000\text{ cm}^{-1}$ wave band. The samples were introduced into KBr and nujol tablets. According to our suppositions and to the indications found in literature as well, we have found that:

— With the complex salts of Hg^{2+} with pyrazolonic protonated ligand the protonation takes place at the atom of oxygen forming a strongly conjugated cation, presented in the following limiting structures:



— The bands specific to the substituents of the pyrazolonic nucleus are not affected, but new bands appear such as $2390–2840\text{ cm}^{-1}$, $1400–1020\text{ cm}^{-1}$. The vibrations characteristic of the free pyridinic nucleus were recorded (Table 2).

— The participation of the tiocarbonyl group at the formation of the coordinative bonding manifests for example, by the splitting of the band from 1412 cm^{-1} , as shown in Table 3.

Thermogravimetric Study of the Complexes. The derivatograms of the complexes were recorded at the Budapest MOM derivatograph. 0.5 g of substance was heated for 50 minutes to 600°C , in air, using Al_2O_3 as actionless ma-

Table 2

The vibrations of the pyridinic nucleus

Compound	δ inside the plane	δ outside the plane
Pyridine	604	405
HgPy ₂ I ₂	653	430

Table 3

The movement of the vibration frequencies in HgT₂Cl₂

Compound	ν_{CS}	ν_{CN}	δ_{NH_2}	γ_{NH_2}
Tiourea	1412 730	1471	1618	1082
HgT ₂ Cl ₂	1440 1390 732 722 710	1480	1610	1090

terial. We have plotted as an example, (Fig. 1) the derivatogram of the complex HgT₂Cl₂. The complexes HgPy₂I₂, HgMorf₂I₂ and HgPip₂I₂ present the lowest thermic stability. We intend to study more thoroughly the behaviour of these complexes at heating, by using a DSC-1B type PERKIN-ELMER differential calorimeter.

The samples weighted with a micronic precision were heated in an inert atmosphere of N₂ — the running speed 15 cm³/min. — dispersed in an actioless suport of Al₂O₃. From the differential calorimetric curves dH/dt = f(T), according to the method described in literature [13], we calculated the activation energy, E and the decomposition enthalpy ΔH . The activation energy was determined aut of the Arhenius curves — log K = f(1/T) presented in Fig. 2. The obtained thermic magnitudes are in accord with the reduced stability of these combinations. (Table 4).

Formation of the Complexes in Solution. Certain complexes in the system Hg—I—L do appear in alcoholic medium, but the rapid decrease in time of the height of the absorption because of the instability of the complex combination, renders it difficult to quantitatively study the stability of these com-

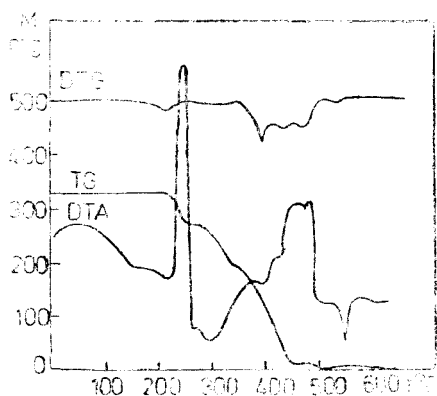


Fig. 1. The derivatogram for the complex HgPy₂I₂

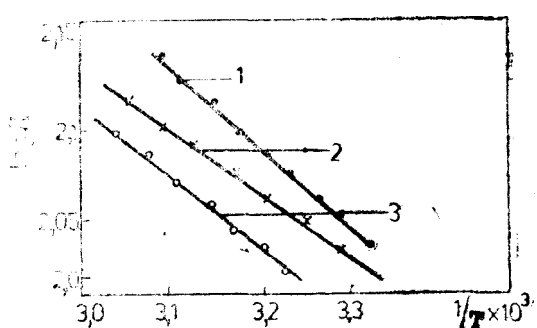


Fig. 2. The Arrhenius curves for the decomposition of the complexes HgPip₂I₂, curve 1, HgPy₂I₂, curve 2 and HgMorf₂I₂, curve 3

pounds. For example, the spectrophotometration of certain HgI_2 and Py solutions after 1 minute post. mixing leads to the UV spectrum presented in Fig. 3 ranging between 240—275 cm^{-1} . Because the ligand absorbs very much in this range, it was put into reference obtaining absorption curves reversed with respect to those of the pyridine. The molar ratios method in the system HgI_2 —Pip, with the ligand in great excess so as to detect all the processes that take place, leads to the distinguishing of the complex corresponding to the ratio $\text{Hg} : \text{Pip} = 1:4$ (Fig. 4).

Determination of the Antiseptic-Disinfectant Action. While making the filamenting test [3] it was observed that some Hg(II) complexes had a bactericide action on the stem of the typhus bacillus isolated during the epidemic in Banat, in the summer of 1974. Relying on this we undertook quantitative tests on bactericide action, determining the phenolic index and the lowest active concentrations of substance which stop the evolution of the respective bacillus. We took as a comparative substance HgI_2 , which, too, presents a bactericide action comparative to the phenol and sodium mertiolate. The results of the tests presented in Table 5 prove the bactericide activity of these combinations.

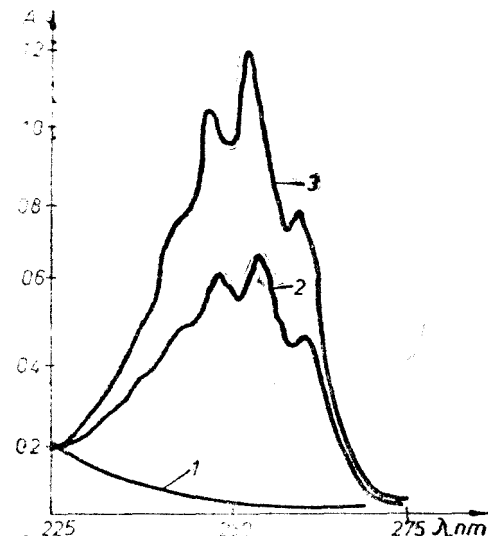


Fig. 3 The UV spectrum in the system HgI_2 —Py, $C_{\text{HgI}_2} = 10^{-3} \text{ M}$, $C_{\text{Py}} = 2 \cdot 10^{-3} \text{ M}$, cuva = 1 cm, ref. Py $2 \cdot 10^{-3} \text{ M}$, $t = 25.5^\circ\text{C}$

Table 4
The activation energies and the decomposition enthalpies of the HgI_3L_2 complexes

Compound	Initiation temperature ($^\circ\text{C}$)	E_a kcal/mol	ΔH kcal/mol
HgPy_3I_2	88	5.9 ± 0.8	12.2 ± 0.9
$\text{HgMorf}_3\text{I}_2$	67	7.3 ± 1.3	17.2 ± 1.1
HgPip_3I_2	82	4.7 ± 1.7	8.8 ± 2.0

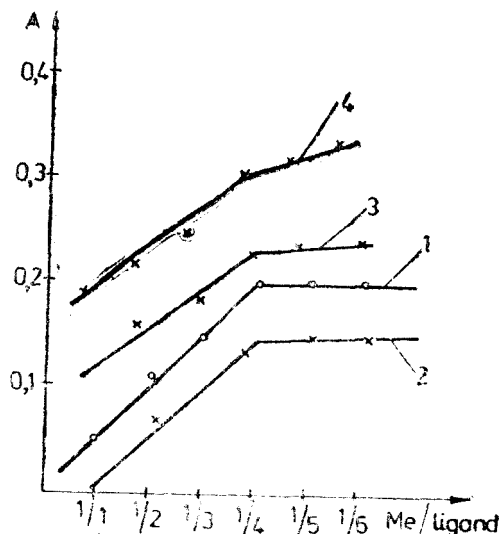


Fig. 4. The molar relations method in the system HgI_2 —Pip — curve 1: $\lambda = 255 \text{ nm}$; curve 2: $\lambda = 265 \text{ nm}$; curve 3: $C_{\text{Hg}} = 10^{-3} \text{ M}$; curve 4: $C_{\text{Hg}} = 2 \cdot 10^{-3} \text{ M}$.

Table 5

The antibactericide action spectrum and the bacteriostatic and bactericide doses of some complexes of Hg(II)

The stem towards which the com- plexes were tested	HgMorf ₄ I ₂ conc.		HgPy ₄ I ₂ conc.		HgI ₂ , conc.	
	B-static mg/100 ml	B-cid	B-static mg/100 ml	B-cid	B-static mg/100 ml	B-acid
B. subtilis	0.138	1.38	0.152	1.52	0.1	1
B. Thypy	1.38	1.38	1.52	1.52	1	1
Micrococcus L.	1.38	13.8	1.52	15.2	1	1
B. pyocyanic	1.38	13.8	1.52	15.2	10	10
B. Thypy (1349)	1.38	1.38	1.52	1.52	1	10
Proteus	1.38	13.8	1.52	15.2	1	1
Stafilococcus	0.13	13.8	0.15	15.2	0.1	1

Conclusions. In comparison with the human typhus bacillus, the complexes HgPy₄I₂ and HgMorf₄I₂ present a bactericide action 10 times greater than that of the phenol. Moreover, their bactericide activity towards the pyocyanic is greater than that of HgI₂. The studied complexes with bactericide action present a reduced thermic stability, manifested by a lower value of the initiating temperature. The obtained activation energies show the easiness with which the first ligand molecule breaks, whereas the values of the decomposition enthalpies reflect the heat that must be absorbed to break both links Hg—L, forming HgI₂. Under these conditions a question arises, namely whether the antiseptic-disinfectant activity is not because of decomposition forming HgI₂. Probably a part of this activity is, indeed, due to the HgI₂ but the 10 factor which it is superior to the bactericide activity of the HgI₂ and phenol favours another mechanism of bactericide action.

REFERENCES

1. B. Rosenberg, L. Van Camp, R. Grimley, J.A. Thomson, *J. Biol. Chem.*, **242**, 1347, (1967).
2. R.W. Talley, *Abstr. Proc. Am. Assoc. Cancer Res.*, **11**, 78 (1970).
3. Gh. Marcu, Maria Jitaru, *Studia*, **31**(2), 8 (1986).
4. V. Guttmann, *Angewandte Chem.*, **82**, 858 (1970).
5. J. Ahlberg, *Acta Chem. Scand.*, **27**, (8), 3003 (1973).
6. C.F. Babak, U.A. Kondrašov, *Zhur. Neorg. Khim.*, **10**, 1642 (1965).
7. A.N. Herlinger, Th. Veachlong, *J. Amer. Chem. Soc.*, **92**, 6481 (1970).
8. F.A. Cotton, *J. Inorg. Nucl. Chem.*, **35**, 1117 (1975).
9. K.J. Tudoryanu, P.K. Migal, *Zh. Neorg. Khim.*, **26**, 2786 (1981).
10. R. Saxena, G.L. Sharma, *Trans. SAEST*, **1**, 45 (1982).
11. V.I. Kumov, *Zhur. Obshchei. Khim.*, **19**, 1236 (1949).
12. W.G. Watt, *J. Inorg. Nucl. Chem.*, **33**, 1319 (1971).
13. H.D. Borchardt, F. Daniels, *J. Amer. Chem. Soc.*, **79**, (41) (1957).

BIOLOGICALLY ACTIVE METALLIC CHELATES

III. Complexes of Co(II) with Amino-Acids with Antitumour Activity

MARIA JITARU* and GHEORGHE MARCU**

Received: October 19, 1985

We isolated in solid state 23 complex combinations of Co(II) with essential aminoacids and other ligands in order to test their biological activity. The nature of the donor atoms established by recording the vibrations of the Co-L link coincides with the existing data in literature. The corresponding values of the stability constants — pK — and of the formation enthalpy — ΔH — for the complex Co—Asp are in perfect concordance with those for the system Co—Norv, whereas the formation enthalpy of the complex Co—αAbut is with 0.7 Kcal/mol lower, that pleads for the coordination of the β-carboxyl group of the aspartic acid. The obtained complexes were tested regarding their activity against the ascitic tumour ERHLICH in both incipient and advanced stage. The complexes CoGlu₂ and CoAsp₂ have proved the maintaining of the carcinostatic activity against the ERHLICH ascitic tumour in an advanced stage.

Cobalt is one of the 20 elements essential to life. The apparition *in vivo*, the biological part and the complexation characteristics of cobalt compared with similar properties of other essential metals are presented in Table 1 [1].

Table 1

Structural and complexation characteristics of the essential metals

The metal	Structure	Biological rôle	Oxidation stages	Preferred donor atoms	Type of complexed	g/70 Kg corp
Na, K	s ¹	Charge carriers and osmotic equilibrium	I	—O—	ionic	70
Mg, Ca	s ²	Frame formation and inhibition reactions	II	—O—	ionic	42 (Mg) 1700 (Ca)
Mn, Fe, Co, Cu, Mo	d ¹⁻⁸	Redox catalysts and enzymes components	II-IV	—O— —N— —S—	charge transfer	1

Of the transitional metals Co is most known, being the central ion in cobalamines and cobinamines — vitamin B₁₂ — . What it is less known is the fact that the complexes of Co(II) are able to transport molecular oxygen as in the case of simple ligands, such as histidine [2]. The essential aminoacids (Table 2) represent the 20 „bricks” of which millions of proteins are formed

* ICECHIM — Institut of Chemical and Biochemical Energetics, Cluj-Napoca Research Group, 3400 Cluj-Napoca.
Romania

** University of Cluj-Napoca, Faculty of Chemical Technology, 3400 Cluj-Napoca, Romania

Table 2

Essential aminoacids R—CH—COOH
 |
 NH

Nature	Group—R Structure	Aminoacid Identification	Abre- viation
1. non-polar aliphatic	$\begin{array}{c} -\text{H} \\ \\ -\text{CH}_3 \end{array}$ $\begin{array}{c} \text{CH}_3 \\ \\ -\text{CH}-\text{CH}_3 \end{array}$ $\begin{array}{c} \text{CH}_3 \\ \\ -\text{CH}_2-\text{CH}-\text{CH}_3 \\ \\ \text{CH}_3 \end{array}$ $\begin{array}{c} \text{CH}_3 \\ \\ -\text{CH}-\text{CH}_2-\text{CH}_3 \end{array}$	glycine alanine valine leucine izoleucine	Gly Ala Val Leu Ile
2. contains the OH group	$\begin{array}{c} -\text{CH}_2-\text{OH} \\ \\ -\text{CH}-\text{CH}_3 \\ \\ \text{OH} \end{array}$ $\begin{array}{c} -\text{CH}_2-\text{C}_6\text{H}_4-\text{OH} \end{array}$	serine threonine tyrosine	Ser Thr Tyr
3. aromatic	$\begin{array}{c} -\text{CH}_2-\text{C}_6\text{H}_5 \end{array}$ $\begin{array}{c} -\text{CH}_2-\text{C}_6\text{H}_4-\text{NH} \end{array}$	phenilalanine tryptophan	Phe Trp
4. radical acid	$\begin{array}{c} -\text{CH}_2-\text{COO}^- \\ \\ -\text{CH}_2-\text{CH}_2-\text{COO}^- \end{array}$	aspartic acid glutamic acid	Asp Glu
5. amino-basic	$\begin{array}{c} -\text{CH}_2-(\text{CH}_2)_3-\text{NH}_3^+ \\ \\ -\text{CH}_2-(\text{CH}_2)_2-\text{NH}-\text{C}\left(\text{NH}_2\right)_2 \\ \\ -\text{CH}_2-\text{C}(=\text{NH})_2 \end{array}$ $\begin{array}{c} -\text{CH}_2-(\text{CH}_2)_2-\text{CH}_2-\text{NH}_3^+ \end{array}$	lysine arginine histidine hydroxylsine	Lys Arg His Hyl
6. radical with —S	$\begin{array}{c} -\text{CH}_2-\text{SH} \\ \\ -\text{CH}_2-\text{S}-\text{S}-\text{CH}_2-\text{CH}\left(\text{COO}^-\right)-\text{NH}_3^+ \\ \\ -\text{CH}_2-\text{CH}_2-\text{S}-\text{CH}_3 \end{array}$	cysteine cystine methionine	Cys Cy Met

[3]. The amino group as well as the carboxyl one are capable of reacting with metallic ions together with other groups presented in the lateral chain. Except glycine, all the essential aminoacids are lefthanded, that is why we have chosen the „levo” form of the acid for the synthesis of the complex, as much as we could. It has been established [4–7] that cancer cells are not able to synthesize certain esential aminoacids and other aminoacids have, themselves, antitumour properties [8, 9].

On the other hand, the cobalt reached in the vicinity of the cancer cell freed from the old links of the complex introduced into the organism as a chemio-therapeutic anti-cancer [10] is able to form new links with the active positions of the cancer cell [10] leading to its degradation. Cobalt, as an intermediate acid, according to the theory of acids and hard and soft bases (ABDM) [11] will form stable with intermediate bases among which fall the $-NH_2$ di-aminoacids group. The complexes Co(II) with aminoacids have been widely studied, some of them recently, in order to test their biological activity. It has, thus, been reported the activity of certain complexes of Co(II) against certain leukaemias [12] and the complex Co-aspartic L acid presents a stimulation action of the oxydation complexes of the organism [13, 14]. Other compounds of Co(III) with cyclic amines inhibit the cellular division of the *E.coli* bacillus [15].

Preparation of the complexes. Generally, we obtained soluble complexes of the form $CoL_n \cdot nH_2O$ either following the reference indications or using our own methods, with the ligands presented in Table 2. The obtaining output of the complex combinations expressed in percentages with respectto the initial quantity of metal decreases with the increase of the solubility of the compounds (Table 3). The complex $CoLeu_3$ and $CoILeu_2$ were prepared from concentrated solutions of $Co(CH_3COO)_3 \cdot 4H_2O$ in a basic medium — pH = 7.5–8 by adding when cooled, the stoechiometric quantity of ligand under the form of the respective sodium salt.

Table 3
Complexes of Co(II) with essential aminoacids

Compound	Colour	Solubility in water	Output %	Dec. temp °C	Bibl. ref.
$Co(1-Leu)_3$	pink-violet	++	87.5	285–290	—
$Co(i-Leu)_3$	pink	++	80.3	250	—
$Co(L-Tyr)_3$	blue	+++	30.3	80	—
$Co(L-Asp)_3$	violet	+++	35.8	75	—
$Co(DL-Met)_3$	pink	—	92.4	80	(16)
$Co(L-Pheala)_3$	pink	+	80.2	55	(17)
$Co(L-Ser)_3 \cdot 2H_2O$	violet	+	81.5	148	(18)
$Co(Gly)_3 \cdot 3H_2O$	violet	+	79.5	—	(19)
$Co(DL-Val)_3$	violet	—	98.4	—	(20)
$Co(D-Ala)_3 \cdot H_2O$	pink	—	91.6	192	(21)
$Co(DL-Thr)_3 \cdot H_2O$	pink	+	76.5	—	(22)
$Co(L-Try)_3$	violet	+-	95.8	hygroscopic	(23)
$Co(DL-Cys)Cl_2$	pink-violet	++	58.6	—	(24)
$Co(L-His)_3Cl_2$	pink	++	52.3	60	(25)
$Co(L-Arg)_3Cl_2$	violet	+	71.5	—	(26)
$Co(L-Glu)_3 \cdot H_2O$	violet	++	59.6	—	(27)
$Co(Cys)_3 \cdot 3H_2O$	brown	+-	91.0	100	(28)
$Co(CySSCys)_3$	pink	—	93.5	—	(29)
$Co(L-Pro)_3$	pink	—	96.7	80	(30)

We get a pink-violet product which cannot be filtered, having the aspect of a foam. The reaction finalizes in three hours, on a water bath at 60°C. We get an abundant precipitate which is separated with a whirler, washed in alcohol and ether and dried at maximum 60°C in vacuum. The great solubility of the complexes Co-LTyr_2 and Co-LAsp_2 in water, represents an impediment when trying to isolate them from the mother solution.

The adding of small amounts of dimethylformamide (DMF) at 8–10°C leads to the forming of some precipitates which can be filtered in time, corresponding to the relation $\text{Co-L} = 1 : 2$. The dissolving of the DMF in the reaction medium being a strongly exothermic process cooling with a mixture of salt and ice is necessary. The composition of the complexes was determined through dosing the Co by atomic absorption and by elementary organic analysis. The analytical results presented in Table 4 show that pure unitary compounds were obtained.

Table 4

Composition and characteristics of some Co(II) complexes with essential aminoacids

Symbolic formula	Brute formula	Molecular mass	%Co Calculated	%Co Found	%N Calculated	%N Found
$\text{Co}(\text{Gly})_2 \cdot 3\text{H}_2\text{O}$	$\text{CoC}_4\text{H}_{14}\text{N}_2\text{O}_7$	261.07	22.60	22.13	10.75	11.04
$\text{Co}(\text{L-Glu})_2 \cdot \text{H}_2\text{O}$	$\text{CoC}_{10}\text{H}_{18}\text{N}_2\text{O}_9$	367.07	16.05	15.76	7.63	7.45
$\text{Co}(\text{L-Asp})_2 \cdot 2\text{H}_2\text{O}$	$\text{CoC}_{10}\text{H}_{18}\text{N}_2\text{O}_9$	359.23	16.40	16.45	7.81	7.92
$\text{Co}(\text{DL-Val})_2 \cdot 3\text{H}_2\text{O}$	$\text{CoC}_{10}\text{H}_{26}\text{N}_2\text{O}_7$	345.13	17.05	17.22	8.10	7.83
$\text{Co}(\text{DL-Met})_2$	$\text{CoC}_{10}\text{H}_{20}\text{O}_4\text{N}_2\text{S}_2$	355.35	16.58	16.35	7.88	8.13
$\text{Co}(\text{L-Leu})_2$	$\text{CoC}_{12}\text{H}_{24}\text{O}_4\text{N}_2$	319.26	18.46	18.35	8.77	9.10
$\text{Co}(\text{DL-iLeu})_2$	$\text{CoC}_{12}\text{H}_{24}\text{O}_4\text{N}_2$	319.26	18.46	18.67	8.77	8.99
$\text{Co}(\text{L-Tyr})_2$	$\text{CoC}_{18}\text{H}_{20}\text{O}_6\text{N}_2$	419.29	14.06	14.03	6.68	6.98
$\text{Co}(\text{L-Trp})_2$	$\text{CoC}_{22}\text{H}_{22}\text{O}_4\text{N}_4$	465.36	12.66	12.20	12.05	12.68

Determination of the Structure of the Complexes. In order to confirm the proposed structures and to correlate the existing data in literature, we have drawn the IR spectra of the synthesized compounds using a PERKIN-ELMER spectrophotometer with a range of work between 250–4000 cm^{-1} to etach the vibration frequencies characteristic of the Co-L link. In the case of the compounds Co(II) — monobasic aminoacids, the elongation vibration of the group $-\text{NH}_2$ moves towards lower frequencies and out of the frequencies corresponding to the carboxyl group λ_{cooas} moves towards higher frequencies and ν_{coosim} towards lower ones. The respective compounds are tetra-coordinated with a plane-square structure and trans geometry (Fig. 1). In CoMet_2 the coordination takes place by N aminic and both atoms of O of the carboxyl group — both ν_{cooas} and ν_{coosim} decrease (Fig. 2). In the case of heterocolic aminoacids — hystidine and tryptophane — it is confirmed

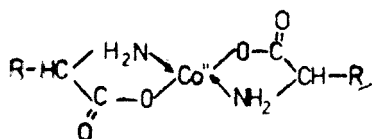


Fig. 1. The structure of the complex combinations of Co(II) with monobasic aminoacids.

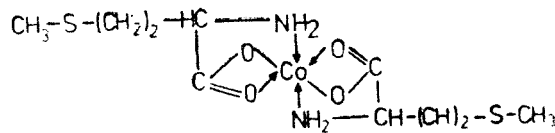


Fig. 2. The structure of the complexes Co(II) with methionine.

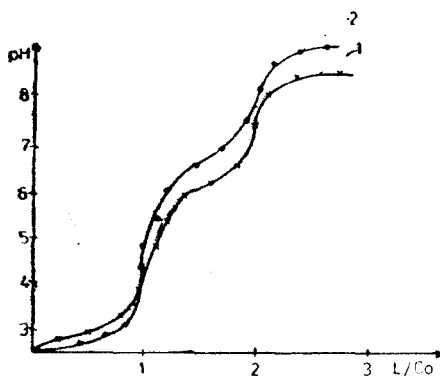


Fig. 3 Potentiometric titration in the system Co(II)-Asp, curves 1 and Co(II)-Glu curve 2

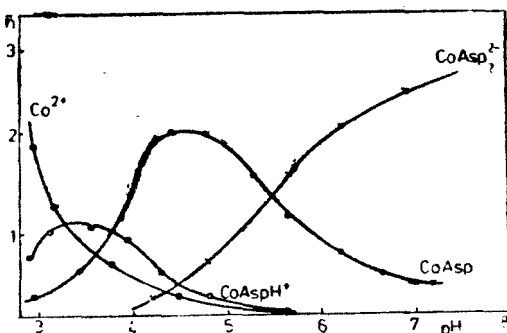


Fig. 4 The distribution of the concentrations of the complexes formed in the system Co(II)-Asp, with respect to the pH.

the fact that the N of the heterocycle does not take part in the coordination. A particular interest presents CoAsp_2 when the coordination of the aspartic acid by the β -carboxyl group is possible as well. To confirm the participation of the β -carboxyl group at the coordination we studied the complexes Co-Asp in solution.

The Potentiometric Study Of the System Co(II) Asp. The potentiometric determinations were done with a PHM-4d radiometer using a glass electrode G-100B as a measure electrode, and the K-100 calomel electrode as reference electrode. During determinations the temperature was constant at $25 \pm 0.1^\circ\text{C}$. The experiment was carried in a medium of KCl 0.2 moles/l in a constant volume of 25 cm^3 . The measurements were done in an aminoacid solution of $6 \cdot 10^{-3}$, varying the metallic ion-ligand ratio from 1:1 to 1:2 and 1:3, respectively. The potentiometric titration curves of the aqueous solution of Co(II) with the respective ligand, present three potential leaps corresponding to the three species which are present in the system depending on its pH (Fig. 3). The distribution of the concentrations of the complexes Co(II) with aspartic acid at a relation $\text{Co-L} = 1:2$ depending on the pH, shows that at a pH = 5 the dominant species is CoAspH^+ which transforms itself in CoAsp at pH = 4.5. Under conditions of a neutral pH similar to those in the organism, the CoAsp_2 is predominant and, anyway, it was isolated in solid state and tested with respect to the antitumour activity. We can see that under certain conditions the concentration of some of the species present in the complex can be neglected and thus we obtain the stability constants of the most components of the compounds in the system at a certain moment (Fig. 4). The thermodynamic parameters obtained on a computer — COMICS programme — are presented in Table 5, compared with the corresponding compounds of Co(II) with norvaline (Norv) and aminobutyric acid (α -Abut) found in literature [31]. To interpret the obtained data we will take into consideration the thermodynamic data as well, regarding the protonation of the aspartic acid and glutamic acid [32] presented in Table 6.

Table 5

Thermodynamic data regarding the complexes Co(II) with glutamic acid (Glu), α -aminobutyric acid (α Abut) and norvaline (Norv) (31)

Process	log K	$-\Delta H$ Kcal/mol	ΔS e.m.u.
$\text{Co}^{2+} + \text{Glu}^- - \text{ClGlu}^+$	8.07	5.9	17
$\text{CoGlu}^+ + \text{Glu}^- - \text{CoGlu}_2^0$	6.77	7.6	6
$\text{Co}^{2+} + \text{Abut}^- - \text{CoAbut}^+$	8.02	5.4	19
$\text{Co}^{2+} + \text{Nva}^- - \text{CoNva}^+$	8.70	5.6	20
$\text{CoNva}^+ + \text{Nva}^- - \text{CoNva}_2^0$	6.75	6.9	8
$\text{CoAbut}^+ + \text{Abut}^- - \text{CoAbut}_2^0$	6.71	6.6	9

Table 6

Thermodynamic data regarding the protonation of the aspartic and glutamic acid (32)

Compound	Group	pK	$-\Delta H$	ΔS
Aspartic acid	$\beta\text{-COO}^-$	3.68	1.96	14.5
	$\alpha\text{-COO}^-$	1.95	1.85	4
	$-\text{NH}_2$	9.63	1.1	26.5
Glutamic acid	$\alpha\text{-COO}^-$	9.12	0.8	7
	NH_2	9.51	9.7	11

Interpretation of the Results. Correlating our data with those reported by other authors [31, 32] certain conclusions must be drawn:

- The stability of the complex CoAsp is greater than that of other complexes of Co(II) containing the same number of carbon atoms;
- There are no important differences between the values pK for the group NH_2 corresponding to the two aminoacids.
- The corresponding values of the pK and ΔH for the system Co(II) are in concordance with those for the system Co-Norv whereas the formation enthalpy of the complex Co-Asp is by 0.7 Kcal/mol greater than that of the complex Co-Abut. This could be due to the participation of the aspartic acid to the coordination of the carboxyl group. The participation of the β -carboxyl group at the coordination in CoAsp° is suggested by the observation that the complex CoAsp° is separated out of solutions containing Co(II) and Asp in a ratio of 1:1 at pH = 4.5, phenomena that does not take place in the system Co-Glu.

Testing of the Antitumour Activity of the Complex Combinations. Our results regarding the testing of certain complexes of Co(II) with respect to the ascith ERHLICH in an incipient phase have already been published. The method of testing the complex combinations which presented a limited antitumour activity [33] regarding the maintenance of this activity against the advanced ERHLICH tumour contained the following stages:

- The transplantations of the tumour ($5 \cdot 10^6$ tumour cells) by interperitoneal injecting (i.p) to mice in the control lot, as well as to those of the experimental ones.
- The injection of animals from the experimental lots on the 4th, 8th, 12th and 18th day with the respective compounds.

The obtained results show that only the complex $\text{Co}(\text{L-Asp})_2$ leads, under these conditions, at a T/C = 150%, to the healing of one animal out of 10 for doses of 20, 40, and 80 mg/Kgcorp. Under these conditions it was put into evidence for certain complexes of Co(II) the late toxicity phenomena: $\text{Co}(\text{L-Leu})_2$, $\text{Co}(\text{LD-Leu})_2$, $\text{Co}(\text{L-Pheala})$ and $\text{Co}(\text{DL-Met})_2$ with T/C 100%. In these cases the time of survival of the treated animals with the dose of over 20 mg/kgcorp decreases with respect to the nontreated animals. Certain

complexes, though not soluble in water, for example $\text{Co}(\text{L}-\text{Glu})_2$, give better results when administered under the form of oily suspension. In this case $T/C = 189\%$ and again one animal out of 6 remains without tumour.

REFERENCES

1. D. R. Williams, "The Metals Of Life", Van Nostrand, London, 1971, p. 376.
2. H. A. O. Hill, J. M. Pratt, R. J. P. Williams, *Chem. Brit.*, **5**, 156 (1969).
3. R. F. Steiner, "Life Chemistry", Van Nostrand, USA, 1968, p. 280.
4. R. W. Talley, *Abstr. Proc. Am. Assoc. Cancer Res.*, **11**, 78 (1970).
5. T. A. Connors, *Chemico-Biol. Interact.*, **5**, 415 (1973).
6. B. J. Leonard, *Nature*, **234**, 43 (1971).
7. J. A. Howle, G. R. Glen, *Biochem. Pharmacol.*, **19**, 2757 (1970).
8. T. A. Connors, *Proc. VII-th Int. Congr. on Chemotherapy*, Avicenum, Prague, 1971, p. 278.
9. C. V. Welch, *Proc. Amer. Assoc. Cancer Res.*, **12**, 25 (1971).
10. J. J. Roberts, J. M. Pascoe, *Nature*, **235**, 282 (1972).
11. H. E. Skipper, *Sci. Horiz.*, **125**, 13 (1971).
12. W. R. Walker, Y.-Ho L.-Shaw, N. C. Li, *J. Coord. Chem.*, **3**, 77 (1973).
13. Kojima Yoshihirp, *Inorg. Chem.*, **12**, 1009 (1974).
14. V. E. Keyes, J. Ivan Legg, *J. Amer. Chem. Soc.*, **95**, 3434 (1973).
15. B. J. Crawford, D. E. Talburt, D. A. Johnson, *Bioinorg. Chem.*, **3**, 121 (1974).
16. C. A. Mc Auliffe, J. V. Quagliano, L. M. Vallarino, *Inorg. Chem.*, **5**, 1996 (1966).
17. E. S. Tchougaeff, *Compt. Rend.*, **154**, 119 (1912).
18. D. A. Buckingham, L. G. Marzilu, A. M. Sargesea, *J. Amer. Chem. Soc.*, **89**, 5659, (1967).
19. Tsuchia Ryokichi, Kanazani Katsuhide, *Bull. Chem. Soc. Jpn.*, **50**, 2805 (1975).
20. S. S. Seehon, S. L. Chopra, *Thermochimica Acta*, **7**, 151 (1973).
21. A. Albert, D. J. Brown, *J. Amer. Chem. Soc.*, **76**, 2061 (1974).
22. B. M. Scoran, M. Cefola, *Arch. Biochim. Biophys.*, **97**, 146 (1952).
23. B. Jezowska-Trzebiatowska, A. Antonov, *Bull. Acad. Pol. Sci., Ser. Sci. Chim.*, **22**, 489 (1974).
24. B. Jezowska-Trzebiatowska, A. Antonov, *Bull. Acad. Pol. Sci., Ser. Sci. Chim.*, **22**, 409 (1974).
25. B. E. Evertsson, *Acta Cryst.*, **B25**, 30 (1969).
26. S. Valladas-Dubois, *Bull. Soc. Chim.*, France, 967 (1961).
27. D. A. Buckingham, J. Dekkers, *Inorg. Chem.*, **12**, 1207 (1973).
28. P. Ray, A. Bhaduri, *J. Indian Chem. Soc.*, **27**, 297 (1950).
29. V. Carasitti, L. Moggia, *Ann. Chim., Rome*, **50**, 602 (1960).
30. Per Saland, K. Kloss, *Nature*, **163**, 565 (1949).
31. R. D. Graham, D. R. Williams, P. A. Yeo, *J. Chem. Soc.*, **A1972** 1876.
32. A. Gergely, J. Sóvagó, *J. Inorg. Nucl. Chem.*, **35**, 4355 (1973).
33. C. Drăgulescu, Maria Jitaru, Iulia Havalik, Ana Maurer, Septimiu Policee, V. Topciu, N. Csaki, *Farmacia*, **29**, 215 (1981).

A SPECTROPHOTOMETRIC KINETIC STUDY OF THE MANGANIC CYSTEINATES DECOMPOSITION IN AQUEOUS SOLUTION

MARIA-MARILENA GIURGIU*

Received: February 8, 1985

Kinetics and mechanism of the manganic cysteinate decomposition in aqueous media has been investigated by means of a fast recording spectrophotometric device. The reaction rate, expressed by the disappearance of the Mn(III) and (IV) complexes, is second order with respect to the concentration of the absorbant complex species at pH = 7.0, and it shows a zero order dependence on the concentration of the reducing substrate. In alkaline solution, the first order kinetic behaviour may become predominant. The intermediate complexes have been detected by means of their absorption spectra. A change of the reaction order with the concentration of the reducing reagent, at pH = 7.0 is to be expected, in accordance with a reaction sequence involving preequilibrium steps. A reaction mechanism has been discussed in connection with our experimental results.

Introduction. Potassium permanganate solution reacts very rapidly with cysteine in excess in alkaline solution to form a red-violet intermediate complex which undergoes a slow decomposition to Mn(II) cysteinate complex and cystine. The manganous cysteinate complex is reoxidized to manganic complex in the presence of the atmospheric oxygen. The rate of reoxidation of Mn(II) compound to one of the manganic state by O₂ is very slow in acidic and neutral media. No catalytic effect was observed in the present instance.

In acidic medium the reaction rate increases considerably. The composition and spectra of the intermediate complexes differ with the pH range of the reaction mixture. In perchloric acid solution both Mn³⁺_{aq} and MnOH²⁺_{aq} species may be involved in the reaction mechanism with organic and inorganic substrates [1].

Some significant aspects connected with the chemistry and equilibria involving manganic complex species in aqueous solution have been discussed by G. Davies [2].

The oxidation processes of some substituted thiourea with Mn(III) species in acidic conditions have been recorded by a stopped-flow device [3]. There is no evidence for complex formation for these systems.

Tanaka, Kolthoff and Stricks [4] have investigated the composition of ferrous and ferric cysteinate complexes in alkaline solution. The principal species are FeOH(Cy)₂²⁻ and Fe(Cy)₃³⁻. They have also found that the disappearance of the ferric cysteinate complexes is second order with respect to total iron concentration and is approximately inversely proportional to the concentration of cysteine. A more detailed study of the Fe(III) — Cysteine reaction was performed by authors [5].

* University of Cluj-Napoca, Faculty of Chemistry, 3400 Cluj-Napoca, Romania

The oxidation of cysteine and thiomalic acid with cobaltic ions in perchloric acid solution [6] demonstrates the existence of an intermediate complex which subsequently decomposes in an intramolecular electron transfer step. A general reaction scheme has been proposed [6].

The oxidation of sulphur-containing compounds such as tiomalic, thiolactic and thioglycolic acids [7] by Ce(IV) has been studied using fast reaction techniques [7]. The kinetics are strictly second order with no evidence for extensive complex formation.

The kinetics of the oxidation of cysteine with Mo(VI) ions [8] is first order with respect to the oxidant concentration and second order with respect to that of the organic substrate [8.a].

The vanadium (V) oxidation of thiomalic acid has been recorded [9]. There is evidence concerning the formation of an intermediate complex.

In the present paper we have performed a kinetic study of the decomposition of inorganic intermediate cysteinate complexes resulting from potassium permanganate reduction in the presence of cysteine. The reaction products of the intramolecular electron transfer processes are manganous cysteinate complex and cystine.

Experimental. 1. *Preliminary observations.* The formation of the intermediates with cysteine in acidic solution becomes instantaneous (within the mixing interval). The optical density values extrapolated to zero time, D_0 , are not additive in respect with the initial reactants (MnO_4^- ions and the equilibrium forms of cysteine).

The kinetic curves in alkaline media of pH=9–11 present a maximum, corresponding to the maximum value of the intermediates concentration [10]. Figure 1 illustrates some kinetic curves in alkaline conditions (at different λ values). The horizontal line of the experimental curves corresponds to the optical density of cysteine, before adding the oxidant solution.

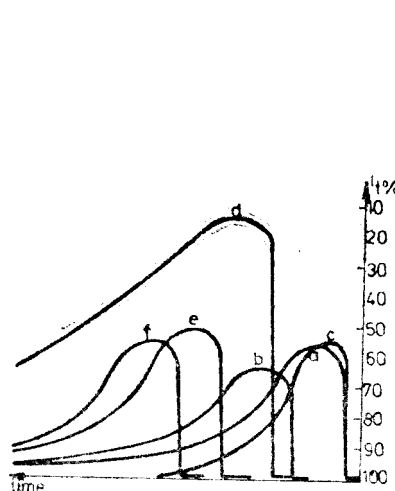


Fig. 1 — Kinetic experimental curves illustrating the existence of the intermediate complexes in alkaline solution: a) 530 nm; b) 590 nm; c) 510 nm; d) 390 nm; e) 410 nm; f) 430 nm.

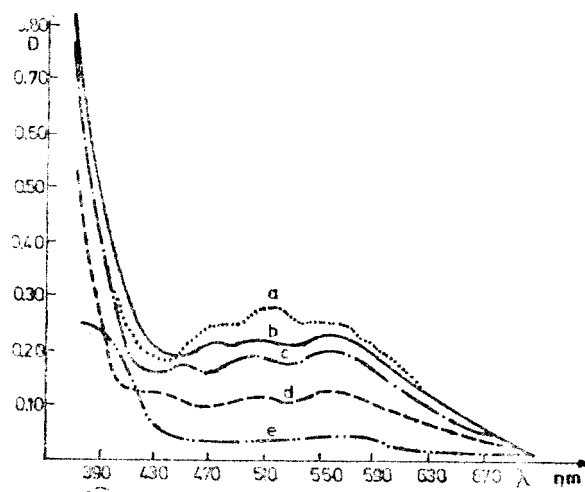


Fig. 2 — Spectra of the intermediate complexes in alkaline solution at pH=11.10
a) $\Delta t_i = t_{\max}$; b) $\Delta t_i < t_{\max}$; c–e) $\Delta t_i > t_{\max}$.
 $(\text{MnO}_4^-)_0 = 1.25 \times 10^{-4} \text{ mol/l}$; $(\text{Cy})_0 = 0.85 \times 10^{-2} \text{ mol/l}$.

The spectra of the intermediate complexes in the pH range of 9–11 have been obtained by means of an indirect method from the kinetic curves recorded experimentally at different λ . The Δt_i values symbolize the time interval from the mixing moment to the observation point [10]. See Figure 2: $\Delta t_i = t_{\max}$; $\Delta t_i < t_{\max}$; $\Delta t_i > t_{\max}$.

The overall reaction of permanganate with cysteine proceeds in two stages: the first one, which is very fast in acidic media, is the MnO_4^- ion reduction to an intermediate oxidation state of the manganese atom (III, IV) with the simultaneous oxidation of the organic substrate. The second stage is the slow decomposition of these intermediates to Mn(II) state and cystine. It is the kinetics of this slow decomposition we have investigated spectrophotometrically, with the hope of further elucidation of the Mn(III) — mercaptide reaction mechanism.

The preliminary overall rate constants, k_{ob} , involving a first order kinetic law, in alkaline media [10] are dependent on the λ — values, suggesting a photochemical catalytic effect on the rate (Table 1).

2. Solutions. Experimental device. Kinetic method. High purity cysteine was used (for biochemistry) without purification. Titration of the reagent in an alchoholic solution with a standard I_2 solution was performed in order to determine the concentration of initial stock solution. Stock solution was prepared by dissolving a weighed amount of 0.6767 gramme into 50 ml phosphate buffer ($\text{pH}=7.0$) solution prepared in twice distilled water. The dilution of this stock solution was performed by using the same buffer solution. The initial concentration range of cysteine is 9.93×10^{-2} — 1.78×10^{-2} mol/l.

The initial value of the optical density, D_0 , experimentally evaluated, is relatively independent on the initial concentration of the reducing agent. An average value of $\epsilon = 2440 \text{ l mol}^{-1}$ has been obtained at $T=288.5 \text{ K}$ and 293 K , suggesting that a single manganic complex is the predominant absorbant species in our conditions. The extinction coefficient of the permanganic ion at 370 nm experimentally determined is $1124 \text{ l mol}^{-1} \text{ cm}^{-1}$.

Potassium permanganate solution of reagent grade purity was standardized against oxalic acid in acidic medium and spectrophotometrically at 530 nm.

The starting time was taken when the oxidant solution (1 ml) was rapidly introduced (by using the syringe technique) into 4 ml aqueous cysteins placed in the thermostated cell. A fast recording Zeiss device was used to follow the reaction course. The recording rate was fixed to be 300 and 600 mm sec $^{-1}$. The optical density value of products is zero in all cases at 370 nm.

All solutions were thermostated in a water-bath before mixing. The experiments were performed at three different temperatures. The mixing time is less than 1.5 seconds, which was evaluated by mixing 1 ml of the oxidant solution into 4 ml buffer of $\text{pH}=7.0$.

The actual values of I_t , I_t^{real} , were obtained from the experimentally recorded values:

$$I_t^{\text{real}} = I_t^{\text{ex}} + \tau \frac{dI_t^{\text{ex}}}{dt}$$

τ — being „the time constant” of the recording device. This correction, however, is not significant in our conditions.

The experimental data for the reaction mixture were converted into D — time values and the kinetics of the overall process was observed according to the second-order rate expression for the disappearance of the intermediate complexes. The reaction order with respect to the concentration of Mn(III) and Mn(IV) complexes was also determined from the linear relationship of the rate against concentration of the absorbant species:

$$\log r \text{ vs } \log D_t$$

Table 1

First order rate constants in alkaline solution
 $298 \text{ K}, J = 0.147 \text{ mol/l}, \text{pH} = 11.10$;
 $(\text{MnO}_4^-)_0 = 1.5 \times 10^{-4} \text{ mol/l}; (\text{Cy})_0 = 9.5 \times 10^{-3} \text{ mol/l}$

λ, nm	$k_{ob} \times 10^3$ sec $^{-1}$	Obs. $\delta \times 10^3$
330	16.60	± 0.10
350	7.00	± 1.00
370	7.10	± 0.60
390	5.50	± 0.20
410	5.95	—
430	8.20	± 1.10
450	12.10	—
470	20.00 ?	—
490	10.70	—
510	19.80	± 0.10
570	19.70	—
590	17.10	± 0.70

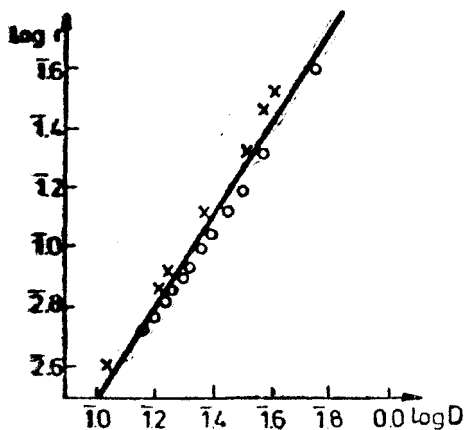


Fig. 3. a — Linear plots, $\log r$ vs $\log D$ at 306.5 K.

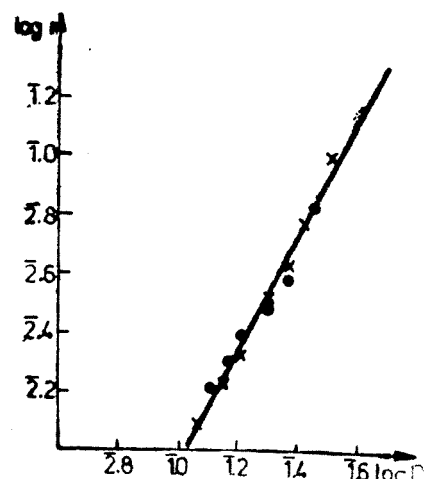


Fig. 3. b — Linear plots, $\log r$ vs $\log D$ at 298 K.

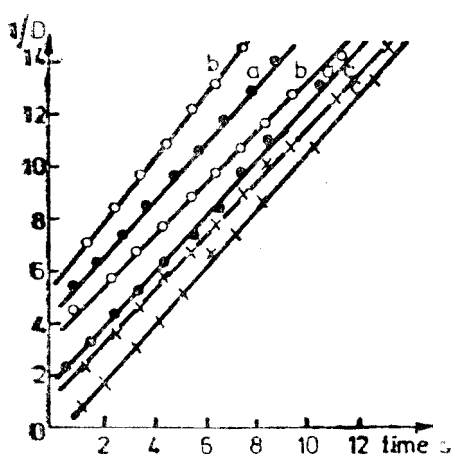


Fig. 4 — Second order kinetic plots, D_t^{-1} vs time, at three different Cysteine concentrations: a) 7.15×10^{-2} mol/l; b) 3.57×10^{-2} mol/l; c) 5.35×10^{-2} mol/l, 284 K, pH = 7.0

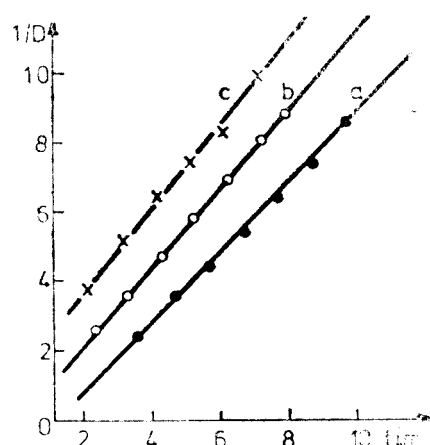


Fig. 5 — Second order kinetic plots D_t^{-1} vs time, at 298 K, pH = 7.0

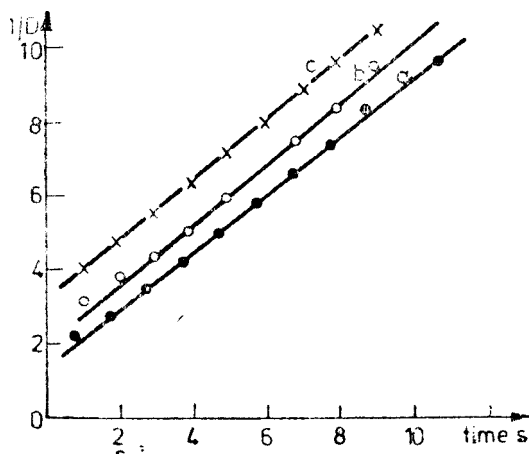


Fig. 6 — Second order kinetic plots, D_t^{-1} vs time, at 306.5 K, pH = 7.0

The reaction rate is expressed by $-dD/dt$.

Figures 3 (*a* and *b*) illustrate these kinetic results at two different temperatures, 298 and 306.5 K, respectively.

The apparent reaction order is independent on temperature, the fact being significant in connection with the reaction mechanism.

3. Kinetic results. Figure 4 illustrates the second-order kinetic plot, D^{-1} vs time, at different values of cysteine concentration (*a*, *b*, *c*) pH = 7.0 and 284 K.

The same kinetic plots are represented in Figures 5 and 6, at 298 and 306.5 K, respectively.

Table 2 presents the apparent second-order rate constants in terms of optical density, at 284 K.

A more detailed experimental study of temperature influence is necessary in order to associate the activation parameters to the reaction mechanism. This will be the object of the next paper.

Discussion. The reactive predominant form of cysteine, calculated from the equilibria in aqueous solution [11] is $\text{H}-\text{S}-\text{R}-\text{HN}_3^+$ at pH = 7.0 with the carboxyl group being dissociated. It is symbolised as /Cy/ in our reaction sequence.

The initial reduction stage, Mn(VII) to Mn(III) being very fast it cannot be subjected to experimental investigation by means of the present technique. Thus the rate of Mn(III) and Mn(IV) cysteinates disappearance was interpreted in connection with the reaction mechanism.

The reaction is second order with respect to the total concentration of the manganese intermediate complexes in neutral solution:

$$r_{\text{ob}} = -dD/dt = k_{\text{app}}(D)^2$$

and of zero order to that of cysteine concentration.

The second order kinetic term in the rate law may result from both Mn(III) and Mn(IV) contribution to the overall process.

The following reaction sequence is in accordance with the rate expression experimentally evaluated:

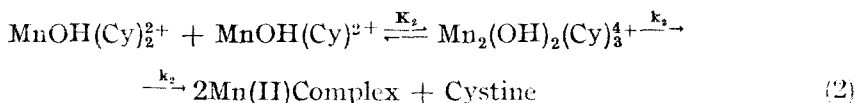
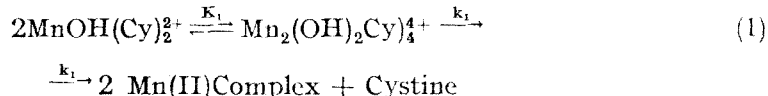
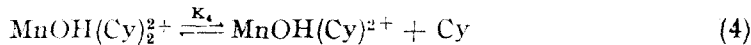
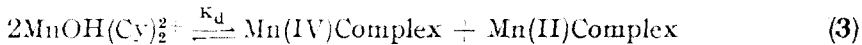


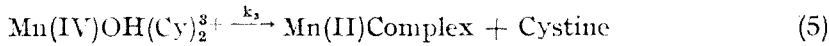
Table 2

Second order rate constants, k_{app} , for the decomposition of manganic cysteinates in phosphate buffer solution, 284 K, pH = 7.0.

$[\text{Cyst}]_0, \text{M}$	7.15×10^{-2}	5.35×10^{-2}	3.57×10^{-2}
k_{op}	1.080	0.900	0.973
(t in sec)	1.050	1.000	1.072
	1.050	0.976	1.173
	..	0.800	1.250
		1.120	1.200
			1.000
			1.123
\bar{k}_{op}	$1.055 \pm$	$0.974 \pm$	$1.104 \pm$
	0.012	0.065	0.040



— determining the equilibrium concentration of the lower manganic complex.



The path (5) is unimolecular with regard to Mn(IV) concentration species but it is bimolecular to that of the manganic complex, on account of the equilibrium step (3).

A first order term may be significant as the pH increases. This kinetic term may be associated to the path:



By expressing the rate by means of the predominant absorbant complex, $\text{Mn(III)OH}(\text{Cy})_2^{2+}$, we obtain:

$$r = -\frac{d(\text{MnOH}(\text{Cy})_2^{2+})}{dt} = \left(k_1 K_1 + \frac{k_2 K_2 K_4}{(\text{Cy})} + \frac{k_3 K_d}{(\text{Mn(II)})} \right) \cdot [\text{MnOH}(\text{Cy})_2^{2+}]^2 \quad (8)$$

$$k_{ob} = k_1 K_1 + \frac{k_2 K_2 K_4}{(\text{Cy})} + \frac{k_3 K_d}{(\text{Mn(II)})} \quad (9)$$

the third term being insignificant in our experimental conditions. The rate constant, k_{ob} , becomes then:

$$k_{ob} = k_a + \frac{k_b}{(\text{Cy})} \quad (10)$$

This reaction sequence gives a rate expression which is linear in $(\text{Cy})_0^{-1}$ at moderate cysteine concentration (in excess to that of the oxidant), with a negative reaction order, and it becomes independent on cysteine concentration ($n = 0$), when the concentration of the complex $\text{MnOH}(\text{Cy})_2^{2+}$ is considerably greater than the concentration of the other manganic complexes (at high excesses of the reducing agent).

The experimental measurements should be completed in order to elucidate these and other important questions. The limiting specific rate, $k_1 K_1$, has been thus evaluated.

REF E R E N C E S

1. C. F. Wells, G. Davies, *Nature*, **205**, 692 (1965); *J. Chem. Soc. A*, **1967**, 1858; C. F. Wells, *Nature*, **205**, 693 (1965).
2. G. Davies, *Coord. Chem. Rev.*, **4**, 199 (1969); G. Davies, *Coord. Chem. Rev.*, **7**, 353 (1972).
3. G. Davies, *Inorg. Chem.*, **11**, 2488 (1972).
4. N. Tanaka, I. M. Kolthoff, W. Stricks, *J. Amer. Chem. Soc.*, **77**, 1996 (1955).
5. D. L. Leussing, J. P. Mislan, R. J. Goll, *J. Phys. Chem.*, **64**, 1070 (1960).
6. J. Hill, A. McAuley, *J. Chem. Soc. A*, **1968**, 2405.
7. J. Hill, A. McAuley, *J. Chem. Soc. A*, **1968**, 156.
- 8.a J. P. Martin, J. T. Spence, *J. Phys. Chem.*, **74**, 2863 (1970); *J. Phys. Chem.*, **74**, 3589 (1970); b. R. Melby, *Inorg. Chem.*, **8**, 349 (1969).
9. W. F. Pickering, A. McAuley, *J. Chem. Soc. A*, **1968**, 1173.
10. M. M. Giurgiu, "Kinetics and Mechanism of the Permanganic Ion Reduction with Thiosulphate in Aqueous Solution", *Doctoral Thesis*, Cluj, **1972**.
11. R. E. Benesch, R. Benesch, *J. Amer. Chem. Soc.*, **77**, 5877 (1955).

UNTERSUCHUNG ÜBER DIE TETRATHIOCYANATO-DIAMIN-CHROMIATE EINIGER AMINE UND PHOSPHINE

GHEORGHE MARCU*, CSABA VÁRIHELYI*, DANA ITUL* und BORBÁLA SZALMA*

Eingegangen am 16. September 1986

Study on the Tetrathiocyanato-Diamine-Chromates (III) of Some Amines and Phosphines. 27 new complex salts of the type AH₂[Cr(NCS)₄(Amine)₂] (amine = NH₃, aniline, p-toluidine, A = imidazole derivatives, isobutylamine, Et₂Ph · P, Et₂(p-tolyl)P, Ph₂Pt · P, Pt₂P) were obtained by double decomposition reactions in acidic medium. The products were characterized by electronic and IR spectra. The thermal decomposition of some derivatives was studied by derivatography.

Einleitung. Die einbasischen Komplexsäuren des Types : H[Cr(NCS)₄(Amin)₂] (Amin = NH₃, verschiedene primäre und tertiäre aliphatische und aromatische Amine) werden oft zur Trennung von verschiedenen N-basischen organischen Substanzen, wie Aminosäuren, Peptiden, Alkaloiden, Antibiotika, usw., verwendet. Sie haben auch in der Analyse verschiedener pharmazeutischer Präparate ein ebensondere Bedeutung. Die Löslichkeit der Ammoniumsalze dieser Säuren im Wasser ist von der Natur des Ammoniumkations bestimmt. Alle diese Salze lösen sich leicht in verschiedenen Ketonen, wie Aceton, Acetylaceton, und in Pyridin [1–3].

Resultate und Diskussion. Wir haben beobachtet, daß die obenerwähnten Komplexsäuren außer den N-Basen auch mit tertiären Phosphinen schwerlösliche Salze bilden können. In dieser Arbeit haben wir 27 neue Ammonium- und Phosphoniumsalze des Typs AH₂[Cr(NCS)₄(Amin)₂] (A = aliphatische und heterocyclische Amine und tertiäre Phosphine) dargestellt und spektroskopisch charakterisiert. Die thermische Zersetzung einiger Salze von dieser Klasse wurde derivatographisch verfolgt.

Die Ammonium- und Phosphoniumsalze wurden aus salzauren, bzw. schwefelsauren Lösungen ausgeschieden. Als Fällungsmittel wurden NH₄[Cr(NCS)₄(NH₃)₂], NH₄[Cr(NCS)₄(Anilin)₂], und p-Toluidin, H[Cr(NCS)₄(p-Toluidin)₂] verwendet. Die letztgenannten Reagenzien entstehen durch eine Substitutionsreaktion aus K₃[Cr(NCS)₆] und den entsprechenden Aminen im Schmelzzustande, also ohne Verwendung von Lösungsmitteln [4]. Als Amine und Phosphine wurden einige Imidazol-Derivate, Alkyl-pheayl- und Triphenylphosphin, usw. in salzaurem, bzw. schwefelsaurem Medium benutzt.

Die neuen Ammonium- und Phosphoniumsalze sind in den Tabellen 1 und 2 charakterisiert.

Die elektronischen Spektren des Et₂Ph · P · H [Cr(NCS)₄(NH₃)₂] und Et₂Ph · P · H [Cr(NCS)₄(Anilin)₂] im Vergleich mit denjenigen des NH₄[Cr(NCS)₄(NH₃)₂] und NH₄[Cr(NCS)₄(Anilin)₂] zeigen, dass die Natur des äusseren Ka-

* Universität Cluj-Napoca, Fakultät für Chemie, 3100 Cluj-Napoca Romania

Tabelle 1

Neue Tetrathiocyanato-diamin-chromate einiger organischen Amine

No.	Formel	Mol. Gew. ber.	Charakteristik	Analyse	
				Ber.	Gef.
1.	Imidazol. HA	387	hellrote glänzende Platten	Cr 13,43	13,52
				S 33,97	32,84
2.	Imidazol. HB	539,4	rotviolette, schimmernde Plättchen	Cr 9,64	9,45
				S 23,74	23,79
3.	Imidazol. HC	567,7	dunkelrote dünne Plättchen	Cr 9,16	9,08
				S 22,60	22,45
4.	Benzimidazol. HA	437,6	schimmernde hellrote Platten	Cr 11,88	12,13
				S 29,32	28,95
5.	Benzimidazol. HB	589,7	rotviolette Platten	Cr 3,81	8,60
				S 21,76	21,54
6.	Benzimidazol. HC	617,7	dunkelrote unregelmässige Krist.	Cr 8,42	8,33
				S 20,77	21,11
7.	2-Methyl-benzimidazol. HA	451,6	glänzende hellrote Platten	Cr 11,51	11,66
				S 28,76	28,90
8.	2-Methyl-benzimidazol. HB	603,8	rotviolette Nadeln	Cr 8,61	8,50
				S 21,24	21,06
9.	2-Methyl-bezimidazol. HC	631,8	dunkelrote unregelmässige Krist.	Cr 8,23	8,09
				S 20,31	20,66
10.	2-Amino-thiazol. HA	419,9	rotviolette mikrokrist. Masse	Cr 12,33	12,24
				S 33,18	38,86
11.	2-Amino-thiazol. HB	572,1	rotviolette glänzende Plättchen	Cr 9,69	8,97
				S 21,2	27,83
12.	2-Amino-thiazol. HC	600,2	dunkelrote unregelmässige Krist.	Cr 8,66	8,50
				S 20,72	26,96
13.	Tri-isobutylamin. HA	504	rotviolette mikrokrist. Masse	Cr 10,31	10,37
				S 15,39	25,18
14.	Tri-isobutylamin. HB	656	rotviolette mikrokrist. Masse	Cr 7,92	7,75
				S 19,51	19,69
15.	Tri-isobutylamin. HC	684,1	dunkelrote mikrokrist. Masse	Cr 7,60	7,76
				S 19,51	19,69

Tabelle 2

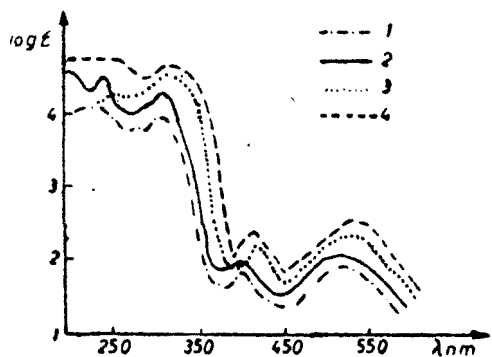
Neue Tetrathiocyanato-diamin-chromate einiger tertären Phosphine

No.	Formel	Mol. Gew. ber.	Charakteristik	Analyse	
				Ber.	Gef.
1.	Et ₃ Ph. P. HA	485,6	rotviolette mikrokrist. Masse	Cr 10,71	10,66
				S 26,42	26,73
2.	Et ₃ Ph.P. HB	637,8	rotviolette Plättchen	Cr 8,15	7,98
				S 20,12	20,33
3.	Et ₂ Ph.P. HC	665,8	dunkelrote mikrokrist. Masse	Cr 7,81	7,88
				S 19,27	19,02
4.	Et ₂ (p-Tolyl)P. HA	499,6	rotviolette, kleine Nadeln	Cr 10,41	10,55
				S 25,68	25,33
5.	Et ₂ (p-Tolyl)P. HB	651,8	rotviolette, unregelmässige Plättchen	Cr 7,98	7,69
				S 19,68	19,81
6.	Et ₂ (p-Tolyl)P. HC	679,9	dunkelrote, kleine unregel- mäss. Krist.	Cr 7,64	7,81
				S 18,87	19,10

Tabelle 2 (continued)

No.	Formel	Mol. Gew. ber.	Charakteristik	Analyse	
				Ber.	Gef.
7.	Ph ₂ Et.P. HA	533,7	rotviolette, kleine Kristalle	Cr 9,74	9,90
				S 24,04	24,23
8.	Ph ₂ Et.P. HB	685,9	rotviolette unregelmäss. Kristalle	Cr 7,57	7,29
				S 18,70	18,87
9.	Ph ₂ Et.P. HC	713,9	dunkelrot mikrokrist. Masse	Cr 7,28	7,33
				S 17,97	18,24
10.	Ph ₃ P. HA	581,7	rotviolette mikrokrist. Masse	Cr 8,94	8,88
				S 22,05	22,15
11.	Ph ₃ P. HB	733,9	rotviolette mikrokrist. Masse	Cr 7,08	7,33
				S 17,48	17,33
12.	Ph ₃ P. HC	761,9	dunkelrote mikrokrist. Masse	Cr 6,82	6,99
				S 16,84	16,69

„A“ = $[\text{Cr}(\text{NCS})_4(\text{NH}_3)_2]^-$; „B“ = $[\text{Cr}(\text{NCS})_4(\text{Anilin})_2]^-$; „C“ = $[\text{Cr}(\text{NCS})_4(\text{p-Toluidin})_2]^-$;
 $\text{Et}_2\text{Ph.P}$ = Diethylphenyl-phosphin; $\text{Et}_2(\text{p-Tolyl})\text{P}$ = Diethyl-p-Tolyl-phosphin; $\text{Ph}_2\text{Et.P}$ = Diphenyl-ethyl-phosphin; Ph_3P = Triphenylphosphin.



A b b. 1. Elektronische Spektren von:
 1. $\text{NH}_4[\text{Cr}(\text{NCS})_4(\text{NH}_3)_2]$; 2. $\text{Et}_2\text{Ph.P. H}[\text{Cr}(\text{NCS})_4(\text{NH}_3)_2]$; 3. $\text{NH}_4[\text{Cr}(\text{NCS})_4(\text{Anilin})_2]$;
 4. $\text{Et}_2\text{Ph. H.}[\text{Cr}(\text{NCS})_4(\text{Anilin})_2]$

Das Auftreten von einer einzigen Bande in diesem Spektralgebiet ist ein Beweis, dass keine Cr-NCS-Kation Brücken im festen Zustand vorhanden sind. Eine solche Erscheinung wurde bei den Ag, Hg und Pb-Tetrathiocyanato-diamin-chromiaten beschrieben [7].

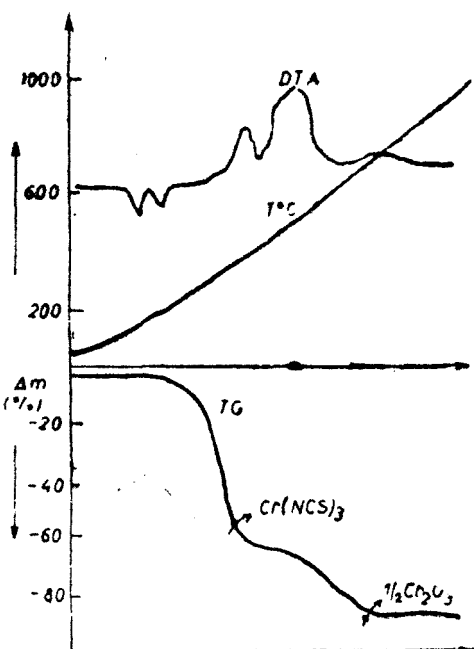
Die thermische Zersetzung einiger Phosphoniumsalze wurde derivatographisch untersucht. Die Derivatogramme von vier Komplexsalzen sind in Abb. 2-5 wiedergegeben.

Wie aus den Thermogrammen ersichtlich ist, kann nach der ersten Zersetzungsstufe ein nicht wohl definiertes Gewichtsverlustanhalt beobachtet werden. Dieses entspricht der Bildung des labilen $\text{Cr}(\text{NCS})_3$ Abbauzwischenproduktes.

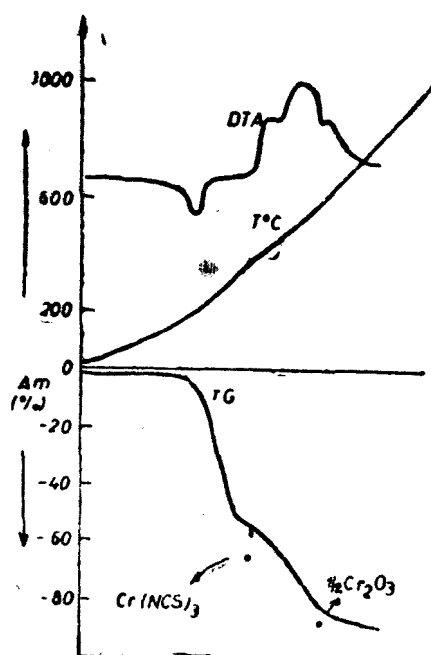
tions nur einen geringen Einfluss auf das Spektrum der Komplexanionen ausübt. (Siehe Abb. 1.)

Die Lage der d-d Übergangsbanden bei 525 und 395 nm (mit NH_3), bzw. bei 540 und 410 nm (mit Anilin) bleibt unverändert. Nur die Absorptionsintensitäten zeigen eine kleine Veränderung. [5].

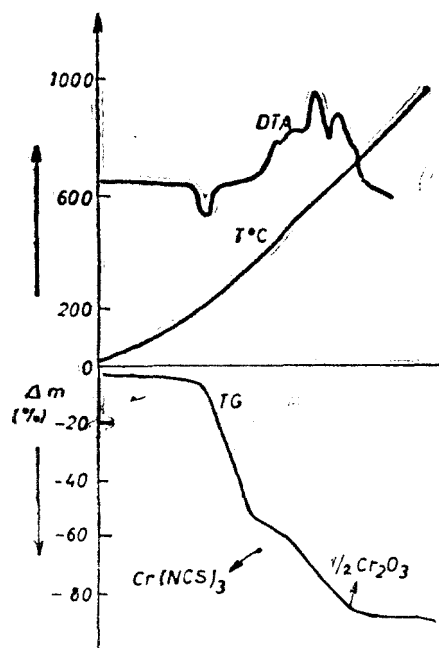
Die $\nu_{\text{C≡N}}$ Valenzschwingungsfrequenzen in den UR-Spektren des $\text{Et}_2\text{Ph.P. H}[\text{Cr}(\text{NCS})_4(\text{NH}_3)_2]$ und $\text{Et}_2\text{Ph.P. H}[\text{Cr}(\text{NCS})_4(\text{Anilin})_2]$ liegen bei 2060-2080 cm^{-1} (starke breite Bande), wie im Falle der Ammoniumsalze, und sind ein Beweis für eine Cr-NCS-Bindung durch das Stickstoffatom (Isothiocyanato-Chrom(III)-Komplex) [6].



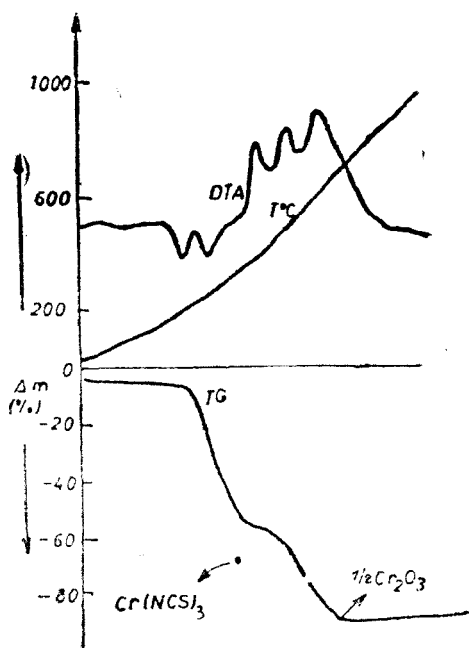
A b b. 2. Derivatogramm von $\text{Et}_2\text{Ph. P. H.}$
 $[\text{Cr}(\text{NCS})_4(\text{NH}_3)_2]$



A b b. 3. Derivatogramm von $\text{Et}_2\text{Ph. P. H.}$
 $[\text{Cr}(\text{NCS})_4(\text{Anilin})_2]$



A b b. 4. Derivatogramm von $\text{Et}_2\text{Ph. P. H.}$
 $[\text{Cr}(\text{NCS})_4(\text{p-Toluidin})_2]$



A b b. 5. Derivatogramm von $\text{Et}_2(\text{p-Tolyl})\text{P. H.}$
 $[\text{Cr}(\text{NCS})_4(\text{Anilin})_2]$

Das Gewicht der Proben an dem Knickpunkt zeigt eine stöchiometrische Menge von $\text{Cr}(\text{NCS})_3$, wenn das Anion $[\text{Cr}(\text{NCS})_4(\text{NH}_3)_2]^-$ ist. [8].

Im Falle der AH. $[\text{Cr}(\text{NCS})_4(\text{Anilin})_2]$ — und AH. $[\text{Cr}(\text{NCS})_4(\text{p-Toluidin})_2]$ — Salze zeigen diese Knickpunkte einen kleineren Gewichtsverlust (im Vergleich mit den stöchiometrischen Mengen) und entsprechen wahrscheinlich zu den $\text{Cr}(\text{NCS})_3 \cdot \text{Anilin}$, bzw. $\text{Cr}(\text{NCS})_3 \cdot \text{p-Toluidin}$ Zwischenprodukten.

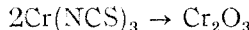
Im Laufe der ersten Zersetzungsetappe:

AH. $[\text{Cr}(\text{NCS})_4(\text{Amin})_2] \rightarrow \text{Cr}(\text{NCS})_3$ kann man zwei endothermische Spalten auf den DTA — Kurven bei $200-220^\circ$, bzw. $290-310^\circ\text{C}$ beobachten.

Die Zersetzung des $\text{Cr}(\text{NCS})_3$ im Luftatmosphäre ist kein einheitlicher Prozess und besteht aus der Überlagerung von mehreren exothermen Vorgängen (zwei, oder drei exotherme Spalten auf den DTA-Kurven bei $380-400$ und $500-520^\circ\text{C}$) [9].

Man kann annehmen, dass diese Prozesse Oxydationsreaktionen mit der Teilnahme des atmosphärischen Sauerstoffs sind.

Das Endprodukt der Pyrolyse ist das grüne Cr_2O_3 , und das Gewicht der Proben erreicht den entsprechenden stöchiometrischen Wert bei annähernd 750°C .



Auf den Thermogrammen zwischen $600-700^\circ\text{C}$ kanu man keine Knickpunkte, welche nach Krausz und Kovács [10] im Falle des $\text{NH}_4[\text{Cr}(\text{NCS})_4(\text{NH}_3)_2]$ dem CrO_3 Abbauzwischenprodukte entsprechen würden, bemerken.

Experimenteller Teil. $\text{NH}_4[\text{Cr}(\text{NCS})_4(\text{Anilin})_2]$ und p-Toluidin . H. $[\text{Cr}(\text{NCS})_4(\text{p-Toluidin})_2]$ wurden durch eine Substitutionsreaktion aus entwässertem $\text{K}_3[\text{Cr}(\text{NCS})_6]$ und Anilin, bzw. p-Toluidin in Schmelzzustand, ohne Verwendung von Lösungsmitteln erhalten. [7]. Das Rohprodukt wurde in Methanol gelöst und aus 15% -iger, überschüssiger NH_4Cl -Lösung umgefällt.

AH. $[\text{Cr}(\text{NCS})_4(\text{Amin})_2] \cdot 15$ mMol Amin, bzw. Phosphin wurden mit 25 ml 10% -iger Salzsäure (Schwefelsäure) behandelt und 20–30 Minuten auf dem Wasserbade erwärmt. Nach Abkühlen wurde das Chlorhydrat (Sulphat) mit 10 mMol Tetrathiocyanato-diaminchromiat in 20–30 ml verd. Methanol versetzt. Die ausgeschiedenen Ammonium- und Phosphoniumsalze wurden nach 15–30 Min. Stehenlassen abfiltriert, mit Wasser gewaschen und an der Luft getrocknet. *Chemische Analysen*. Der Chromgehalt der Proben wurde gravimetrisch als Cr_2O_3 , bzw. jodometrisch nach Oxydation zu CrO_4^{2-} bestimmt. Der Schwefelgehalt wurde gravimetrisch als BaSO_4 ermittelt. Die *derivatographischen Messungen* wurden mit einem Derivatographi MOM (Budapest) durchgeführt. Probe menge: 100 ± 1 mg. Heizungsgeschwindigkeit $20^\circ/\text{Min}$.

Die *elektronischen Spektren* wurden mit einem Specord Spectrophotometer (Carl Zeiss Jena) in Methanol aufgenommen.

LITERATUR

1. R. Coupechoux, *J. Pharm. Chim.*, **30**, 113 (1939).
2. P. Duquennois, M. Fallér, *Bull. Soc. Chim. France* (**5**), **1**, 998 (1939).
3. M. Bergmann, *J. Biol. Chem.*, **110**, 476 (1935).
4. Cs. Várhelyi, I. Gănescu, *Monatsh.*, **98**, 472 (1967).
5. G. Boda, Cs. Várhelyi, *Stud. Univ. Babes-Bolyai, Chem.*, **12**, (2), 81 (1967).
6. M. Chamberlain, J. C. Bailar, *J. Amer. Chem. Soc.*, **81**, 6412 (1959).
7. Cs. Várhelyi, I. Gănescu, *Stud. Univ. Babes-Bolyai, Chem.*, **30**, 67 (1985).
8. G. Boda, Cs. Várhelyi, Á. Mostis, *Stud. Univ. Babes-Bolyai, Chem.*, **10**, (2), 63 (1965).
9. J. Zsakó, G. Liptay, Cs. Várhelyi, E. Brandt-Petrić, *J. Thermal Anal.*, **23**, 123 (1982).
10. P. J. Krausz, J. Kovács, *Ann. Univ. Sci. Budapestinensis, de R. Eötvös nom. Sect. Chim.*, **4**, 37 (1962).

KATALYTISCHER UMSATZ DES METHANOLS MIT WASSERDAMPF

I. Stöchiometrie, Gleichgewicht und Wärmebilanz des Vorganges

I. SIMINICEANU, I. TODEA, M. STANCA* und A. POP*

Eingegangen am 29. November 1986

Catalytic Conversion of Methanol with Water Vapours. I. Stoichiometry Equilibrium and Thermic Balance of the Process. The present paper deals with some aspects concerning stoichiometry and balance in the process of methanol conversion with water vapours, in order to get hydrogen. It is demonstrated that the mathematical description of this process may be performed by taking into account two stoichiometrical equations. The equations are set down and on their grounds, the mathematic staff balance model was elaborated. The model was also elaborated by solving it, and its solution emphasize the way the main parameters act upon the balance of the process. The mathematical thermic balance model was elaborated, too. It is demonstrated that the specific heat consumption is strongly influenced by the conversion, the water excess and by the existing temperature of the reaction products.

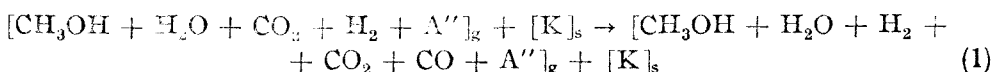
Wasserstoff gehört zu den Stoffen, die in der chemischen Industrie in grossen Mengen zu den verschiedensten Zwecken verwendet werden. Als Energiequelle und idealer Brennstoff, und in riesen Mengen vorkommend, ist Wasserstoff eine der energetischen Lösungen der Zukunft. [1-3]

Zur Zeit sind die Kohlenwasserstoffe die Hauptquelle für Wasserstoff weil die Technologien zur Verarbeitung und Verwertung an diese Rohstoffe gebunden sind. Bei der Wasserstoffherstellung können aber auch alternative Energiequellen wie Ammoniak und Methanol Bedeutung finden.

Die Wasserstoffherstellung ist von einer zusätzlichen Energiequelle abhängig, egal welcher Rohstoff verwendet wird und deshalb muss sie in andere Technologie integriert werden, um deren Effizienz zu erhöhen. Eine technologische Lösung wäre die Kupplung der Wasserstoffproduktion aus Methanol mit einer Atomzentrale (Figur 1). Methanol wird vorgezogen weil er leichter zu transportieren ist als die Naturgase. Deshalb gibt es mehrere Forschungsarbeiten über die Reaktion zwischen Methanol und Wasser [4-8]. In der Fachliteratur wurde aber keine mathematische Beschreibung des Prozesses gefunden, ohne die die Optimisierung und Integrierung der Anlage in eine Atomzentrale zwecks Konsum der überschüssigen Energie bei geringem Verbrauch nicht möglich ist.

In dieser Arbeit verfolgen wir die Stöchiometrie das Gleichgewicht und Masse sowie Wärmebilanz im Gleichgewichtszustand. Es wird versucht diese genannten Probleme mathematisch zu beschreiben.

1. Struktur und Stöchiometrie des Vorganges. Der katalytische Umsatz von Methanol auf Wasserdampf gehört zu den Kontaktverfahren [9] und wird durch die charakteristische Gleichung (1) beschrieben.



* Universitatea Cluj-Napoca, Fakultät für Chemie, 3400 Cluj-Napoca, Romania

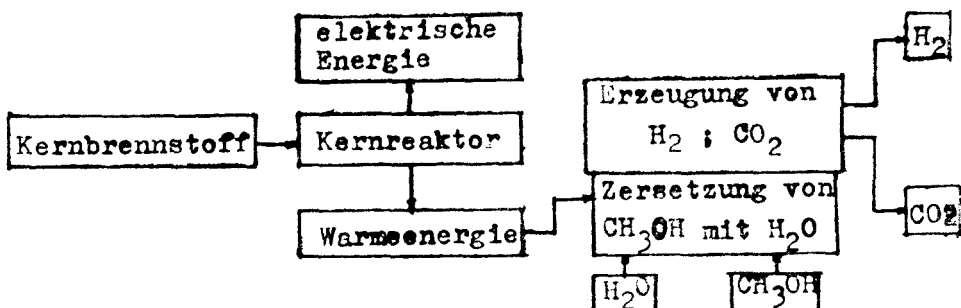
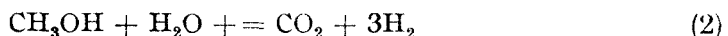


Abb. 1. Integrieranlageneschema der Wasserstoff production in einem Kernkraftwerk.

Die stöchiometrischen Gleichungen sind folgende: (2—4)



Die Thermodynamik dieser Reaktionen zeigt uns, dass unter den Bedingungen eines industriellen Reaktors alle drei Reaktionen möglich sind. Beim Aufstellen der algebraischen Bilanzgleichungen müssen nicht alle Gleichungen verwertet werden sondern nur die unabhängigen [9—11].

Um diese herauszufinden verwendet man die Methode der Orthogonalisierung [12] wo die Anzahl der unabhängigen Gleichungen nach der Formel (5) berechnet wird.

$$L = N - C \quad (5)$$

C ist der Rang der Matrix der Elemente. Die Matrix A die den Molekülarten entspricht die in der Reaktionsmasse auftrete wird in der Beziehung (6) wiedergegeben:

Tabelle 1
Reaktionsmatrix der möglichen Reaktionen

Matr.-reakt-kompon.	A _{R2}	A _{R3}	A _{R4}
CH ₃ OH	1	1	0
H ₂	3	2	1
CO	0	1	1
H ₂ O	1	0	1
CO ₂	1	0	1

$$\begin{array}{ccccc}
 & & C & H & O \\
 \text{CH}_3\text{OH} & | & 1 & 4 & 1 \\
 \text{H}_2 & | & 0 & 2 & 0 \\
 \text{CO} & | & 1 & 0 & 1 \\
 \text{H}_2\text{O} & | & 0 & 2 & 1 \\
 \text{CO}_2 & | & 1 & 0 & 2
 \end{array} = A_a \quad (6)$$

Diese Matrix hat den Rang 3 ($C=3$). Unter Verwendung der Formel (5) erhalten wir $L = 2$.

Aus Tabelle 1 folgt dass die Unabhängigkeitsbedingung (6) erfüllt ist, und zwar für die Reaktionen (3) und (4).

$$A_{RI}^T \cdot A_a = 0 \quad i = 2, 3, 4$$

Verwendet man die Definitionen der Umsätze der Reaktanten (8—9) in den unabhängigen Reaktionsgleichungen und die Gleichungen die die kon-

unterten Bedingungen ausdrücken (10) erhält man die primären Bilanzgleichungen, wiedergegeben in Tabelle 2 und 3, ausgedrückt in Mol und Molenbrüchen.

$$\eta_1 = \eta_M = \frac{n_M^{03} - n_M^3}{n_M^{03}} = \frac{n_{CO}^3 - n_{CO}^{03}}{n_M^{03}} = \frac{n_{H_2}^3 - n_{H_2}^{03}}{2n_M^{03}} \quad (8)$$

$$\eta_2 = \eta_{CO} = \frac{n_{CO}^{04} - n_{CO}^4}{n_{CO}^{04}} = \frac{n_{H_2O}^{04} - n_{H_2O}^4}{n_{CO}^{04}} = \frac{n_{CO_2}^4 - n_{CO_2}^{04}}{n_{CO}^{04}} = \frac{n_{H_2}^4 - n_{H_2}^{04}}{n_{CO}^{04}} \quad (9)$$

$$n_M^{03} = n_M^0 \quad n_{H_2}^{03} = n_{H_2}^0 \quad n_{CO_2}^{04} = n_{CO_2}^0$$

$$n_M^3 = n_M \quad n_{H_2}^3 = n_{H_2}^{04} \quad n_{CO_2}^4 = n_{CO_2}^0$$

$$n_{CO}^{03} = n_{CO}^0 = 0 \quad (10)$$

$$n_{CO}^3 = n_{CO}^{04} \quad n_{H_2}^4 = n_{H_2}$$

$$n_{CO}^4 = n_{CO} \quad n_{H_2O}^{04} = n_{H_2O}^0$$

$$n_{H_2}^3 = n_{H_2}^{04} \quad n_{H_2O}^4 = n_{H_2O}$$

Tabelle 2

Algebraische Massebilanzgleichungen primärer Form, in Mol.

KOMPON.	BILANZGLEICHUNGEN	
	Form. a	Form. b
CH ₃ OH	$n_M = n_M^0 = (1 - \alpha)$	$n_M = n_M^0 (1 - \alpha)$
CO	$n_{CO} = n_M^0 = (\alpha - \beta)$	$n_{CO} = n_M^0 (1 - \beta)$
CO ₂	$n_{CO_2} = n_{CO_2}^0 + n_M^0 \cdot \beta$	$n_{CO_2} = n_M^0 (\dot{\chi}_{CO_2}^0 + \beta)$
H ₂	$n_{H_2} = n_{H_2}^0 + 2n_M^0 \cdot \alpha + n_M^0 \cdot \beta$	$n_{H_2} = n_M^0 (\dot{\chi}_{H_2}^0 + 2\alpha + \beta)$
H ₂ O	$n_{H_2O} = n_{H_2O}^0 - n_M^0 \cdot \beta$	$n_{H_2O} = n_M^0 (\dot{\chi}_{H_2O}^0 - \beta)$
A"	$n_{A''} = n_{A''}^0$	$n_{A''} = n_M^0 \cdot \dot{\chi}_{A''}^0$
	$n_T = n_T^0 + 2n_M^0 \cdot \alpha$	$n_T = n_M^0 (A + 2\alpha)$

Setzt man die Gleichungen (11) in die primären Bilanzgleichungen ein, erhält man die sekundären Bilanzgleichungen die in Tabelle 4 aufgezeichnet sind.

$$n_M^0 \cdot \alpha = n_M^0 - n_M$$

$$n_M^0 \cdot \beta = n_{CO_2} - n_{CO_2}^0 \quad (11)$$

Tabelle 3

Algebraische Massebilanzgleichungen primärer Form, in Molenbrüche

KOMPON	BILANZGLEICHUNGEN	
	Form. a	Form. b
CH_3OH	$X_M = \frac{x_M(1-\zeta)}{1 + 2x_M^\circ \cdot \zeta}$	$x_M = \frac{1-\zeta}{A+2\zeta}$
CO	$x_{\text{CO}} = \frac{x_{\text{CO}}^\circ(\zeta-\beta)}{1 + 2x_M^\circ \cdot \zeta}$	$x_{\text{CO}} = \frac{\zeta-\beta}{A+2\zeta}$
CO_2	$x_{\text{CO}_2}^\circ + x_M^\circ \cdot \beta$ $1 + 2x_M^\circ \cdot \zeta$	$x_{\text{CO}_2}^\circ + \beta$ $A+2\zeta$
H_2	$x_{\text{H}_2} = \frac{x_{\text{H}_2}^\circ + x_M^\circ(2\zeta+\beta)}{1 + 2x_M^\circ \cdot \zeta}$	$x_{\text{H}_2} = \frac{x_{\text{H}_2}^\circ + 2\zeta + \beta}{A+2\zeta}$
H_2O	$x_{\text{H}_2\text{O}} = \frac{x_{\text{H}_2\text{O}}^\circ - x_M^\circ \cdot \beta}{1 + 2x_M^\circ \cdot \zeta}$	$x_{\text{H}_2\text{O}} = \frac{x_{\text{H}_2\text{O}}^\circ - \beta}{A+2\zeta}$
A	$x_A^\alpha = x_A^\circ$	$x_A^\alpha = \frac{x_A^\circ}{A+2\zeta}$
	$\sum x_i = 1$	$\sum x_i = 1$

Sie haben den Vorteil dass sie als Unbekannte nur zwei Augangskonzentrationen enthalten und zwar die von Methanol und Kohlendioxyd, die beim Reaktoraugang während des Experiments gemessen werden müssen.

Die Bilanzgleichungen die in Tabelle 3 und 4 aufgezeichnet sind, verwendet man zum Aufstellen der theoretischen und reellen Masse und Wärmebilanzen im ganzen Reaktor.

2. Mathematisches Modell des Gleichgewichtsprozesses. Die Gleichgewichtskonstanten der unabhängigen Reaktionsgleichungen (3,4) werden durch die Beziehungen (12) definiert:

$$K_{f1} = \frac{f_{\text{CO}} \cdot f_{\text{H}_2}^2}{f_M} \quad K_{f2} = \frac{f_{\text{CO}_2} \cdot f_{\text{H}_2}}{f_{\text{CO}} \cdot f_{\text{H}_2\text{O}}} \quad (12)$$

Beachtet man die Gleichungen von Lewis-Randal und die algebraischen Bilanzgleichungen erhält man aus den Gleichungen (12) folgende Formen (13, 14).

$$K_{p1} = \frac{K_{f1}}{K_{\gamma_1}} = \frac{(\alpha-\beta)(x_{\text{H}_2}^\circ + 2\alpha + \beta)^2 \cdot P}{(1-\alpha)(2\alpha+A)^2} \quad (13)$$

$$K_{p2} = \frac{K_{f2}}{K_{\gamma_2}} = \frac{(x_{\text{CO}_2}^\circ + \beta)(x_{\text{H}_2}^\circ + 2\alpha + \beta)}{(\alpha-\beta)(x_{\text{H}_2\text{O}}^\circ - \beta)} \quad (14)$$

Tabelle 4

Algebraische Massebilanzgleichungen secundärer Form, in Mol. und Molenbrüche

KOMPON.	BILANZGLEICHUNGEN	
CH ₃ OH	$n_M = \left[\frac{1+2X_M^0}{1+2X_M} \cdot X_M \right] \cdot n_T^0$	$X_M = X_M$
CO	$n_{CO} = \left[X_M + X_{CO_2}^0 - \frac{1+2X_M^0}{1+2X_M} (X_M + X_{CO_2}) \right] n_T^0$	$X_{CO} = \left[\frac{1+2X_M^0}{1+2X_M} (X_M + X_{CO_2}^0) - X_M - X_{CO_2} \right]$
CO ₂	$n_{CO_2} = \left[\frac{1+2X_M^0}{1+2X_M} \cdot X_{CO_2} \right] \cdot n_T^0$	$X_{CO_2} = X_{CO_2}$
H ₂	$n_{H_2} = \left[X_{H_2}^0 + 2X_M^0 - X_{CO_2}^0 + \frac{1+2X_M^0}{1+2X_M} (X_{CO_2} - X_M) \right] \cdot n_T^0$	$X_{H_2} = \left[\frac{1+2X_M^0}{1+2X_M} (X_{H_2}^0 + 2X_M^0 - X_{CO_2}^0) + X_{CO_2} - 2X_M \right]$
H ₂ O	$n_{H_2O} = \left[X_{H_2O}^0 + X_{CO_2}^0 - \frac{1+2X_M^0}{1+2X_M} \cdot X_{CO_2} \right] n_T^0$	$X_{H_2O} = \left[\frac{1+2X_M^0}{1+2X_M} (X_{CO_2}^0 + X_{H_2}^0) - X_{CO_2} \right]$
A''	$n_{A''} = n_T^0 \cdot X_{A''}^0$	$X_{A''} = \left[\frac{1+2X_M^0}{1+2X_M} \right] \cdot X_{A''}^0$
TOTAL	$n_T = \left[\frac{1+2X_M^0}{1+2X_M} \right] \cdot n_T^0$	$\sum X_i = 1$

Die Gleichungen (13,14) drücken die Abhängigkeit der Gleichgewichtssumssätze η_1 und η_2 von dem Druck P , Temperatur T und der Anfangszusammensetzung der Reaktionsmasse $X_{CO_2}^0$, $X_{H_2}^0$, $X_{H_2O}^0$, $X_{A''}^0$ aus.

Dieses Gleichungssystem, ergänzt von den Gleichungen der Konstanten K_{p1} und K_{p2} bilden das mathematische Modell der Gleichgewichtsreaktion.

Die Abhängigkeit der Gleichgewichtskonstanten K_{p1} und K_{p2} wurde mit Hilfe der isobaren von van't Hoff [13] berechnet.

$$\frac{d(\ln K_p)}{dT} = \frac{\Delta H}{RT^2} \quad (15)$$

Die thermodynamischen Daten, die für die Bestimmung der Abhängigkeit der Gleichgewichtskonstanten K_{p1} und K_{p2} von der Temperatur verwendet wurden, wurden nach einer kritischen Analyse der Daten der Literatur aus-

gewählt [14–17]. Die Lösung der Gleichung (15) für die Reaktionen (3) und (4) führte zu folgenden Beziehungen (16, 17).

$$\ln K_{p1} = \frac{-9330,441}{T} + 7,6248 \ln T - 5,683 \cdot 10^{-3}T + 5,02 \cdot 10^{-7}T^2 - 21,054 \quad (16)$$

$$\ln K_{p2} = \frac{5072,4}{T} + 0,29 \ln T + 48,012 \cdot 10^{-4} T - 1,17 \cdot 10^{-7}T^2 - 7,53 \quad (17)$$

Die Aktivitätskoeffizienten γ_i der Komponenten des Systems wurde mit der Zustandsgleichung von Berthelot [13] gültig für gemässigte Drucke ausgerechnet.

$$\ln \gamma_i = \frac{9}{128} \frac{P \cdot T_c}{P_c \cdot T} \left(1 - 6 \frac{T_c^2}{T^2} \right) \quad (18)$$

3. Analyse des Vorganges aufgrund der mathematischen Beschreibung des Gleichgewichtes. Dies algebraische Gleichungssystem (13–14) ergänzt mit den Gleichungen von K_{p1} und K_{p2} wurde numerisch nach der Newton-Raphson Methode [18–19] mit Hilfe des Rechners Felix C-256 ausgerechnet.

Die unabhängigen Variablen nehmen Werte an die die Parameter des industriellen Reaktors einschliessen. Ein Teil der erhaltenen Werte für η_1 und η_2 sind in den Figuren 2–7 enthalten.

Diese Ergebnisse zeigen den bedeutenden Einfluss der Anfangszusammensetzung, vor allem des Molbruchs $x_{H_2O}^0$ auf den Umsatz während des Gleichgewichtes. Bei Werten $x_{H_2O}^0 > 1,4$ wird sein Einfluss so gross dass η_2 dieselbe Größenordnung wie η_1 annimmt, wen der Gesamtdruck im System eine Atmosphäre beträgt. Bei grösseren Drucken ist der Einfluss der Konzentration des Wasserdampfes noch grösser. Aus den Daten von Figur 2–7 folgt noch dass der Einfluss der Molenbrüche $x_{CO_2}^0$, x_H^0 und x_A^0 unbedeutend im Vergleich zu $x_{H_2O}^0$ ist, unabhängig von den Werten von Temperatur und Druck.

Im allgemeinen beeinflusst die Druckvergrösserung den Vorgang negativ weil die Reaktion (3) eine Volumenvergrösserung zur Folge hat, während die Reaktion (4) ohne Volumenänderung verläuft.

Grossen Einfluss auf das Gleichgewicht hat die Temperatur. Die Reaktion (3) ist endotherm und somit von hohen Temperaturen begünstigt während Reaktion (4) exotherm ist, also von hohen Temperaturen benachteiligt ist.

Die optimale Temperatur liegt zwischen 200–220°C in Funktion des Wasserüberschusses $x_{H_2O}^0$ (Figuren 2–3).

4. Mathematische Beschreibung des Wärmebilanzes. Der Umsatz von Methanol mit Wasserdampf ist, global gesehen endotherm. Es ist wichtig herauszuheben welches die wichtigsten Parameter sind und die Art und Weise wie diese den spezifischen Wärmeverbrauch des Vorganges beeinflussen.

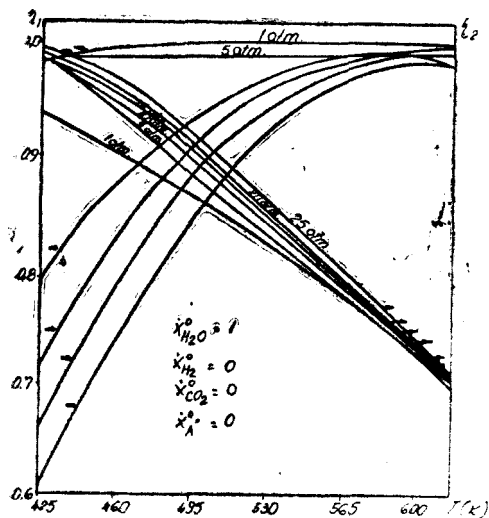


Abb. 2. Einfluss der Temperatur auf das Gleichgewicht.

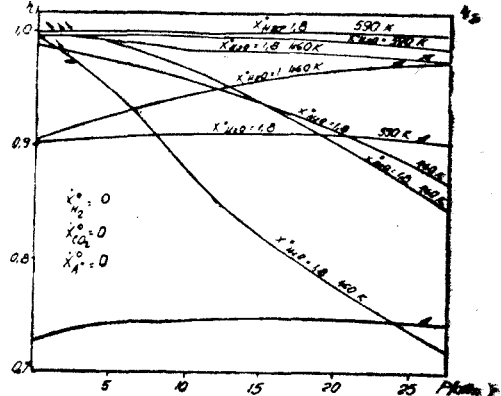


Abb. 3. Einfluss des Drucks auf das Gleichgewicht.

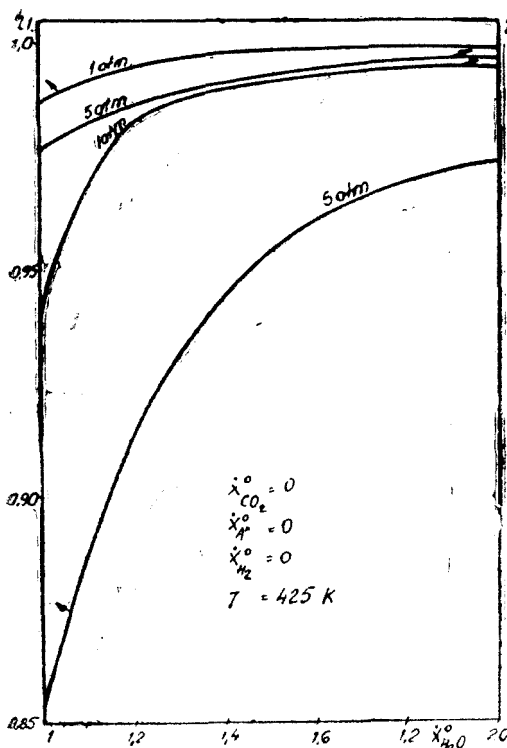


Abb. 4. Einfluss des Wasserdampfs auf das Gleichgewicht.

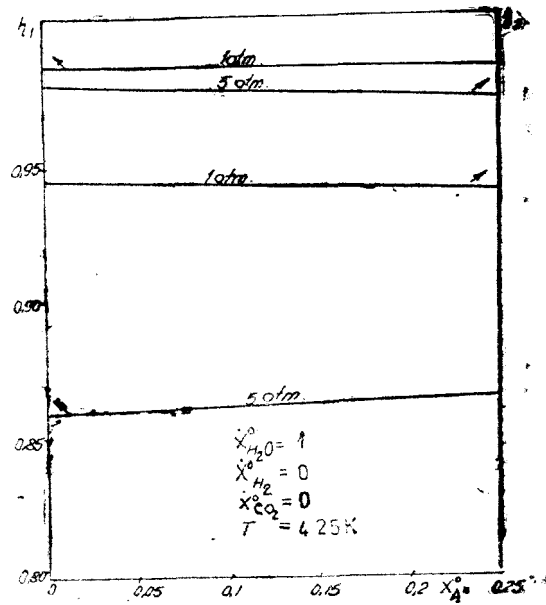


Abb. 5. Einfluss der Inerten auf das Gleichgewicht.

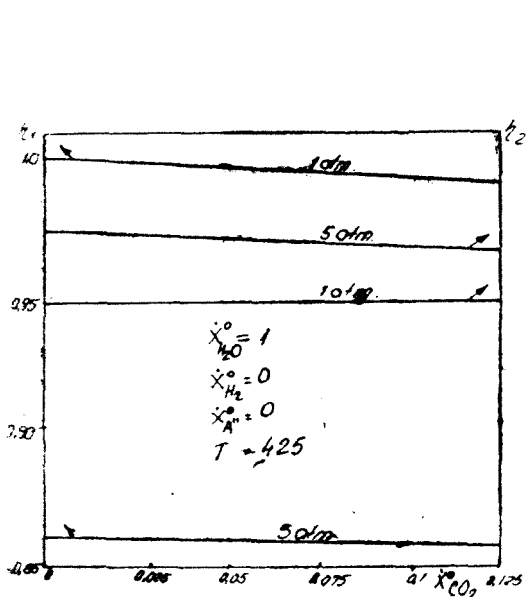


Abb. 6. Einfluss des Kohlendioxys auf das Gleichgewicht.

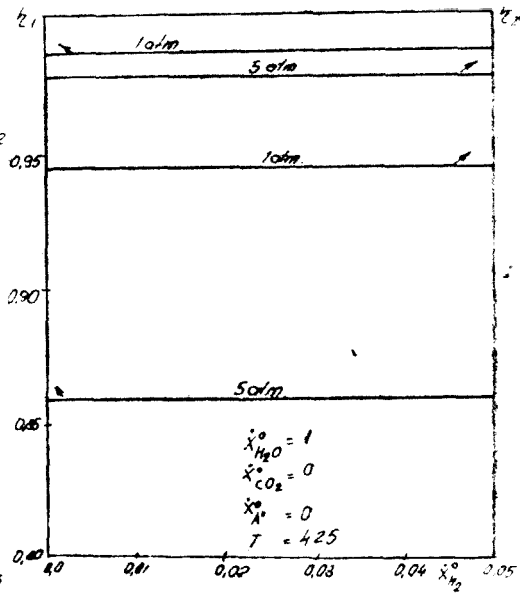


Abb. 7. Einfluss des Wasseroffs auf das Gleichgewicht.

Aus diesem Grund wird die Wärmebilanz aufgestellt (Gleichung 19).

$$\Delta H_0 + \Delta H_{\text{pr. tr.}}^{(R4)} + \Delta H_{\text{rec}} = \Delta H + \Delta H_{\text{pr. tr.}}^{(R, 3)} + \Delta H^{\text{ev}} + \Delta H_p \quad (19)$$

Die Angangs-und Endenthalpie wird durch die Beziehungen (20–21) erhalten und die Enthalpie der Umsätze durch die Gleichung (22).

$$\Delta H^\circ = \sum_{i=1}^n n_i^0 \int_{273}^{T_i} c p_i \cdot dT \quad (20)$$

$$\Delta H = - n_i^0 \sum_{i=1}^n \int_{273}^T c p_i \cdot dT \quad (21)$$

$$H \Delta H_{\text{pr. tr.}} = n_{AK}^\circ \cdot \gamma_{AK} (\pm \Delta R H_T^\circ) \quad (22)$$

Unter Verwendung der primären Bilanzgleichungen aus Tabelle 2 und der Gleichungen (20–22) erhält man mathematische Beschreibung der Wärmebilanz die durch die Gleichungen (23–27) ausgedrückt wird. Diese Beschreibung

zeigt die Abhängigkeit des spezifischen Wärmeverbrauchs von den wichtigsten Parametern die den Vorgang beeinflussen.

$$\frac{\Delta H_{\text{rec}}}{\eta_M^0} = A \cdot T_e + B \cdot T_e^2 + C \cdot T_e^3 + 20 \cdot 252,231 \cdot \alpha - 9784,09 \cdot \beta + D \quad (23)$$

$$A = 4,88 + 15,13 \cdot \alpha + 0,59 \cdot \beta + 6,89 \cdot \dot{x}_{H_2O}^0 + 6,88 \dot{x}_{H_2}^0 + 6,85 \cdot \dot{x}_{CO_2}^0 + 11,2 \dot{x}_{A''}^0 \quad (24)$$

$$B = 1,237 \cdot 10^{-2} - 1,1125 \cdot 10^{-2} \cdot \alpha + 1,6125 \cdot 10^{-3} \cdot \beta + 1,6415 \cdot$$

$$- 10^{-3} \dot{x}_{H_2O}^0 + 3,3 \cdot 10^{-5} \dot{x}_{H_2}^0 + 4,26 \cdot 10^{-3} \cdot \dot{x}_{CO_2}^0 \quad (25)$$

$$C = - 1,96 \cdot 10^{-6} - 1,926 \cdot 10^{-6} \alpha - 7,676 \cdot 10^{-7} \beta - 1,1433 \cdot 10^{-7} \dot{x}_{H_2O}^0 + \\ + 9,3 \cdot 10^{-8} \dot{x}_{H_2}^0 - 8,25 \cdot 10^{-7} \dot{x}_{CO_2}^0 - 1,15 \cdot 10^{-7} \dot{x}_{A''}^0 \quad (26)$$

$$D = 20,252,231 \alpha - 9784,1 \beta + 8482,65 \dot{x}_{H_2O}^0 - 3915,88 \dot{x}_{H_2}^0 - \\ - 4,54 \cdot 10^3 \dot{x}_{CO_2}^0 - 6,5 \cdot 10^3 \dot{x}_{A''}^0 \quad (17)$$

Die Analyse dieser Gleichungen führt zu den Darstellungen von Figur 8. Man kann beobachten, dass der Wärmeverbrauch mit der Temperatur der Reaktionsprodukte am Reaktorausgang sowie mit den Wachsen von $\dot{x}_{H_2O}^0$ steigt. Der Wärmeverbrauch steigt mit den Fallen des Wirkungsgrades weil dadurch die Menge der durch den Reaktor transportierten Stoffe steigt und somit das kalorische Inhalt unter Form von sensibler Wärme.

Zusammenfassung. 1. Durch Verwendung der Methode der Orthogonalisierung von Gramm Schmidt wurde bewiesen, dass für die mathematische Beschreibung des Vorganges nur zwei der möglichen Reaktionen notwendig sind.

2. Aufgrund der unabhängigen stöchiometrischen Gleichungen und der Definition der Umsätze wurden die primären und sekundären Bilanzgleichungen aufgestellt.

3. Es wurde die mathematische Beschreibung des Gleichgewichtsvorgangs aufgestellt. Sie besteht aus zwei nichtlinearen algebraischen Gleichungen, die mit den Gleichungen der Gleichgewichtskonstanten ergänzt sind.

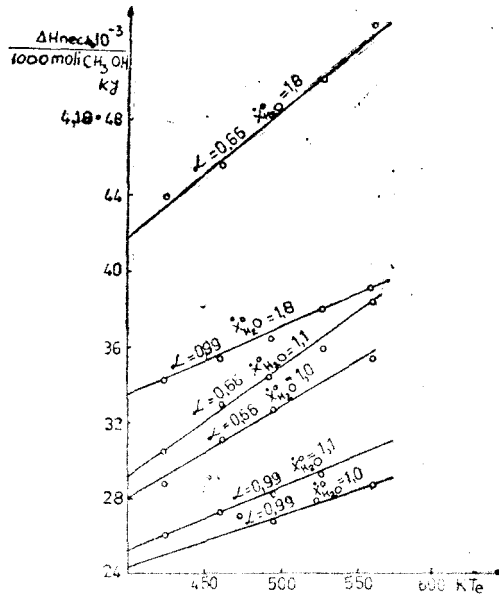


Abb. 8. Einfluss depr Ausgangstemperatur der Produkten auf dem Wärmeverbrauch.

4. Es wurde die mathematische Beschreibung der Wärmebilanz aufgestellt und dadurch die Faktoren hervorgehoben die den Wärmeverbrauch bestimmen.

Notierungen :

A''	— Inerte;
A	= Konstante definiert durch die Gleichung $A = 1 + \dot{x}_{\text{CO}_2}^0 + \dot{x}_{\text{H}_2\text{O}}^0 + \dot{x}_{\text{H}_2}^0 + \dot{x}_{\text{A}''}^0$;
A_{Ri}^T	= Überführungsmatrix der Reaktion „i“
A_a	= Elementenmatrix
f	= Fugazität, Index für Konstante K ;
$[K]_s$	= katalysator im Festbett;
K_{f1}, K_{f2}	= Gleichgewichtskonstanten (Gl. 12);
K_{p1}, K_{p2}	= Gleichgewichtskonstanten (Gl. 13, 14);
P	= Gesamtdruck;
x_i	= Molbruch des Komponenten i;
$\dot{x}_{\text{CO}_2}^0 \dots \dot{x}_{\text{A}''}^0$	= Anfangs-Molverhältnis der Komponenten im Vergleich zu Methanol;
C_p	= spezifische Wärme der Komponenten;
L	= unabhängige Stöchiometrische Gleichungen;
N	= Anzahl der aktiven molekularen Spezies aus der Reaktionsmasse;
T_i, T_e	= Temperatur der Reaktionsmasse beim Eintritt bzw. Austritt aus dem Reaktor;
ΔH_{port}	= Enthalpien der Vorgänge;
$\Delta_R H_T^0$	= warmeffekt bei Temperatur T;
$\Delta H_i^0; \Delta H$	= sensible Wärme der Reaktionsmasse;
$\eta_1; \eta_2$	= Umsatz in den Reaktionen (3) und (4);
$\alpha; \beta$	= Größen definiert durch die Beziehungen: $\alpha = \eta_1; \beta = \eta_2; \eta_1; \eta_2$;
γ_i	= Aktivitätskoeffizient;
σ	= überschrieben — für Anfangsgrößen;
i	= subskribiert für Komponente i;
AK subskribiert	= wertvoller Komponent;
M subskribiert	= Methanol.

LITERATUR

1. V. I. Nițu, „Bazele teoretice ale energeticii”, Ed. Acad. RSR, București, 1977, s. 198.
2. V. Părușanu, M. Cazobea, G. Muscă, „Economia hidrocarburilor”, Ed. Științifică și Encyclopedică, București, 1980.
3. M. Florescu, *Rev. Chim. (București)*, **31**(5) (1980).
4. H. Kobayashi, N. Takezawa, C. Minochi, *J. Catal.*, **69**(2), 487 (1981). *Chem. Abstr.*, 15731 p.
5. H. Kobayashi, N. Takezawa, C. Minochi, *Hokkaido Daigaku Kogakubu Kenkyū Hokoku*, **102**, 13, (1981). *Chem. Abstr.* **95**: 6411t (1981).
6. *Pat. Japan* 8126, 992, 16 Mart. 1981. *Chem. Abstr.* **95**, 65236n (1981).
7. *Pat. Japan* 8148, 252, 01 May 1981; *Chem. Abstr.* **95**, 31124j (1981).
8. C. Calistru, C. Leonte, „Tehnologia substanțelor anorganice”, Ed. didactică și pedagogică, București, 1972, s. 58.
9. C. Calistru, I. Siminiceanu, C. Hagiu, C. Petrilă, *Rev. Chim. (București)*, **24**(11), 880 (1973).
10. I. Siminiceanu, A. Pop, L. Cormoș, *Chemische Technik (Leipzig)*, **33**(2), 77 (1981).
11. I. Siminiceanu, C. Calistru, A. Pop, *Stud. Univ. Babeș-Bolyai, Chem.*, **26**(1), 40(1981).
12. E. I. Henley, E. M. Rose, „Material and Energy Balance Computations”, John Wiley, New York, 1964, s. 34.
13. M. H. Karapetiant, „Termodinamică chimică”, (Übersetzung aus russisch), Ed. tehn., București, 1955.

14. * * * Landolt—Börstein "Zahlenwerte und Funktionen" II Band Springer Verlag, Berlin, 1964.
15. * * * „Manualul inginerului chimist”, vol. II, Ed. tehn. Bucureşti, 1952.
16. F. O. Rosini, "Selected Values of Physical and Thermodynamic Properties of Hydrocarbons and Related Compounds", Carnegie Press, Pittsburgh, 1953.
17. K. Schwabe, "Physikalische Chemie", Band 1, Akademie-Verlag, Berlin, 1975.
18. B. Demidovici, I. Maron, „Elements de calcul numerique”, Ed. Mir. Moskou, 1973, s. 112.
19. T. M. Ter-Mikadian, B. M. Kogan, „Rezolvarea problemelor ingineresti cu calculatoare numerice”, Ed. tehn., Bucureşti, 1965, s. 210.

KATALYTISCHER UMSATZ VON METHANOL UND WASSERDAMPF II. Kinetik des Vorganges

I. SIMINICEANU, I. TODEA, M. STANCA*, A. POP* und A. GHITĂ

Eingegangen am 26. November 1986

Catalytic Conversion of Methanol with Water Vapours. II. Kinetics of the Process. The present paper is a study of the kinetics of methanol conversion process with water vapours on copper catalytic, of BASF/K₃ type, used in ammonia factories for conversion. Out of the kinetics data, the activating energy was calculated and, on these grounds, it was settled that at temperatures lower than 230°, limiting in the display process are the phenomena of mass changing. At temperatures higher than 230°, the activating energy is under 3 kcal/mol (the fact proves that the processes of mass changing are limiting).

Obwohl die katalytische Reaktion von Methanol und Wasserdampf von mehreren Autoren [1—5] behandelt wurde gibt es wenig Daten in der Fachliteratur über die Kinetik der Reaktion, die zu ihrer mathematischen Beschreibung dienen könnten.

In dieser Arbeit wird die Kinetik des Vorganges behandelt um die wichtigsten Faktoren die die Geschwindigkeit der Reaktion beeinflussen. Ebenso wird die Aufstellung eines realen makrokinetischen Modells des Vorganges verfolgt.

Makrokinetische Modellierung. Der beschriebene Vorgang gehört zu den Kontaktverfahren und ist schematisch in Figur 1 dargestellt.

Der Gesamt vorgang ist endotherm und deshalb muss neben den Umwandlungen und dem Massetransfer auch der Wärmetransfer berücksichtigt werden, der in Figur 2 schematisch dargestellt ist.

Aus diesen Schemata folgt, dass der Vorgang, je nach Arbeitsbedingungen, nach einfachen oder kombinierten makrokinetischen Modellen stattfinden kann. [6].

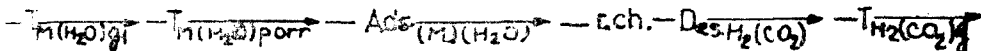


Abb. 1. Strukturschema der Massenprozesse.

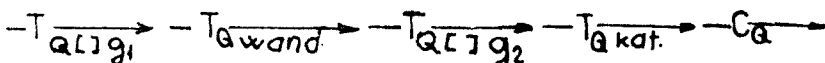


Abb. 2. Structurschema der Wärmeprozesse.

* Universität Cluj-Napoca, Fakultät für Chemie, 3400 Cluj-Napoca, Romania

Experimenteller Teil. Zur Aufstellung des makrokinetischen Modelles wurde eine Laboranlage verwendet, dargestellt in Figur 3, die die experimentellen Daten für das Modell liefern soll.

Der Reaktor ist isotherm. Als geschwindigkeitsbeeinflussende Parameter wurden die Temperatur und die Granulation des Katalysators gewählt. Da die Geschwindigkeit der Gase gross genug ist, wirkt der Massetransfer durch die Gasphase nicht geschwindigkeitshemmend.

Der verwendete Katalysator beruht auf Kupferbasis, vom Typ BASF/k₂-10, der in der zweiten Stufe des Kohlenmonoxydumsatzes aus den Ammoniaklinien verwendet wird. Die Zusammensetzung ist 29–33% CuO, 40–45% ZnO, die spezifische Oberfläche 98,2 m²/g und die Porosität 0,336 cm³/g. Die Temperatur schwankte in den Grenzen 180–320°C, da hier der Katalysator aktiv ist.

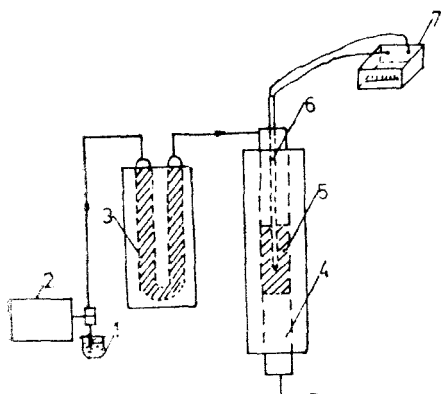


Abb. 3. Versuchsanlagen-schema: 1 — Gefäß für Reaktionskomponenten, 2 — Dosier-pumpe, 3 — Abdampf-kessel und Vorwärme der Reaktionskomponenten, 4 — Reaktor, 5 — Katalysatorschicht, 6 — Elektrischer Ofen, 7 — Mess und reglergerät der Temperatur.

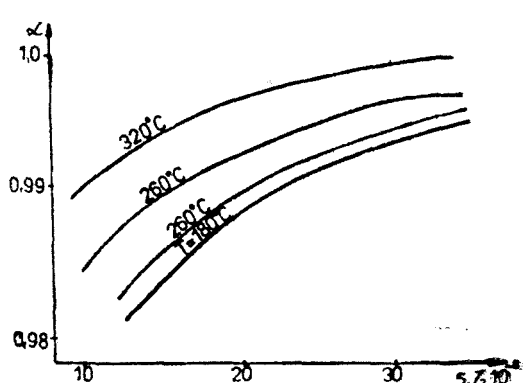


Abb. 4. Einfluss der Korngrösse auf die Geschwindigkeit des Prozesses.

Ergebnisse deu Diskussion. Um der Einfluss den Granulation, also des Massetransfers durch die Poren des Katalysators zur Reaktionsoberfläche auf die Reaktionsgeschwindigkeit zu zeigen, wurde mit zwei Granulationen — 5 und 0,3 mm — gearbeitet, bei verschiedenen Temperaturen und derselben Kontaktzeit. Die Ergebnisse sind in Figur 4 dargestellt.

Mann kann beobachten, dass im ganzen Temperaturintervall der Umsatz des Methanols mit der Verkleinerung der Granulation steigt, aber dieses Ansteigen ist unbedeutend. Daraus folgt dass im Temperaturintervall 180–260°C der Massentransfer durch die Poren des Katalysators die Geschwindigkeit des Vorganges nicht beeinflusst.

Die Versuche die den Einfluss der Temperatur hervorheben sollen, wurden mit tabletiertem katalysator, der mit dem industriellen identisch ist durchgeführt. Er besteht aus Zylinder der Dimension 5 × 5 mm.

Die Ergebnisse sind in Figur 5 dargestellt.

Man kann den starken Einfluss der Temperatur auf die Geschwindigkeit feststellen. Die Verarbeitung der experimentellen Daten aus Figur 5 in den Koordinaten — $\ln(1 - \alpha)$ — τ führt zu den Darstellungen aus Figur 6.

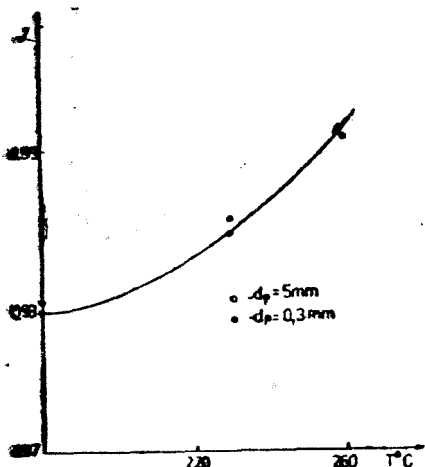


Abb. 5. Einfluss der Temperatur auf die Geschwindigkeit des Prozesses.

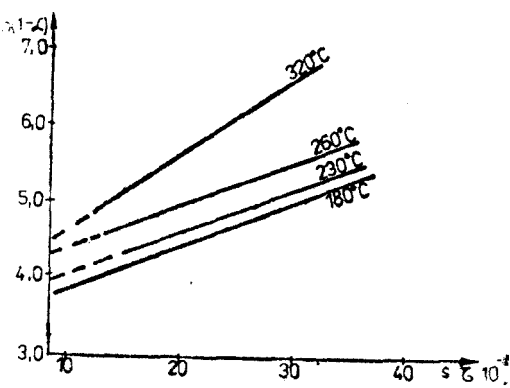


Abb. 6. Diagramm $\ln(1-\alpha) - \tau$.

Die Steigung der Geraden aus Figur 6 zeigen die Geschwindigkeitskonstanten der Reaktion bei der entsprechenden Temperatur.

Wird die Geschwindigkeitskonstante in den Koordinaten $\ln k - \frac{1}{T}$ grafisch dargestellt erhält man Figur 7.

Man kann erkennen, dass die erhaltene Linie bei 230°C ihre Steigung verändert.

Aus den Steigungen der beiden Segmente Figur 8 wurde die Aktivierungsenergie berechnet und die Werte 1,82 kcal/mol bei Temperaturen grösser als 230°C und 12,15 kcal/mol bei Temperaturen kleiner als 230°C gefunden. Diese Werte zeigen dass in den industriellen Bedingungen und entsprechender Granulation, bei Temperaturen unter 230°C der Masseumsatz Reaktionsgeschwindigkeit bestimmt, und bei Temperaturen über 230°C, der Massetransfer durch die Poren des Katalysators.

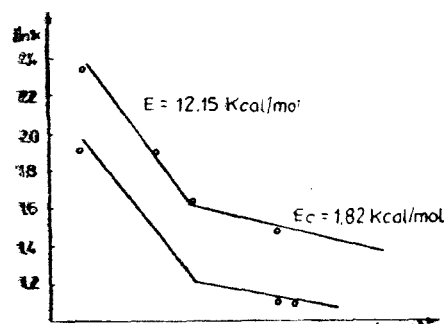


Abb. 7. Diagramm $\ln k - \frac{1}{T}$.

Notierungen

- T_M — Elementarvorgang des Massentransports.
- T_Q — Elementarvorgang des Wärmedurchgangs.
- C_Q — Elementarvorgang des Wärmeverbrauchs.
- K — Konstante der Reaktionsgeschwindigkeit.
- α — Umsatz des Methanols.
- [] g — Gasphase.

LITERATUR

1. G. Salvi, E. Zanella, E. Parodi, *Riv. Combustibili*, **32**(7-8), 233, (1978).
2. H. Kobayashi, N. Takezawa, C. Minochi, *J. Catal.* **69**(2), 487 (1981), *Chem. Abstr.* **95**, 157313p.
3. H. Kobayashi, N. Takezawa, C. Minochi, *Hokkaido Daigaku Kogakubu Kenkyu Hokoku*, **102**, 13 (1981), *Chem. Abstr.* **95**, 6411t (1981).
4. *Pat. Japan. Kokai Tokkyo Koho*, 81 26,992 (16 Mart. 1981); *Chem. Abstr.* **95**, 65236n (1981).
5. *Pat. Japan. Kokai Tokkyo Koho*, 81 48, 252; *Chem. Abstr.* **95**, 31124j.
6. C. Calistrut, C. Leontie, „Tehnologia substanțelor anorganice”, Ed. did. și ped., București, 1972.

RS_H stands for HOOCCH₂-SH. Conditions were chosen such that the redox reaction was quite slow. Three to five individual readings were made for each set of conditions. The results are summarized in Table 1.

Table 1
Experimental conditions and equilibrium state absorbances at 25°C and $\mu = 0.2$ in an 1 cm path lenght cell

$10^4(H^+)$	$10^4(Cr^{VI})_0$	$10^4(RSH)$	A_e	$\epsilon_{obs} = \frac{A_e}{(Cr^{VI})_0}$
1.00	4.00	0.383	0.160	400
2.00		0.393	0.163	401
1.00		0.786	0.198	495
2.00		0.786	0.200	500
1.00		1.57	0.238	570
		3.97	0.310	775
		4.00	0.320	800
1.00	5.00	11.80	0.433	866
2.00		11.80	0.430	860
1.00	4.00	15.70	0.340	850

The absorbance at equilibrium is

$$A = \epsilon_0 [(Cr^{VI})_0 - (RSCrO_3^-)] + \epsilon(RSCrO_3^-) \quad (2)$$

where ϵ_0 and ϵ are absorption coefficient for HOCrO₃⁻ and RSCrO₃⁻ respectively. Expressing (RSCrO₃) in terms of equilibrium constant K and observed absorption coefficient $\epsilon_{obs} = A/(Cr^{VI})_0$, equation (2) yields

$$\epsilon_{obs} = \epsilon - \frac{\epsilon_{obs} - \epsilon_0}{(RSH)_f} \cdot \frac{1}{K} \quad (3)$$

which shows a linear dependence of ϵ_{obs} versus $(\epsilon_{obs} - \epsilon_0)/(RSH)_f$ having the intercept ϵ and the slope $-1/K$. The values ϵ_{obs} are available from experimental data, $\epsilon_0 = 230 \text{ M}^{-1}\text{cm}^{-1}$. Some iterations have been carried out, first using

the total (RSH) for the free concentration. The formation constant was calculated from the slope of the line described by (3). Using it, corrected values for $(RSH)_f$ were determined and used again to compute a new and better value for K. The computation was repeated until a convergence was achieved. The plot of equation (3) is shown in Figure 2. Values of $\epsilon = 900 \pm 40 \text{ M}^{-1}\text{cm}^{-1}$ at 420 nm and $K = (1.10 \pm 0.15) \times 10^3 \text{ M}^{-3}$ have been considered. An objective least-square method was

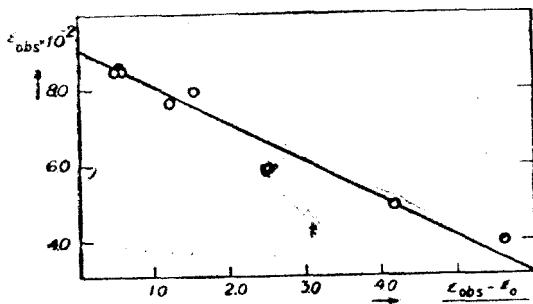


Fig. 2. Linear dependence described by equation (3).

used. The experimental errors are larger as compared to the other chromate-thiol compounds because of the fact that redox reaction proceeds faster in this case.

To study the formation Cr(VI)-thiol complex kinetics, stopped-flow traces were obtained under pseudo-first-order conditions at 420 nm. The plots $\log (A_e - A)$ vs. time were linear up to 80–85% of reaction, and first-order rate constants for different conditions were evaluated from these plots. A_e and A represents absorbance at equilibrium and at time t respectively. The observed first-order rate constants increased with both the thiol and mineral acid concentrations as shown in Table 2. Values in Table 2 are means of 3–4

Table 2

Kinetic data for the formation of RSCrO_4^- at 25°C $\mu = 0.2$ and $(\text{HCrO}_4^-) = 5 \times 10^{-4}$

$10^3(\text{H}^+)$	$10^3(\text{RSH})$	k_{obs}	$k_f = k_{\text{obs}}/[1/K + (\text{RSH})]$	
0.50	1.50	1.22	76.25	Mean : 76.3
1.00	0.56	0.53	89.59	92.0
	1.00	1.01	92.25	
	1.18	1.14	89.65	
	1.50	1.54	96.76	
	1.50	1.43	89.85	
	2.00	1.97	94.19	
2.00	1.18	1.50	117.96	115.5
	1.50	1.80	113.09	
4.00	0.42	0.85	166.11	165.1
	0.61	1.13	161.06	
	1.18	2.10	165.15	
	1.50	2.60	163.36	
	1.79	3.01	160.00	

individual measurements which do not differ to more than 5%. Second-order rate constants were calculated as $k_f = k_{\text{obs}}/[(\text{RSH}) + 1/K]$. At constant acidity specific second-order velocities were close together within the limits of experimental errors (column 4 in the table) and linear dependent on perchloric acid concentration. A fractional order of 0.4 with respect to the hydrogen ion concentration has been deduced from a graph of $\log k_f$ as a function of $\log(\text{H}^+)$. This fact indicated the involvement of two concurrent ways, one of zero-order and the other of first-order with respect to (H^+) . When second-order rate constants k_f were plotted as a function of perchloric acid concentration, a straight line was obtained, which did not pass through the origin. An objective least-square method gave the intercept as the second-order rate constant of $k_f^0 = 66.3 \pm 1.2 \text{ M}^{-1}\text{s}^{-1}$ and the slope as the third-order rate constant of $k_f^H = (2.47 \pm 0.05) \times 10^3 \text{ M}^{-1}\text{s}^{-1}$. Therefore, the overall rate law for the thioglycolate-chromate complex formation can be written as:

$$\frac{d(\text{RSCrO}_4^-)}{dt} = \{[k_f^0 + k_f^H(\text{H}^+)(\text{RSH})]\}(\text{HOCrO}_4^-) \quad (4)$$

indicating a first-order dependence on thiol. Observed first-order and calculated second-order rate constants are collected in Table 4. On the other hand, when (H^+) was varied from 5×10^{-3} to 3.69×10^{-2} M at constant 1.04×10^{-2} M thiol concentration, a fractional order, lower than unity, was obtained. As figure 3 illustrates, there appears a linear dependence of k_{obs} (or second-order

Table 4

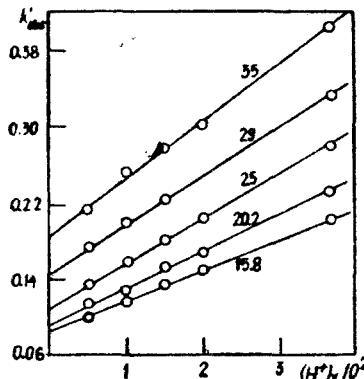


Fig. 3. The effect of the acidity on the reaction rate constant for the oxidation process.

The effect of thioglycolic acid on the redox reaction
 $\mu = 2.2$, $t = 25^\circ C$, $(HCrO_4^-) = 4 \times 10^{-4}$ and $(H^+) = 1.0 \times 10^{-2}$.

$10^2(RSH)$	k_{obs}^{-1}	$k_{obs} / (RSH) M^{-1} \cdot s^{-1}$	
0.518	0.0771	14.9	Mean: 15.0 ± 0.3
	0.0764	14.7	
	0.0794	15.3	
	0.0771	14.9	
	0.0780	15.1	
0.78	0.115	14.8	15.0 ± 0.3
	0.120	15.3	
	0.117	15.0	
	0.156	15.0	15.2 ± 0.2
1.04	0.161	15.4	
	0.159	15.2	
	0.161	15.4	
	0.253	16.2	15.8 ± 0.4
	0.248	15.8	
	0.244	15.6	
	0.248	15.8	

rate constant as well) on the mineral acid concentration. Each point on the graph is a mean of 3–7 individual runs which do not differ to more than 5%. These results indicate the following rate law for the redox disappearance of thioester:

$$-\frac{d(RSCrO_3^-)}{dt} = [k_2 + k_3(H^+)] (RSH)(RSCrO_3^-) \quad (7)$$

This rate law is similar to that obtained for the oxidation of cysteine [7].

Temperatures between 15.8 and $35^\circ C$ were used to investigate the effect on the redox reaction rate. The values of second-order and third-order rate constants, as deduced from the intercepts and the slopes of lines in figure 3 respectively, are collected in Table 5. The activation parameters are:

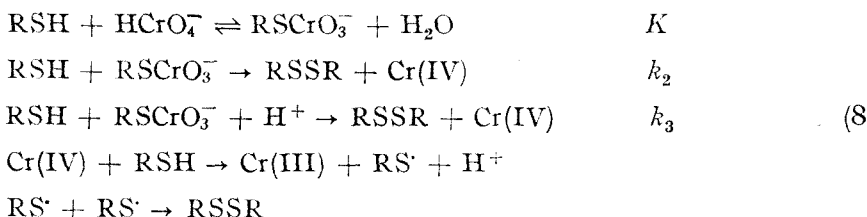
$$\begin{array}{ll} \Delta H_f^\ddagger = 31 \pm 4 \text{ kJ/mol} & \Delta S_f^\ddagger = -121.3 \pm 8.3 \text{ J/mol} \cdot K \\ \Delta H_s^\ddagger = 19.2 \pm 1.2 \text{ kJ/mol} & \Delta S_s^\ddagger = -129.7 \pm 8.3 \text{ J/mol} \cdot K \end{array}$$

Activation enthalpies are comparable with those for oxidation of thiosulfate [12] and methionine [13] and about 20 kJ lower than that for the oxidation of cysteine [7]. Activation entropies are negative as found for all cited systems, and quite large.

4. *Free radical identification.* In order to prove the presence of free radicals during the reaction, thioglycolic acid — chromate system was used to initiate polymerization of ethylacrylate. Temperature increase of 2.5–4.0 degrees has been noticed when monomer was added to reaction mixture. No thermic

effect was observed when only reducing agent or oxidant agent solutions were shaken with monomer in the reaction vessel. These facts lead to the conclusion that some free radicals are involved in the redox process.

5. *Redox reaction mechanism.* The evidence for extensive complex formation, the reaction stoichiometry, the proof for free radicals involved and the kinetics of the reaction are consistent with the following reaction scheme:



The path by which chromium (VI) is reduced by one-equivalent thiol reagent include the participation of two reducing agent molecules. A sulfur-sulfur bond is rapidly formed beside chromium (IV). Under the thiol excess, chromium (IV) reacts fast with another thioglycolic molecule in one-equivalent step, to form Cr(III) and free radicals, which unite to yield disulfide. Such mechanisms are quite common for the oxidation of thiosulfate [12], other thiols [13], thiocyanide [2] and iodide [14] by chromate, when a dimer from a free radical and Cr(IV) are formed. Activation entropies — large and negative — agree with the above reaction mechanism.

REFERENCES

1. K. A. Muirhead, G. P. Haight, J. K. Beattie, *J. Amer. Chem. Soc.*, **94**, 3006 (1972).
2. C. T. Lin, J. K. Beattie, *J. Amer. Chem. Soc.*, **94**, 3011 (1972).
3. K. A. Muirhead, G. P. Haight, *Inorg. Chem.*, **12**, 1116 (1973).
4. F. H. Westheimer, *Chem. Rev.*, **45**, 419 (1949).
5. I. Baldea, G. Niac, *Inorg. Chem.*, **7**, 1232 (1968).
6. G. Niac, S. Schön, I. Baldea, *Studia Univ. Babes-Bolyai, Chem.*, **31**(2), 31 (1986).
7. I. Baldea, G. Niac, *Studia Univ. Babes-Bolyai, Chem.*, **31**(2), 41 (1986).
8. K. K. Sengupta, J. K. Chakrader, *J. Chem. Soc., Dalton Trans.*, **1974**, 222; J. G. Mason, A. D. Kowalak, *Inorg. Chem.*, **3**, 1248 (1964).
9. A. Haim, *Inorg. Chem.*, **11**, 3147 (1972).
10. D. L. Leusing, I. P. Mislan, R. J. Goill, *J. Phys. Chem.*, **64**, 1070 (1960).
11. I. Baldea and S. Schön, *Stud. Univ. Babes-Bolyai, Chem.*, **18**(1), 47 (1973).
12. I. Baldea, G. Niac, *Inorg. Chem.*, **9**, 110 (1970).
13. A. Petri, I. Baldea, *Stud. Univ. Babes-Bolyai, Chem.*, **20**(2), 67 (1975).
14. K. E. Howlett, S. Sarsfield, *J. Chem. Soc.*, **1968A**, 683.

Table 5

Temperature dependence of third- and second-order rate constants for the redox process

Temp. °C	$k_2 \text{ M}^{-1} \cdot \text{s}^{-1}$	$10^{-2} \times k_3 \text{ M}^{-2} \cdot \text{s}^{-1}$
15.8	7.5 ± 0.4	3.23 ± 0.08
20.2	9.5 ± 0.5	3.43 ± 0.09
25.0	11.0 ± 0.6	4.33 ± 0.06
29.0	14.5 ± 0.4	4.71 ± 0.09
35.0	18.2 ± 0.3	5.60 ± 0.10

ON THE DIOXIMINE COMPLEXES OF TRANSITION METALS. LXIX.
Kinetics and Mechanism of the Hydrolysis of Nyoxime in acidic medium

FERENC MÁNOK*, GABRIELLA DÉNEZSI*, CSABA VÁRHELYI* and ANDRÁS BENKŐ*

Received: January 7, 1987

The polarographic behaviour of the nyoxime (1,2-cyclohexane dione dioxime) in acidic solutions (0.1, 0.2 and 0.4 N HClO_4) showed a protolytic process followed by a deoximation reaction. Some kinetic parameters of these reactions were determined and a possible mechanism was established and discussed.

Introduction. The alycyclic 1, 2-dioximes (nyoxime, heptoxime) are well known reagents used in the analytical chemistry of some transition metals ($M(\text{Diox.H})_2$, ($M = \text{Ni, Pd, Pt}$). The $[\text{Co}(\text{Diox.H})_2\text{X}_2]^-$ and $[\text{Co}(\text{Diox.H})_2(\text{amine})\text{X}]^-$ chelate compounds have been studied from several coordination chemical point of views [1].

The α — dioximes are very weak dibasic acids ($K_1 = 10^{-11} - 10^{-12}$). They are stable in neutral and weakly basic solutions and participate only in reversible, fast acid-base reactions. In acidic media the situation is more complicated. The protonization of the oxime group occurs and parallel with this phenomenon other reactions can be also observed. Shlenskaya; et al. [2] have determined the acidity constants of some aliphatic and alycyclic α — dioximes by means of ultraviolet spectrophotometric measurements. These authors mentioned that the absorbancy of the sample solutions varies with the time. The comparison of the spectra taken in neutral and acidic aqueous solutions of some — dioximes showed that in acidic media hydrolysis processes occur with the liberation of hydroxylamine and free α -diketones.

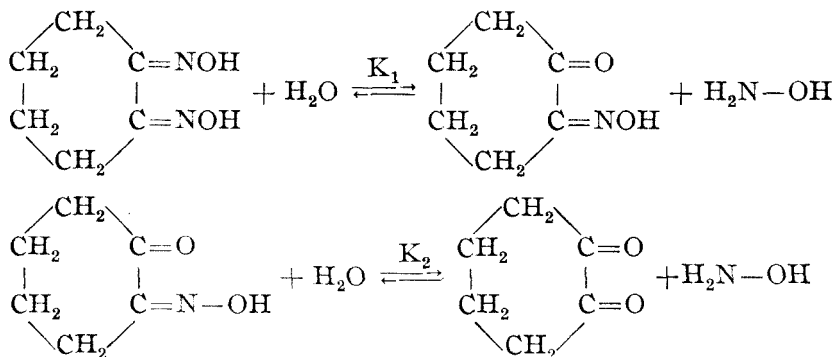
Results and Discussion. We observed that the α -dioximes and some of their hydrolysis products give well defined polarographic waves. This phenomenon allowed us the quantitative determination of the unreacted dioximes and their decomposition derivatives and the determination of the kinetic parameters of the deoximation reactions.

In a previous paper [3] the polarographic behaviour of 1, 2, 3-cyclohexane trione trioxime was studied in acidic media.

The present paper deals with the polarographic behaviour of „nyoxime” (1, 2-cyclohexanedione dioxime) in acidic solutions (0.1, 0.2 and 0.4 M HClO_4).

* University of Cluj-Napoca, Faculty of Chemistry, 3400 Cluj-Napoca, Romania

In the case of the hydrolysis of this substance the following equilibria can be assumed:



The transformations occurring in acidic solutions of nyoxime are illustrated by the polarograms in the Fig. 1.

These polarograms were taken in 0.1 N HClO_4 solutions 7, 24 and 150 minutes after mixing the nyoxime and HClO_4 solutions. The constant ionic strength of the solutions (1M) was ensured by addition of NaClO_4 .

On the polarograms 1 and 2 two waves appear (I and II) with $E_{1/2}$ values of -0.32 V and -0.58 V (vs. SCE), respectively. The second curve shows that the wave I increases and the II one decreases on standing.

After a longer period of time (150 minutes) the wave II practically disappears and wave I decreases slowly. The rate of the decrease of the wave

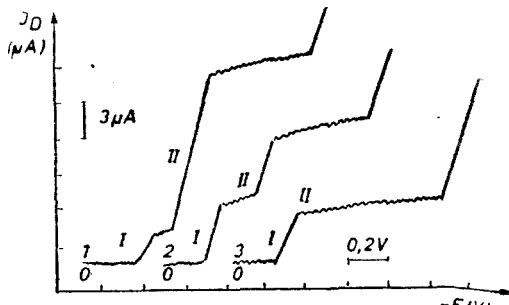


Fig. 1. Polarographic waves of nyoxime in acidic media

$C_{\text{Niox. H}_2} = 10^{-3}$ M; $C_{\text{HClO}_4} = 0.1$ M; $C_{\text{ClO}_4} = 1$ M;
I. $t = 7$ min. after mixing; II. $t = 24$ min. after mixing; III. $t = 150$ min. after mixing.

Table I
Variation of the height of polarographic waves of nyoxime with the time by various acidities

Time min	C_{HClO_4}	II. wave $I_D(\mu\text{A})$	I. wave $I_D(\mu\text{A})$	C_{HClO_4}	II. wave $I_D(\mu\text{A})$	I. wave $I_D(\mu\text{A})$	C_{HClO_4}	II. wave $I_D(\mu\text{A})$	I. wave $I_D(\mu\text{A})$
1	0.1 M	9.36	—	0.2 M	9.2	—	0.4 M	9.0	—
2	..	9.00	—	..	8.4	—	..	8.2	—
5	..	7.64	1.00	..	6.8	1.4	..	6.2	1.0
10	..	6.10	2.30	..	4.9	2.4	..	3.9	2.6
15	..	4.70	2.90	..	3.4	2.9	..	2.4	3.3
20	..	3.70	3.10	..	2.4	3.1	..	1.56	3.3
25	..	2.84	3.10	..	1.7	3.0	..	1.0	3.2
30	..	2.24	3.00	..	1.2	2.9	..	0.64	3.2

temp. 20° , $C_{\text{Niox. H}_2} = 10^{-3}$ M; $C_{\text{ClO}_4} = 1$ M

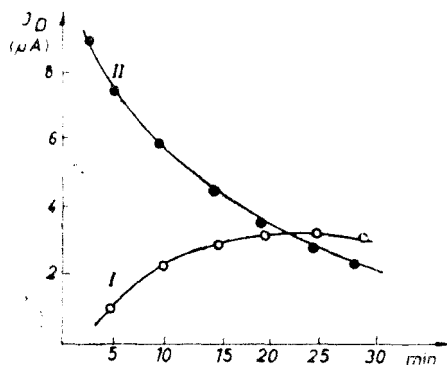


Fig. 2. Variation of the height of the polarographic waves with time at 20°C by $C_{\text{HClO}_4} = 0.1 \text{ M}$; $C_{\text{Niox-Hg}} = 10^{-3} \text{ M}$; $C_{\text{ClO}_4^-} = 1 \text{ M}$.

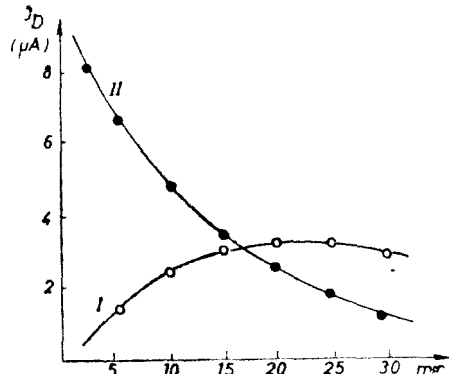


Fig. 3. Variation of the height of the polarographic waves with time at 20°C by $C_{\text{HClO}_4} = 0.2 \text{ M}$

II becomes greater with increasing acidity of the solution. At a pH ≤ 4 the heights of the polarographic waves practically do not alter with the time. In order to obtain the kinetic data of the hydrolysis necessary for the elucidation of the above mentioned phenomenon three series of measurements were carried out. The concentration of the perchloric acid was 0.1, 0.2 and 0.4 M. After a period of time in thermostated conditions (15, 20, 25°C) the polarograms were taken using the forced dropping method.

The results of these measurements for 20°C are presented in Table 1 and in Figs. 2, 3 and 4, respectively.

The log values of the diffusion currents corresponding to the second wave (II) enable us to determine the rate constants of the reaction (see Table 2).

The plot of the $\log I_d$ values versus time gives straight lines (see Fig. 5). Using I_d values extrapolated to zero time and various initial concentrations of nyoxime, the dependence of the diffusion current from the concentration of the above mentioned chelating agent was determined.

On the basis of these functions one can calculate the half life time of the decomposition of myoxime.

The rate constant of this reaction can be given by:

$$k = \frac{0.693}{t_{1/2}} \quad (1)$$

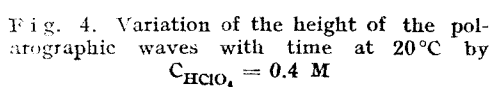


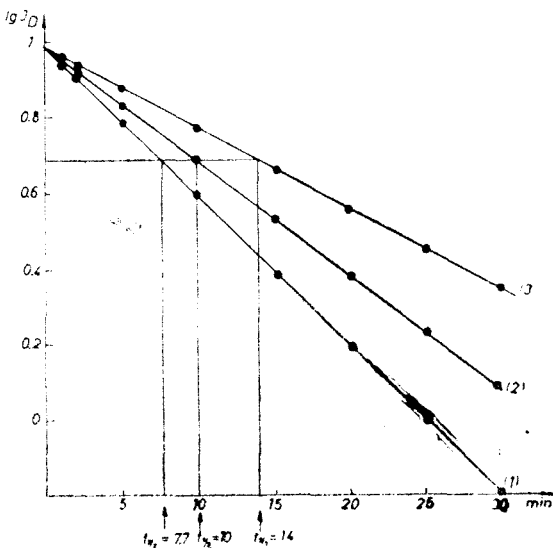
Fig. 4. Variation of the height of the polarographic waves with time at 20°C by $C_{\text{HClO}_4} = 0.4 \text{ M}$

Table 2

Kinetic data on the hydrolysis of nyoxime by 20°C

Time min	$C_{HClO_4} = 0.1 \text{ M}$			$C_{HClO_4} = 0.2 \text{ M}$			$C_{HClO_4} = 0.4 \text{ M}$		
	II. wave $I_D(\mu\text{A})$	$\lg I_D$	$C \cdot 10^3$ (Mol/l)	II. wave $I_D(\mu\text{A})$	$\lg I_D$	$C \cdot 10^3$ (Mol/l)	II. wave $I_D(\mu\text{A})$	$\lg I_D$	$C \cdot 10^3$ (Mol/l)
1	9.36	0.971	0.93	9.2	0.964	0.92	9.0	0.954	0.90
2	9.00	0.954	0.90	8.4	0.924	0.84	8.2	0.914	0.82
5	7.64	0.883	0.76	6.8	0.833	0.67	6.2	0.792	0.62
10	6.1	0.785	0.61	4.9	0.690	0.50	3.9	0.591	0.39
15	4.7	0.672	0.47	3.4	0.531	0.34	2.4	0.380	0.25
20	3.7	0.568	0.37	2.4	0.380	0.24	1.56	0.193	0.15
25	2.84	0.453	0.28	1.7	0.230	0.17	1.0	0.000	0.09
30	2.24	0.350	0.22	1.2	0.079	0.11	0.64	-0.194	0.06
$k(\text{min}^{-1})$		4.92×10^{-2}		6.9×10^{-2}		9.0×10^{-2}			
$C_{\text{Nyox H}_2} = 10^{-3} \text{ Mol/l}; C_{\text{ClO}_4^-} = 1 \text{ M}$									

Fig. 5. Variation of the $\log I_D$ values with time at 20°C I. $C_{HClO_4} = 0.4 \text{ M}$; II. $C_{HClO_4} = 0.2 \text{ M}$; III. $C_{HClO_4} = 0.1 \text{ M}$.



Our investigations showed a tendency of increase of these rate constants with the concentration of the perchloric acid.

$$C_{HClO_4} = 0.4 \text{ M}; k_1 = 9.0 \times 10^{-2} \text{ min}^{-1}$$

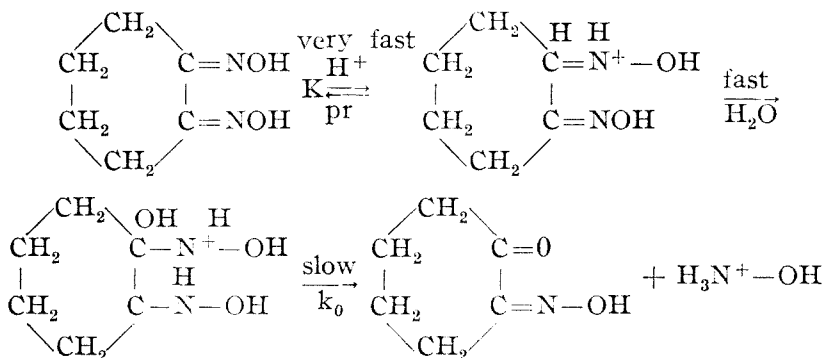
$$C_{HClO_4} = 0.2 \text{ M}; k_2 = 6.9 \times 10^{-2} \text{ min}^{-1}$$

$$C_{HClO_4} = 0.1 \text{ M}; k_3 = 4.9 \times 10^{-2} \text{ min}^{-1}$$

In order to determine the enthalpy and entropy of activation of the deoximation reaction analogous measurements were carried out at three different temperatures (15, 20, 25°C).

On the basis of some literature data [4] referring to the hydrolysis of acetophenone oxime and acetoxyime, respectively, the first polarographic step can be attributed to the reduction of 1, 2-cyclohexane dione monoxime, which is formed by the partial hydrolysis (deoximation) of the nyoxime. The second wave is due to the reduction of the non transformed nyoxime.

For the explication of the increase of the rate of the hydrolysis with increasing perchloric acid concentration the following successive reactions can be presumed:



According to our presumption in the first step of the reaction a pre-equilibrium between the protonated and non protonated forms of the nyoxime is established. (K_{pr} = the acidity constant of the protonated species).

This process is followed by an elementary reaction, viz. the addition of a water molecule, facilitated by the polarization of the π -bonding because of the protonization of the nitrogen atom. The presumed pre-equilibrium is very probable due to the great value of the recombination constant of the protonated form ($k_r = 9.6 \times 10^{11}$) [5].

The addition of water is a pseudo-monomolecular reaction. The final elementary reaction is the elimination of hydroxylamine.

To resolve the problem, which of these elementary reactions: the addition of a water molecule or the elimination of hydroxylamine can be considered as rate determining process (characterized by the rate constant k_0), it is necessary the calculation of the kinetic parameters, and especially the activation entropy value.

If our presumption concerning the protolytic pre-equilibrium is correct, between the apparent rate constant k_m ($m = 1, 2, 3$), the pH independent rate constant k_0 , and the acidity constant of the protonated form K_{pr} , the following relation is valid:

$$k_m = \frac{k_0[H_m^+]^2}{K_{pr} + [H_m^+]} \quad (2)$$

For the ratio of the rate constants the following relation can be obtained:

$$k_m = \frac{[H_m^+]K_{pr} + [H_n^+][H_m^+]}{[H_m^+][H_n^+] + K_{pr}[H_n^+]} \quad (3)$$

From these equations results the K_{pr} value:

$$K_{pr} = \frac{[H_m^+][H_n^+] \left(1 - \frac{k_m}{k_n} \right)}{\frac{k_m}{k_n} [H_n^+] - [H_m^+]} \quad (4)$$

On the basis of equation (4), using different apparent rate constant values, the following K_{pr} values were obtained:

$$K_{pr} = 0.140 \ (k_1, k_2)$$

$$K_{pr} = 0.135 \ (k_2, k_3)$$

$$K_{pr} = 0.148 \ (k_1, k_3)$$

Mean value: $K_{pr} = 0.141$

Using this mean value, $k_0 = 12.2 \times 10^{-2} \text{ min}^{-1}$ was calculated.

From the rate constants obtained at different temperatures (15, 20, 25°C) the activation enthalpy and entropy were calculated using the Eyring [6] and Evans and Polanyi [7] relation.

$$\Delta H^\ddagger = 47.4 \text{ kcal/mole}$$

$$\Delta S^\ddagger = 89 \text{ e.u.}$$

The positive entropy value is in agreement with the formation of an activated complex by addition of a water molecule.

This activated species has strongly stabilized bondings as compared to the initial substance. This phenomenon leads to the elimination of hydroxylamine in a successive step.

The positive entropy value is in agreement with the presumption, that the elimination of hydroxylamine from the activated water addition product, is the rate determining step.

Contrary, if the water addition were the rate determining process, the mobility of the activated species would be smaller as compared to the initial nyoxime, leading to a negative entropy value.

Experimental. The polarograms were taken on a Radelkis Type OH-120 polarograph with a Tast-Rapid-OH 9991 adapter to ensure a forced dropping of the mercury. A conventional polarographic cell was used with a saturated calomel electrode, connected to the cell by means of an agar-agar bridge (1 M KNO₃). The oxygen was eliminated from the solutions with purified methane. The dropping mercury electrode has a flow rate of 1.3 mg s⁻¹ and a drop time of 5.20 s in 1 M NaClO₄ and with a mercury reservoir height of 60 cm.

REFERENCES

1. V. M. Peshkova, V. M. Savostyna, E. K. Ivanova: „Oksimi”, Izdat. „Nauka”, Moskva, 1977, p. 52–112.
2. V. I. Shlienskaya, T. I. Tikhvinskaya, A. A. Bir'yukov, *Vestnik Moskov. Univ. Ser. II. Khim.*, **1970**, 337.
3. F. Mánok, Cs. Várhelyi, A. Benkő, M. Tarsoly-Magyari, *Monatsh.*, **109**, 1329 (1978).

4. C. Calzolari, C. Furlani, *Triest Mem.*, **2**, 22, 43, 63 (1953); *Chem Abstr.*, **49**, 938 (1955).
5. F. Mánok, G. Dénezsí, Cs. Várhelyi, *Stud. Univ. Babeş-Bolyai, Chem.*, **31**(2), 3 (1986).
6. H. Eyring, *J. Chem. Phys.*, **3**, 107 (1935).
7. M. G. Evans, M. Polányi, *Trans. Faraday Soc.*, **31**, 875 (1936).

NEUE TETRACHLORO- UND TETRABROMO-PLATINITE (II) DER KOBALT(III)AMINEN

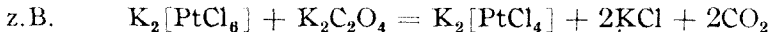
CSABA VÁRHELYI* and ION GĂNESCU**

Eingegangen am 7 Januar, 1987

New Tetrachloro- and Tetrabromo-Platinite (II) Type Cobalt (III) Amines.

A number of 25 new complex salts of the $H_2[PtCl_4]$ and $H_2[PtBr_4]$ acids with monoacido-pentamine -- (cis-[Co(en)₂Cl(amine)]²⁺) and diacido-tetramine [(Co(en)₂X₂)⁺, [Co(DH)₂(amine)₂]⁺, [Co(ec)(amine)₂]⁺) „en” -- ethylenediamine, „ec.” H₂” -- ethylendiimino-bis-acetylacetone, „DH₂”-dimethylglyoxime) type cobalt(III) amines were obtained by double decomposition reactions. The products were characterized by chemical and thermogravimetical analysis.

Einleitung. Die Tetrahalogeno-platinite : $[PtCl_4]^{2-}$ und $[PtBr_4]^{2-}$ entstehen leicht durch die partielle Reduktion unter gelinden Unständen der Hexachloro-, bzw. Hexabromo-platinaten (IV). Es ist empfehlenswert für diesem Zweck Sulfit, CuCl, Oxalsäure und Alkalioxalat zu verwenden. [1-2].



Die starken Reduktionsmittel wie SnCl₂, Hydroxylamin, Hydrazin, usw. führen, im allgemeinen, zur Auscheidung von metallischem Platin. Die Tetrahalogeno-platinite bilden leicht neutrale Salze mit Metallen, Aminen und Phoophinen in saurem Medium ((Amin, H)₂[PtX₄], (Phosphin, H)₂[PtX₄]). In wässrigen Lösungen hydratisieren sich stufenweise die $[PtCl_4]^{2-}$ und $[PtBr_4]^{2-}$ -Ionen unter Bildung von verschiedenen Halogeno-aquo-komplexen. Dieser Vorgang wurde auch von kinetischem Standpunkt aus untersucht [3-4]. Ihre Alkalisalze dienen als Ausgangssubstanzen für verschiedene Substitutionsreaktionen mit NH₃, Aminen, Aminosäuren, usw. Die Reaktionsprodukte sind cis- oder trans Diacido-Nichtelektrolyte. $[Pt(Am)_2X_2]$ [5-7]. Es ist bemerkenswert, dass einige cis-Derivate von diesem Typ in der Chemotherapie der Krebserkrankungen eine besondere Bedeutung haben [8-9].

Resultate und Diskussion. Nach Literaturangaben wurden nur einige Komplexsalze der obenerwähnten Säuren mit Metall-aminen erhalten. Die energetischen Faktoren begünstigen die Bildung von schwerlöslichen Komplexsalzen vom AB, bzw. AB₂ Typ, insbesonders mit Kobalt(III)- und Chrom(III)-aminen. Wir haben beobachtet, dass die wässrige Lösungen der K₂[PtCl₄] und K₂[PtBr₄] mit ein-, bzw. zweiwertigen Kompexkationen des Kobalts charakteristische, kristalline Fällungen abscheiden. Zu diesem Zweck wurden von den Monoacido-pentaminen einige Co(en)₂X(Amin)²⁺-Derivate verwendet. Von den zahlreichen Diacido-tetraminen benützten wir einige Chelatkatione vom Typ : [Co(en)₂X₂]⁺, [Co(DH)₂(Amin)₂]⁺, bzw. [Co(ec)(Amin)₂]⁺ für die doppelten Umsetzungsreaktionen („en” -- Äthylendiamin, DH₂ — Dimethylglyoxim, „ec.” H₂” — Schiff'sche Base aus Äthylendiamin und Acetylacetone). Die erhaltenen neuen Salze sind in den Tabellen 1-2 charakterisiert.

* Universitate Cluj-Napoca, Facultăt für Chemie, 3400 Cluj-Napoca, Romania

** Universität Craiova, Facultät für Naturwiss., 1100-Craiova, Romania

Tabelle 1

Nene Tetrachloro--Platinite mit Kobalt (III)-aminen.

No.	F o r m e l	Mol. Gew. ber.	Charakteristik	Analyse	
				Ber.	Gef.
1.	[Co(DH) ₂ (Pyridin) ₂] ₂ [PtCl ₄] · H ₂ O	1253,5	gelbbraune, hexagonale Platten	Pt 15,56 Co 9,40 N 13,40 H ₂ O 1,43	15,47 9,40 13,28 0,96
2.	[Co(DH) ₂ (NH ₃) ₂] ₂ [PtCl ₄] · H ₂ O	1005,3	gelbbraune mikrokrist. Masse	Pt 19,40 Co 11,72 N 16,71 H ₂ O 1,79	19,16 11,51 16,58 1,28
3.	[Co(DH) ₂ (m-Xylidin) ₂] ₂ [PtCl ₄]	1403,9	gelbbraune hexagonale Plättchen	Pt 13,89 Co 8,39 N 11,96	13,73 8,19 11,82
4.	[Co(DH) ₂ (m-Aminophenol) ₂] ₂ [PtCl ₄]	1355,4	braune rhomb. Prismen	Pt 14,39 Co 8,69 N 12,39	14,32 8,67 12,19
5.	[Co(DH) ₂ (m-Toluidin) ₂] ₂ [PtCl ₄]	1347,5	gelbbraune Dendryte	Pt 14,47 Co 8,74 N 12,46	14,38 8,69 12,28
6.	[Co(ec)(Pyridin) ₂] ₂ [PtCl ₄] · H ₂ O	1233,6	gelbbraune mikrokrist. Masse	Pt 15,81 Co 9,55 N 9,07 H ₂ O 1,49	15,67 9,47 8,96 1,68
7.	[Co(ec)(NH ₃) ₂] ₂ [PtCl ₄] · H ₂ O	985,5	dunkelgelbe Nadeln	Pt 19,79 Co 11,96 N 11,36 H ₂ O 1,82	19,78 11,82 11,22 1,03
8.	[Co(ec)(m-Aminophenol) ₂] ₂ [PtCl ₄]	1335,6	gelbbraune Nadeln	Pt 14,60 Co 8,82 N 8,38	14,45 8,77 8,21
9.	[Co(ec)(p-Toluidin) ₂] ₂ [PtCl ₄]	1327,7	sternförmige kurze Prismen	Pt 14,69 Co 8,87 N 8,43	14,64 8,81 8,30
10.	[Co(ec)(m-Xylidin) ₂] ₂ [PtCl ₄]	1384,1	gelbraune, kurze Prismen	Pt 14,09 Co 8,51 N 8,09	13,96 8,50 7,92

Die erhaltenen Tetrahalogeno-platinite (II) sind beständig in saurem Medium und zersetzen sich leicht in Gegenwart von Alkalien. Die charakteristischen Platinite lösen sich, im allgemeinen, in DMF, DMSO und THF und sind unlöslich in nichtpolaren organischen Lösungsmitteln.

Tabelle 2
Neue Tetrabromo-platinite mit Kobalt(III)-aminen

Nr.	Formel	Mol. Gew. ber.	Charakteristik	Analyse	
				Ber.	Gef.
1.	$[\text{Co}(\text{DH})_2(\text{NH}_3)_2]_2$ $[\text{PtBr}_4] \cdot \text{H}_2\text{O}$	1183	gelbbraune hexagonalne Plättchen	Pt 16,49 Co 9,96 N 14,20 H_2O 1,53	16,40 9,83 14,06 1,06
2.	$[\text{Co}(\text{DH})_2(\text{Anilin})_2]_2$ $[\text{PtBr}_4]$	1469,1	gelbbraune rhomb. Platten	Pt 13,27 Co 8,02 N 11,43	13,21 7,94 11,29
3.	$[\text{Co}(\text{DH})_2(\text{m-Cl-Anilin})_2]_2$ $[\text{PtBr}_4]$	1611	gelbbraune Dendryte	Pt 12,11 Co 7,31 N 10,42	12,00 7,16 10,21
4.	$[\text{Co}(\text{DH})_2(\text{m-Xylidin})_2]_2$ $[\text{PtBr}_4]$	1581,6	gelbbraune rhomb Platten	Pt 12,33 Co 7,45 N 10,62	12,19 7,17 10,46
5.	$[\text{Co}(\text{DH})_2(\text{p-Phenetidin})_2]_2$ $[\text{PtBr}_4]$	1645,3	Quadratischen braune Platten	Pt 11,85 Co 7,16 N 10,21	11,67 7,11 10,03
6.	$[\text{Co}(\text{DH})_2(\alpha\text{-Naphthylamin})_2]_2$ $[\text{PtBr}_4]$	1669,2	unregelmässige, kleine, braune krist.	Pt 11,68 Co 7,06 N 10,06	11,42 7,14 9,87
7.	$[\text{Co}(\text{DH})_2(\text{Thioharnstoff})_2]_2$ $[\text{PtBr}_4]$	1401,3	grosse, braune Tafeln	Pt 13,92 Co 8,41 N 15,98	13,81 8,39 15,69
8.	$[\text{trans-Co(en)}_2\text{Cl}_2]_2$ $[\text{PtBr}_4] \cdot \text{H}_2\text{O}$	1032,7	gelbgroße Nadeln	Pt 18,89 Co 11,41 N 10,66	18,82 11,30 10,84
9.	$[\text{trans-}[\text{Co(en)}_2\text{Br}_2]_2$ $[\text{PtBr}_4] \cdot \text{H}_2\text{O}$	1210,2	glänzende gelb- grüne Dendryte	Pt 16,12 Co 9,74 N 9,25	16,02 9,56 9,17
10.	$\text{trans-}[\text{Co(en)}_2(\text{NCS})_2]_2$ $[\text{PtBr}_4] \cdot \text{H}_2\text{O}$	1122,9	gelbbraune mikrokrist. Masse	Pt 17,37 Co 10,49 N 14,96	17,24 10,44 14,80
11.	$\text{cis-}[\text{Co(en)}_2(\text{NCS})_2]_2$ $[\text{PtBr}_4]$	1104,8	rotbraune mikrokrist. Masse	Pt 17,65 Co 10,66 N 15,20	17,44 10,60 15,04
12.	$\text{trans-}[\text{Co(pn)}_2(\text{NCS})_2]_2$ $[\text{PtBr}_4]$	1161,3	rotbraune, kleine unregel- mäss. Krist.	Pt 16,79 Co 10,15 N 14,46	16,68 10,07 14,30
13.	$\text{trans-}[\text{Co(pn)}_2\text{Cl}_2]_2$ $[\text{PtBr}_4] \cdot \text{H}_2\text{O}$	1088,9	grüne Dendryte	Pt 17,91 Co 10,82 N 10,28	17,84 10,67 10,06
14.	$\text{cis-}[\text{Co(en)}_2\text{Cl}(\text{m-Toluidin})]$ $[\text{PtBr}_4]$	836,1	rotbraune kleine unregelmäss. Krist.	Pt 23,33 Co 7,04 N 8,34	23,27 6,99 8,20
15.	$\text{cis-}[\text{Co(en)}_2\text{Cl}(\text{Benzylamin})]$ $[\text{PtBr}_4]$	836,1	rotbraune mikrokrist. Masse	Pt 23,33 Co 7,04 N 8,34	23,14 6,97 8,13

„en“ — Äthyldiamin; „pn“ — 1,2-Propyldiamin; „DH“ — deprotoniertes Dimethylglyoxim;
„ec. H₂“ — Äthyldiimino-bis-Acetylaceton

Die thermische Stabilität einiger Komplexsalze wurde auf thermogravimetrischem Wege untersucht. Diese Derivate sind beständig bis 150–220°C in Funktion der Natur des Komplexkations und zersetzen sich über diesem Temperaturbereich durch mehrere parallele und sukzessive nicht stöchiometrische Prozesse ohne Abbauzwischenprodukte. Das Endprodukt der Thermolyse um 800–900°C ist ein stöchiometrisches Gemisch von $\text{Co}_3\text{O}_4 + \text{Pt}$. Die thermische Stabilität der Tetrachloro-platinite (II) ist ein wenig grösser als jene der Tetra-bromo-platinite (II) mit demselben Kation.

Experimenteller Teil. $\text{K}_2[\text{PtCl}_4]$ und $\text{K}_2[\text{PtBr}_4]$ wurden aus $\text{K}_2[\text{PtCl}_6]$, bzw. $\text{K}_2[\text{PtBr}_6]$ im wässrigen Suspension durch Erhitzen mit Kaliumoxalat (Molarverhältnis: 1 : 1) erhalten. Die Hexahalogenate lösen sich nach 8–10 Stunden erwärmen und nach Abkühlen kristallisieren die Tetrahalogenate aus.

Zur doppelten Umsetzungreaktion wurden je 0,2–0,3 mMol $\text{K}_2[\text{PtCl}_4]$, bzw. $\text{K}_2[\text{PtBr}_4]$ in 30–35 ml Wasser und 3–4 mMol Komplexsalz in 30–50 ml Wasser, oder verd. Methanol verwendet. Die ausgeschiedenen kristallinen Substanzen wurden nach 15–30 Min Stehenlassen abgesaugt, mit Wasser gewaschen und an der Luft getrocknet.

Die Synthese der verwendeten Kobalt(III)-amine wurde in vorhergehenden Arbeiten beschrieben. **Analyse.** Das Platin wurde mikrogravimetrisch, der Kobaltgehalt nach Abtrennung des Platins komplexometrisch, in Anwesenheit von Murexidindikator, in Acetatpufferlösung, bestimmt.

LITERATUR

1. M. Vèzes, *Bul. Soc. Chim. France (3)*, **19**, 879 (1898).
2. R. Klement, *Z. anorg. Chem.*, **164**, 200 (1927).
3. I. L. Eilding, *Acta Chem. Scand.*, **24**, 1331, 1341 (1970); **24**, 1527 (1970).
4. A. K. Morgan, M. M. Jones, *J. Inorg. nucl. Chem.*, **35**, 275 (1972).
5. Yu. N. Kukushkin, V. A. Yurinov, *Zhur. neorgan. Khim.*, **18**, 182 (1973).
6. G. N. Sedova, L. N. Demachenko, *Zhur. neorgan. Khim.*, **26**, 435 (1981).
7. Yu. N. Kukushkin, V. B. Ukrainstev, *Zhur. neorgan. Khim.*, **17**, 2687 (1972).
8. B. Rosenberg, L. Van Camp, J. E. Trosko, V. H. Mansour, *Nature*, **222**, 385 (1969).
9. M.J. Cleare, J.D. Hoeschell, *Bioinorg. Chem.*, **2**, 187 (1973).
10. Cs. Värhelyi, I. Gănescu, *Stud. Univ. Babeş-Bolyai, Chem.*, **31**(2), 26 (1986).

SUITABILITY OF GRAPHITE ELECTRODES FOR COMBINATION WITH PLATINUM, IN BIAMPEROMETRIC INDICATION

USHA SHUKLA* and B. B. PRASAD*

Received: January 19, 1987

Biamperometric indication has been examined with the combination of platinum with different graphite electrodes utilising the couple iodine-iodide for aqueous and copper(II)-copper(I) for non-aqueous media. The impregnated ones yield better breaks and improved reproducibility.

Wax-impregnated graphite, in combination with a platinum electrode, has been adopted in recent years for biamperometric determination [1-4] employing the halogen and some of the non-halogen current indicating reversible couples; effect of the variation [5] in the polarising emf, and of interchange in the polarity has also been examined. Attempt is now made to explore the suitability of differently processed graphite electrodes from the standpoint of assessing the extent of its response towards sharpness of the equivalence point and reproductibility of the current values.

Experimental. The electrodes employed were of thin cylindrical shape having approximately equal cross-section ($\sim 40 \text{ mm}^2$) and consisted of the following — Electrode (A) was the graphite rod supplied by Union Carbide, India, and that cut from a pyrolytic solid block was (B); (C) and (D) were prepared in a mould using molten wax and graphite powder of respectively pyrolytic and nuclear grade samples. The electrodes (A) and (B) after careful cleaning were impregnated with molten wax, whereas (C) and (D) were employed as such. The tip of each of these, before use, was rubbed gently over zero number emery paper and kept dipping in distilled water when not in use.

The electrode assembly, being one of the above graphite and a micro-platinum electrode, was fitted in a rubber disc with a fixed inter-electrode distance ($\sim 3 \text{ cm}$).

The experimental procedure followed was essentially the same as reported earlier [1-4] and consisted of adding the titrant from a semimicro-burette to a known test amount in the titration cell and measuring the current at fixed polarising emf (25–300 mV) obtained from a battery-operated potentiometer. The solution was kept stirred throughout with a magnetic stirrer.

The combination with each one of the above graphite electrodes was examined both in aqueous as well as in non-aqueous media utilising the couples iodine-iodide and copper(II)-copper(I) respectively for the two cases.

All chemicals used were of analytical grade except otherwise stated; for the preparation and dilution to the titration volume (30 ml), exclusively the relevant solvent was used.

The test iodine solution was prepared, stored and standardised according to the recommended procedure [6].

Ascorbic acid (S.D. and Sarabhai) for aqueous medium was prepared by dissolving a weighed amount in double distilled water and for non-aqueous experiments by using a little warm glacial acetic acid first and then diluting with acetonitrile. Both of these were standardised [7] iodimetrically in aqueous medium.

Stock solution of uric acid (Sigma) was prepared using minimum amount of aqueous NaOH which before titration [8] was neutralised with HCl and the solution was made alkaline with sodium bicarbonate.

* Banaras Hindu University, Department of Chemistry, Varanasi – 221005, India

Solution of copper perchlorate was obtained from the sample (prepared for the purpose) following the recommended method [9] which consisted of adding a slight excess of perchloric acid (S.D., 70%) to a suspension of copper(II) carbonate in water and subsequent removal of carbon dioxide by boiling. The blue crystalline compound obtained on cooling was dried in vacuum. A weighed quantity was dissolved in acetonitrile to obtain the stock which was standardised iodometrically in aqueous medium.

For the first series of experiments involving iodine-iodide couple, the following two sets (i) and (ii) were selected: (i) where the couple existed from the beginning and vanished at the equivalence point and (ii) where the couple appeared just on completion of the oxidation. Estimation of iodine (5.9–72.60 mg) with ascorbic acid, constituted set (i) and that of uric acid (7.23–39.05 mg) with iodine, set (ii). The corresponding ranges of emf employed were 25–100 mV and 100–300 mV. Typical results are shown in Table 1 (i) and (ii); curves A and B in Fig. 1 represented the current-volume variations obtained with wax-impregnated Union Carbide sample and pyrolytic graphite rod.

In the second series of experiments, use was made of the acetonitrile medium for the estimation of ascorbic acid with copper perchlorate in the emf range 200–300 mV. The results are shown in the same Table 1 being separated in (iii) and by curves C and D (Fig. 1).

Instead of reproducing the comparative curves pertaining to any particular set of experiments with different graphite electrodes, only one from each has been selected with an intention to indicate simultaneously the general nature obtainable in different types of estimation as well and with large variation of emf.

Results and Discussions. It is apparent from the titration curves that though the above graphite electrodes are capable of adoption with the present technique, the raw ones after impregnation (A and B) yield better breaks. This has been seen in both the cases of disappearance and appearance of the couple. On the other hand, electrodes (C and D) prepared from the two varieties of graphite powder yield slightly greater current values. However, these lack many

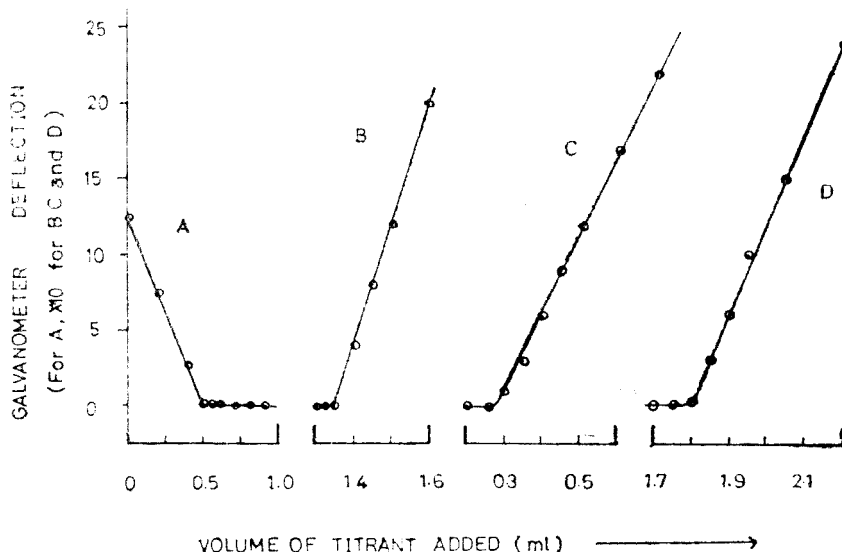


Fig. 1. Platinum Graphite Biampereometric Indication. Graphite electrode: A — Union Carbide, 5.9 mg Iodine, 50 mV; B — Pyrolytic, 5.97 mg Uric acid, 200 mV; C — Prepared from Pyrolytic, 10.74 mg Ascorbic acid, 250 mV; D — Prepared from Nuclear Grade, 28.87 mg Ascorbic acid, 300 mV.

Table 1
Platinum Graphite Biamperometric Indication

(A) Union Carbide Graphite		(B) Pyrolytic Graphite		(D) Prepared from Pyrolytic Graphite Powder		(D) Prepared from Nuclear grade Graphite Powder	
Amount of the substance (mg)							
Taken	Found	Taken	Found	Taken	Found	Taken	Found
(i) Aqueous Iodine; Applied emf — 50 mV							
5.92	5.95	6.02	6.01	6.25	6.24	6.20	6.18
17.70	17.70	18.05	18.04	18.75	18.75	18.74	18.71
(ii) Aqueous Uric Acid; Applied emf — 100 mV							
7.23	7.27	5.99	5.98	5.53	5.53	6.56	6.56
14.47	14.35	11.86	11.96	7.37	7.36	13.11	13.05
(iii) Non-aqueous Ascorbic Acid; Applied emf — 200 mV							
10.76	10.6	10.8	10.9	10.8	10.9	10.8	10.6
64.3	62.9	30.95	29.95	28.86	28.84	77.35	77.32

times exact reproduction especially at higher emf values in spite of the fact that the entire set of points in a particular run lies faithfully on the resulting titration curve.

It is seen further, that a higher emf is needed to obtain measurable current magnitudes in non-aqueous medium (200—300 mV) as compared to that in aqueous one (25—100 mV). The influence of increase in emf is found to enhance the current in all cases without affecting either the general nature of the curve or the location of the end point. In addition, use of impregnated graphite helps in improving the stability and the reproducibility of the current values and the reliability of estimation.

Acknowledgement. Our thanks are due to Profs. S. M. Verma and I. S. Ahuja, previous and present Head of the Department of Chemistry, for providing necessary facilities. Financial assistance in the form of a sanction for the scheme by University Grants Commission, New Delhi is gratefully acknowledged.

R E F E R E N C E S

1. B. B. Prasad, G. D. Khandelwal, M. I. Quraishi, M. M. Sharma, *Stud. Univ. Babes-Bolyai, Chem.*, **18**(2), 111 (1973).
2. B. B. Prasad, G. D. Khandelwal, *J. Sci. Res. B.H.U.*, **21**, 107 (1970—71).
3. D. Ghose, B. B. Prasad, *J. Electrochem. Soc.*, **32**, 295 (1983).
4. T. B. Singh, B. B. Prasad, *ibid.* **28**, 99 (1979); **29**, 141 (1980).
5. G. D. Khandelwal, M. I. Quraishi, B. B. Prasad, *J. Ind. Chem. Soc.*, **48**, 1053 (1971).
6. A. I. Vogel, "A Text Book of Quantitative Inorganic Analysis", London, Longmans Green and Co. Ltd., (1962).
7. A. Berka, J. Vulterin, J. Zykla, "Newer Redox Titrants", Pergamon Press Ltd., (1965).
8. M. R. F. Ashworth, W. Walish, *Z. analyt. Chem.*, **181**, 193—9 (1961); *Chem. Abstr.*, **55**, 23185e.
9. B. C. Verma, S. Kumar, *Talanta*, **24**, 694 (1977).

DISTRIBUTION COEFFICIENTS AND CATION EXCHANGE BEHAVIOUR OF Cd(II) AND Zn(II) IONS IN WATER-HYDROCHLORIC ACID AND ACETONE-WATER-HYDROCHLORIC ACID MEDIA

GHEORGHE MARCU*, LIVIA CRIVEI**, and NICOLAE PASCU**

Received: January 21, 1987

Cation exchange distribution coefficients with Vionit CS-3 (a sulfonated polystyrene cross-linked with 8% divinylbenzene) were determined for Cd(II) and Zn(II) in water-hydrochloric acid and acetone-water-hydrochloric acid media. In water-hydrochloric acid system, the acid concentration ranges from 0.1 to 2.0 M was covered. In acetone-water-hydrochloric acid system, the acid concentration ranges from 0.2 to 1.0 M and the acetone concentration ranges from 0 to 90% were covered. In both systems, Cd(II)-Zn(II) separation was achieved. A rapid and efficient separation method was given.

Introduction. The use of the ion exchange resins in view of the metal ions recovery and separation was proved to be efficient and economic, especially in the case of diluted solutions.

A great attention was paid to the cationic exchange studies and to the separations of different elements in the presence of complexing agents. The complexing agent is selected so that the strongly adsorbed metal ions should form the complexes less stable with the elution agent.

The complexing action of the hydrochloric acid [1, 2] was the basis of some separations of metal ions, by ion-exchange chromatography, taking into account different stability of the chlorocomplexes.

The use of organic solvent-mineral acid (HCl) mixture for the selective elution of the cations adsorbed on the ion exchange resins was investigated in [3-5].

Acetone one of the most used organic solvent, enhances the differences among the distribution coefficients of the cations, which constituted the basis of their separation into mixture.

In this paper, water-hydrochloric acid and acetone-water-hydrochloric acid solutions were used as complexing agents, for the elution and separation of the Cd(II) and Zn(II) ions adsorbed on the cationic exchange resin Vionit CS-3.

The investigation is based on the fact, that Cd(II) and Zn(II) are difficult to separate and the ion exchange constituted a simple and rapid method of separation, removing the precipitation and filtration operations and high consumption of the reagents.

* University of Cluj-Napoca, Faculty of Chemistry, 3400 Cluj-Napoca, Romania

** Institute of Chemistry Cluj-Napoca, 3400 Cluj-Napoca, Romania

Experimental. *Ion-Exchange Resin.* Indigenous, ion-exchange resin strongly acid cationit Vionit CS-3 (styrene copolymer of 8% divinylbenzene with sulphonic groups), 50–100 mesh particle size, in the H⁺form was used.

The H⁺ type cationit was purified by a method earlier described [6].

The air dried (~25°C) resin has the humidity of 35.38%; the ion-exchange capacity was of 4.25 mVal/g. of dried resin and 1.90 mVal/ml of wet resin.

The Ion-Exchange Column A: glass column of 1.7 × 20.4 cm was used.

Metallic Ion Solutions were prepared by dissolving the Cd(II) and Zn(II) sulphates or nitrates in distilled water. Cd(II) and Zn(II) ions were determined by titration with Complexon III solution, using Erio T as indicator [7].

Reagents. Hydrochloric acid, analytical-reagent grade (Merck, d = 1.19; minimum content 37%) Organic solvent: acetone, analytical-reagent grade (minimum content 99%).

Distribution Coefficients Measurements. The coefficients K_D for studied elements were determined by batch method and calculated according [6].

The measured amounts of H⁺ form resin (1.0 g) were stirred with 50 ml aqueous solutions of hydrochloric acid or hydrochloric acid-acetone of varied concentrations, containing the same amount of metallic ion (1 mmol cadmium or zinc).

For the ion exchange equilibrium establishment, the samples were stirred 24 hs. at room temperature (25°C). After the resin particles filtration, the solution was evaporated on a water bath to near dryness, for the acid and organic solvent removing, and the metal ion content was determined by [7].

The adsorption was achieved under a ratio q of resin loading:

$$q = \frac{\text{total amount of cations (in equivalents)}}{\text{Total amount of the resin (in equivalents)}} = 0.4$$

The solutions are so prepared, that the amount of water and organic solvent is expressed as percent by volume and the hydrochloric acid concentration as molarity.

Results and Discussion. Measurement of the distribution coefficients offers the possibility of choosing the suitable elution conditions.

For two cations separation, the elution conditions are chosen such [8] that, one of the cation has a high distribution coefficient (strongly retained by the resin) and the other cation has a low distribution coefficient (may be eluted from the resin).

From the data presented in Table 1, we observed that the distribution coefficient decreases with the increase of the hydrochloric acid concentration.

For Cd²⁺, the adsorbability is small at the hydrochloric acid concentrations higher or equal with 0.5 M. Cadmium form the chlorocomplex CdCl₃⁻, unretained by the cationic resin.

The positive ion of Zn²⁺, is retained by the resin, and a hydrochloric acid concentration equal to 2M, for complete desorption of zinc is required.

Table 1

Distribution coefficients in aqueous hydrochloric acid solutions at various concentrations and resin in H⁺ form (q = 0.4)

Concentration HCl (M)	Element	
	Cd	Zn
0.1	338.63	838.45
0.2	82.06	252.80
0.3	47.96	107.10
0.4	19.62	85.81
0.5	12.17	60.37
0.8	11.34	56.00
1.0	8.66	17.93
2.0	6.22	1.68

Table 2

Distribution coefficients in aqueous hydrochloric acid solutions containing acetone and resin in H^+ form

Acetone %	Cadmium			Zinc		
	HCl(M)			HCl(M)		
	0.2	0.5	1.0	0.2	0.5	1.0
20	72.12	13.62	1.27	305.39	97.00	12.11
40	60.03	11.60	1.02	294.20	56.02	9.52
60	9.37	9.20	0.60	70.31	38.12	4.27
80	6.77	8.91	0.50	30.43	20.50	1.31
90	4.21	5.35	0.20	28.92	21.50	0.90

periments, the separation of the two elements studied was achieved.

In Figure 1, the separation of cadmium (II) from Zinc (II) in aqueous solutions of hydrochloric acid is given: cadmium (II) ions were eluted with 280 ml 0.5 M hydrochloric acid solution, at an elution rate of 1.3 ml/minute; Zinc (II) ions were eluted with 250 ml 2.0M hydrochloric acid solution, at an elution rate of 5 ml/minute.

In Figure 2, the separation of cadmium (II) ions from zinc (II) ions in water hydrochloric acid-acetone solution is given: for the elution of Cd(II), 350 ml 0.5 M HCl in 30% acetone was used (elution rate 2.0 ± 0.5 ml/minute); for the elution of Zn(II), 350 ml 0.5 M HCl in 70% acetone was used (elution rate 3.0 ± 0.5 ml/minute).

On the same column (1.77×20.4 cm) and with the suitable elution rates, we achieved the separation of the mixture: Cd (57.2 mg) — Zn(32.3 mg).

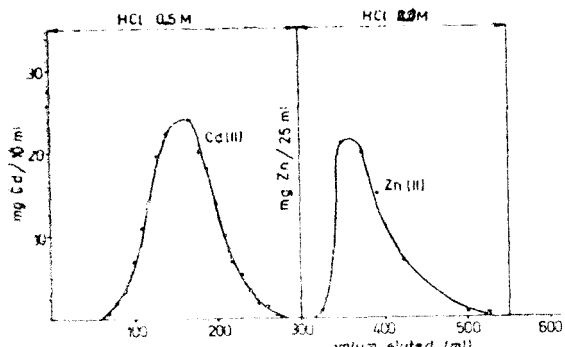


Fig. 1. Elution curve for Cd(II) and Zn(II) in aqueous hydrochloric acid solutions. Column of 50 ml (1.77×20.4 cm) Vionit CS-3, 50–100 mesh, resin in H^+ form. Elution rate 1.3 ± 0.5 ml/minute for Cd(II) and 5.0 ± 0.5 ml/minute for Zn(II). Cd 0.261 g; Zn 0.064 g.

The acetone effect on the distribution coefficients may be observed in Table 2.

At small acid and acetone concentrations, the K_D value is high, but with the increase of the solvent concentration, the K_D value decreases. This decrease is due to the formation of chlorocomplexes less retained by the resin.

Acetone offers suitable conditions for the separation of the metal ions at small hydrochloric concentrations.

Elution Curves. On the base of experiments.

On the base of experiments studied was achieved.

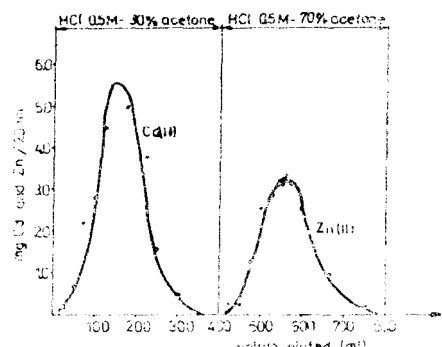


Fig. 2. Elution curve for Cd(II) and Zn(II) in water-hydrochloric acid-acetone solutions. Column of 50 ml (1.77×20.4 cm) Vionit CS-3, 50–100 mesh, resin in H^+ form. Elution rate 2.0 ± 0.5 ml/minute for Cd(II) and 3.0 ± 0.5 ml/minute for Zn(II). Cd 0.5 mmol; Zn 0.5 mmol.

Cd(II) with 300 ml 0.2M HCl in 60% acetone and Zn(II) with 350 ml 0.5 M HCl in 70% acetone.

Conclusions. The distribution coefficients for Cd(II) and Zn(II) on the Vionit CS-3 (a sulfonated polystyrene resin) were studied in HCl media or organic solvent (acetone) — HCl media and their separation conditions were established.

- in aqueous hydrochloric acid solution:
0.5 M HCl for cadmium (II) and 2.0 M HCl for zinc (II)
- in aqueous hydrochloric acid solution containing acetone:

0.5M HCl in 30% acetone } for Cd(II)
0.2M HCl in 60% acetone }

and

0.5M HCl in 70% acetone for Zn(II).

Cadmium and zinc ions were quantitatively retained on the Vionit CS-3 type resin and they might be eluted selectively and completely.

R E F E R E N C E S

1. F. W. Strelov, *Analyt. Chem.*, **32**, 1185 (1960).
2. F. Nelson, T. Murase și K. A. Kraus, *J. Chromatog.*, **13**, 505, (1964).
3. J. Korkisch și S. S. Ahluwalia, *Talanta*, **14**, 155, 1967.
4. S. P. Peterson, F. Terra și C. H. Morrison, *J. Radioanalyt. Chem.*, **2**, 115, (1969).
5. N. Pasca, V. Săcelean, L. Crivei, E. Kiss și N. Bojan, *Rev. Roumaine Chim.*, **17**, 505, (1972).
6. Gh. Marin, L. Crivei și N. Pasca, *Stud. Univ. Babeș-Bolyai, Chem.*, **31**, 27 (1986).
7. C. Liteanu, „Analiza chimică cantitativă — volumetria”, Ed. didactică și pedagogică, București, 1964, p. 596 și p. 597.
8. J. S. Fritz și T. A. Rettig, *Analyt. Chem.*, **34**, 1562 (1962).

CLASSIFICATION OF MINERAL WATERS BY PATTERN RECOGNITION PROCESSING OF CHEMICAL COMPOSITION DATA

DUMITRU DUMITRESCU* and LÁSZLÓ KÉKEDY**

Received: December 2, 1986

Classification of 30 native mineral waters has been attempted using a hierarchical fuzzy pattern recognition technique. The analytical chemical data of eight major components have been considered. Three distinct clusters have been obtained, revealing real differences in composition.

Pattern recognition techniques acquire extended applications in analytical chemistry for signal interpretation, for the interpretation of analytical chemical data (mainly for classification) as well as for solving general analytical chemical problems, e.g. selection of the best analytical method for a given analysis [1-8]. To our knowledge only two papers deal with the pattern recognition classification of waters [9,10]. The purpose of this paper is to attempt a classification of a group of Roumanian mineral waters on the basis of their chemical composition, using pattern recognition techniques.

A number of 30 waters were selected from three different geographical area of the country. The criterion of selection was to have analysis data concerning the same analytes. For identification the waters were labelled by a code number. The chemical composition of the waters selected is given in Table I [11], eight components being considered. From the Ca, Mg and Fe-ion content we computed the total hardness in german degrees, which of coarse was not considered in the classification calculations, serving only for the characterization of the clusters (classes) obtained. In our opinion the number of 30 waters as well as that of 8 components considered is great enough to obtain reliable classification results. Tentatively, classification calculations were made considering a smaller number of components omitting successively the components present in greater concentration in order to investigate the possible influence on the classification of analytes present in smaller concentrations. Thus calculations were performed considering successively only 7 constituents (mineralization omitted), 6 constituents (mineralization and HCO_3^- content omitted) or only 5 constituents (the previous ones and CO_2 content omitted), respectively.

The Classification Method. The most real-world classes being fuzzy in nature, a hierarchical fuzzy classification has been used. A class of patterns may be conceived as a fuzzy set. Let $X = \{x_1, \dots, x_n\}$ be a set of pattern vectors. Every pattern x_i is specified by the values of d features. The real number x_{ij} represents the value of the j -th feature with respect to x_i . In this way x_i is a vector in R^d . The cluster structure of the data set X may be given by a fuzzy partition of X . A fuzzy set A on X is a function $A : X \rightarrow \{0, 1\}$. $A(x)$ is the membership degree of x to the class A or the plausibility degree of the affirmation „ x is an element of A ”.

* University of Cluj-Napoca, Faculty of Mathematics-Physics, 3500 Cluj-Napoca, Romania

** University of Cluj-Napoca, Faculty of Chemistry, 3500 Cluj-Napoca, Romania

Table 1

Chemical composition of the waters (mg/l [11], total hardness in german degrees)

Code	HCO_3^-	Cl^-	Ca^{2+}	Mg^{2+}	Na^+	Fe^{2+}	CO_2	Mineralization	Total hardness
1	3568.5	58.4	629.9	224.5	202.5	7.6	1834.5	6703.40	140.6
2	1346.6	47.4	234.6	65.6	162.8	0.1	344.5	2312.29	48.0
3	1614.3	20.4	294.4	101.2	70.8	9.8	1653.4	3866.88	65.5
4	1985.3	22.2	393.6	107.9	98.0	1.95	2472.5	5183.41	80.1
5	2897.5	46.4	551.5	147.4	185.4	6.8	1760.6	5712.37	111.8
6	3019.5	51.7	580.5	118.0	250.1	13.4	2417.0	6563.11	109.8
7	2318.0	30.0	449.3	118.1	120.3	36.8	2087.2	5233.89	93.7
8	1758.7	14.2	409.8	68.9	56.9	15.9	2094.0	4508.75	74.8
9	2440.5	35.4	446.0	111.4	153.2	65.4	2296.4	5658.74	94.6
10	1739.3	15.9	359.6	97.5	69.9	2.3	2365.0	4745.05	73.0
11	1692.7	21.5	330.8	74.8	121.3	2.1	2085.7	4402.23	63.7
12	2360.9	40.8	436.7	139.7	130.2	4.0	2204.9	5429.78	93.7
13	2342.4	35.9	433.9	111.4	177.9	2.4	2520.4	5739.59	86.6
14	1738.5	19.8	335.9	102.1	82.9	3.0	1961.0	4323.88	70.8
15	2144.7	35.7	401.7	137.4	113.12	0.41	2333.0	5290.93	87.9
16	3849.1	76.5	588.2	168.4	470.7	5.5	1545.4	6873.37	121.6
17	4148.0	89.1	617.8	282.5	344.0	6.8	1476.6	7160.80	152.1
18	768.5	8.4	119.0	48.2	64.4	1.6	2500.0	5315.00	27.9
19	2220.0	815.6	315.0	118.0	720.0	40.4	1506.0	5911.00	75.3
20	1976.0	496.4	316.0	122.0	372.0	48.6	1804.0	5318.00	77.2
21	2318.0	851.0	360.0	1887.0	623.0	11.0	2112.0	6652.00	485.6
22	1464.0	266.0	218.6	95.6	262.0	35.0	1760.0	4258.00	56.1
23	549.0	106.0	72.4	0.0	139.8	15.4	1023.0	2016.6	11.7
24	390.0	88.6	41.0	10.0	133.5	3.0	3310.0	4079	8.3
25	964.0	189.0	10.8	6.2	464.6	6.2	0.0	1724	3.6
26	813.0	19.0	197.2	36.4	16.6	0.97	330.3	1447.74	36.1
27	817.4	0.2	198.6	40.0	6.5	1.5	312.2	1407.34	37.2
28	866.5	1.5	209.0	44.3	7.3	1.3	328.1	1489.96	39.6
29	827.8	1.9	214.3	39.2	5.7	1.1	0.0	1119.42	39.1
30	872.6	3.4	214.1	40.7	13.1	1.4	189.0	1355.14	46.8

The cluster substructure of a fuzzy class C may be described by a fuzzy partition of C [12]. The family A_1, \dots, A_n of fuzzy sets is a fuzzy partition of the fuzzy set C if, and only if:

$$\sum_{i=1}^n A_i(x) = C(x), \quad \forall x \in X \quad (1)$$

Let $P = \{A_1, \dots, A_n\}$ be a fuzzy partition of C . Every member (or atom) A_i of P represents a fuzzy class of points. A fuzzy class A_i is represented by a prototype $L_i \in R^d$. The dissimilarity between x_j and the prototype L_i is given by [11, 12]:

$$D_i(x_j, L_i) = (A_i(x_j))^2 d^2(x_j, L_i), \quad (2)$$

where d is a distance on R^d . The inadequacy $I(A_i, L_i)$ between the fuzzy class A_i and its prototype L_i may be defined as

$$I(A_i, L_i) := \sum_{j=1}^p D_i(x_j, L_i) = \sum_{j=1}^p (A_i(x_j))^2 d^2(x_j, L_i) \quad (3)$$

The inadequacy $J(P, L)$ between the fuzzy partition P and its representation $L = (L_1, \dots, L_n)$ is given by

$$J(P, L) = \sum_{i=1}^n I(A_i, L_i) = \sum_{i=1}^n \sum_{j=1}^p (A_i(x_j))^2 d^2(x_j, L_i) \quad (4)$$

The detection of the cluster substructure of the fuzzy class C reduces to the search for the partition P and its representation L which minimize the function J . The necessary and sufficient conditions to minimize P are given by

$$A_i(x_j) = \frac{C(x_j)}{\sum_{k=1}^n \frac{d^2(x_j, L_k)}{d^2(x_j, L_i)}}, \quad \forall j, i. \quad (5)$$

$$L_i = \frac{\sum_{j=1}^p (A_i(x_j))^2 \cdot x_j}{\sum_{j=1}^p (A_i(x_j))^2}, \quad \forall i. \quad (6)$$

Successive iterations with (5) and (6), starting with an arbitrary partition of C , lead to a solution. This iterative procedure will be called the Generalized Fuzzy Isodata (or FIG) [13, 14] algorithm.

We may now describe a divisive hierarchical clustering procedure which generates a fuzzy hierarchy [13]. A binary fuzzy partition A_1, A_2 of X is computed. If A_1 and A_2 don't represent „real” cluster, there is no structure in X . If A_1 and A_2 correspond to „real” clusters, then put $P^1 = \{A_1, A_2\}$. Using the FIG algorithm we compute a binary fuzzy partition for every member of P^1 . If the members (or atoms) of this fuzzy partition of A_i describe real clusters, they will be atoms in a new fuzzy partition P^2 of X . Otherwise A_i will be allocated to P^2 . A_i is marked in any way and remains unsplitted. For the atoms of P^2 non-marked, i.e. obtained by splitting the atoms of P^1 , the same procedure is used. P^l is the fuzzy partition of X at the decomposition level l . The process ends when no „real” clusters are obtained, i.e. two successive partitions are identical. The Fuzzy Divisive Hierarchical clustering algorithm (FDH) corresponding to this procedure is presented in detail in [12].

We admit that a binary fuzzy partition of C , $P = \{C_1, C_2\}$ describes „real” clusters if for either of its atoms there exists a pattern vector with the membership degree greater than 0.5 and $R(P) \geq t$. $R(P)$ is the polarization degree [12] of P and t is an appropriate threshold. $R(P)$ is defined by

$$R(P) = \frac{\sum_{j=1}^p (\bar{C}_1(x_j) + \bar{C}_2(x_j))}{\sum_{j=1}^p C(x_j)}, \quad (7)$$

where

$$\bar{C}_i(x) = \begin{cases} C_i(x), & \text{if } C_i(x) > 0.5 \\ 0, & \text{otherwise} \end{cases} \quad \forall x \in X \quad (8)$$

An appropriate value for t is 0.8.

For our problem $X = \{x_1, \dots, x_{30}\}$, where x_j is the sample vector corresponding to the j -th mineral water, i.e. x_j is the j -th line in Table 1. We have for example $x_{11} = 3568.5$, $x_{12} = 58.4$, $x_{13} = 629.9$. The FDH algorithm was programed in FORTRAN, for details see [12].

Results and Discussion. Considering 8 components, the above mentioned calculations yielded 3 clusters (Table 2), the waters being classified in 3 distinct classes (clusters). The twodimensional representation of the clusters is

Table 2

Clusters obtained considering 8 components, with the indication of degree of membership and the concentration of major components (mg/l; total hardness in german degrees)

Code	Degree of membership	HCO_3^-	CO_2	Mineralization	Total hardness
Cluster 1					
28	0.995	866.50	328.10	1489.96	39.6
26	0.994	813.00	330.30	1447.74	36.1
27	0.993	817.40	312.20	1407.34	37.2
30	0.990	872.60	189.00	1355.14	46.8
25	0.983	964.0	0.00	1724.0	3.6
29	0.976	827.80	0.00	1119.42	39.1
2	0.965	1346.60	344.50	2312.29	48.0
23	0.965	549.0	1023.0	2016.60	11.7
Cluster 2					
10	0.922	1738.30	2365.00	4745.05	73.0
15	0.894	2144.70	2333.00	5290.93	87.9
8	0.877	1758.70	2094.00	4508.75	74.8
7	0.860	2318.00	2087.20	5233.89	93.7
11	0.842	1692.70	2085.70	4402.23	63.7
20	0.822	1976.00	1804.00	5318.00	77.2
14	0.813	1738.50	1961.00	4323.83	70.8
12	0.761	2360.90	2204.90	5429.78	93.7
18	0.721	768.50	2500.00	5315.00	27.9
22	0.721	1464.0	1760.00	4258.00	56.1
4	0.690	1985.30	2472.50	5183.41	80.1
13	0.588	2342.40	2520.40	5737.59	36.6
3	0.586	1614.30	1653.40	3866.88	65.5
9	0.582	2440.50	2296.40	5658.74	94.6
24	0.524	390.00	3310.00	4079.00	8.3
Cluster 3					
1	0.873	3568.50	1834.50	6703.40	140.6
6	0.870	3019.50	2417.00	6563.11	109.8
16	0.804	3849.10	1545.40	6873.37	121.6
17	0.745	4148.00	1476.06	7160.80	152.1
5	0.725	2897.50	1760.60	5712.37	111.8
21	0.565	2318.00	2112.00	6652.00	485.6
19	0.523	2220.00	1506.00	5911.00	75.3

given in Fig. 1. For this purpose the selected characteristics were : total hardness (H) and mineralization (M). From the data of Table 2 it can be seen that the clusters correspond to groups of mineral waters with distinct characteristics as follows :

Cluster 1 : mineralization 1000–2000 mg/l, total hardness less than 50 degrees, CO_2 and HCO_3^- content small. The cluster is compact, the degree of membership of waters being between 99.5 and 96.5% respectively.

Cluster 2 : increased mineralization (3000–6000 mg/l), total hardness between 50 and 100 german degrees, higher CO_2 and HCO_3^- content than in the previous

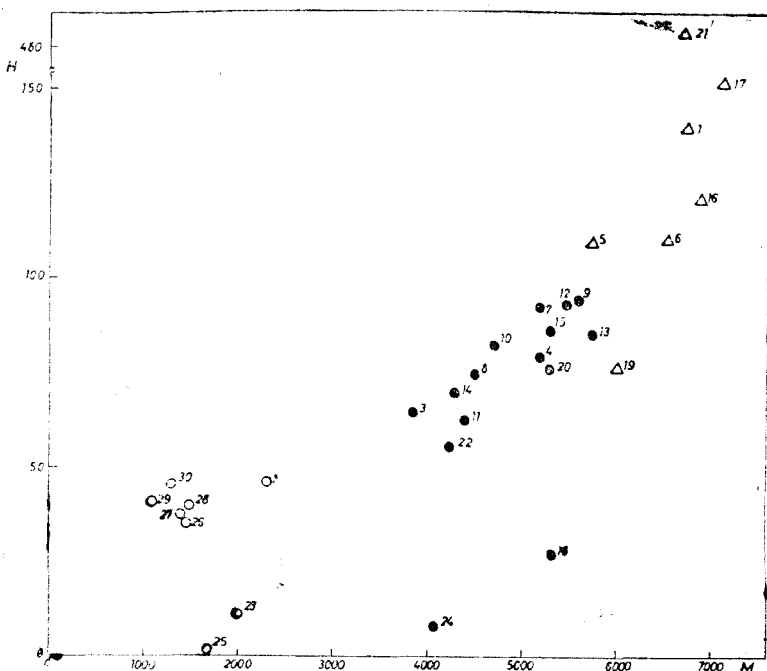


Fig. 1. Twodimensional representation of data from Table 2. Selected characteristics: total hardness (H) and mineralization (M).
 ○ — cluster 1; ● — cluster 2; △ — cluster 3

cluster. The cluster is less compact, the degree of membership of waters ranging between 99,2 and 54,4%. The waters 18 and 24 on the basis only of their HCO_3^- content would belong to cluster 1, but their high mineralization as well as their high CO_2 content group them in this cluster.

Cluster 3: mineralization higher than 6000 mg/l, total hardness greater than 100 degress, high CO_2 and HCO_3^- content as well.

Reducing gradually the components considered at the classification, no significant changes have been observed. Considering only 7 or 6 components, 3 clusters have been obtained again, cluster 1 remained unchanged, small modifications appearing in clusters 2 and 3 associated with the decrease of the degree of membership. Classification with 5 components yielded no clusters indicating that components present in small amounts do not influence the classification.

REFERENCES

1. B. R. Kowalski, *Analyt. Chem.*, **47**, 1152A (1975).
2. D. L. Massart, L. Kaufman, "The Interpretation of Analytical Chemical Data by the Use of Cluster Analysis", Wiley, Chichester, 1983.
3. K. Varminza, *Analyt. Chim. Acta*, **122**, 227 (1980).
4. I. Krüger, *Talanta*, **28**, 871 (1981).

5. G. Katemann, F. W. Pijspers, "Quality Control in Analytical Chemistry", Wiley, New York, 1981.
6. F. W. Pijspers, *Analyst*, **109**, 299 (1984).
7. "Pattern Recognition in Analytical Chemistry". Part B, Modern Trends in Analytical Chemistry. Ed. E. Pungor and G. E. Veress, Akadémiai Kiadó, Budapest, 1984.
8. G. E. Veress, *Trends in Analys. Chem.*, **1**, 16 (1982).
9. I. S. Scarminio, R. E. Burns, E. A. G. Zaggatto, *Energ. Nucl. Agric.*, **4**, 99 (1982).
10. J. H. M. Bartels, T. A. H. M. Janse, F. W. Pijspers, *Analys. Chim. Acta*, **177**, 35 (1985).
11. Ministerul Sănătății, „Indicații și contraindicații de trimitere la cură balneo-climatice”. Editura Medicală, București, 1975.
12. D. Dumitrescu, "Hierarchical Classification With Fuzzy Sets". University of Cluj-Napoca, *Fac. Math. Res. Seminars*, **4**, 36 (1984).
13. D. Dumitrescu, *Stud. Univ. Babeș-Bolyai, Ser. Math.*, **31**, 3 (1986).
14. D. Dumitrescu, Hierachial Pattern Classification, Fuzzy Sets and Systems. In the press.

TLC OF SOME DERIVATIVES OF FLUORENE

ILEANA OLTEANU*, FLORICA PAIU** and VALER FĂRCĂŞAN**

Received: January 28, 1987

The behaviour of some derivatives of fluorene and related compounds by TLC were followed and the chromatographic data correlated.

By the synthesis of certain new derivatives of fluorene (I) /1,2/ we followed the reactions and checked the purity of the obtained compounds by TLC.

The aim of this paper is to report and correlate some of these chromatographic data.

The TLC was performed on "Silicagel RFUV" plates manufactured by the Institute of chemistry Cluj-Napoca. As eluent toluene, ethanol or n-heptane were used.

Table 1 listed the data for fluorene (I) and of his derivatives substituted in position 2.

Table 1

The hRf values for compounds I ... XI



R	Compound	hRf values	Eluent
H	I	100	Toluene
NO ₂	II	79	Toluene
NH ₂	III	22	Toluene
NHOOC ₆ H ₅	IV	18	Toluene
NHOOC ₆ H ₅ O	V	10	Toluene
NHOOC ₄ H ₂ OBr	VI	24	Toluene
NHCSC ₆ H ₅	VII	47	Toluene
NHSO ₂ C ₆ H ₅	VIII	8	Toluene
NHSO ₂ C ₆ H ₄ NO ₂	IX	6	Toluene
NHSO ₂ C ₆ H ₄ NH ₂	X	0	Toluene
NHSO ₂ C ₆ H ₄ NHCOCH ₃	XI	23	Toluene+alcool
		0	Toluene
		15	Toluene+alcool

The hRf values for compounds I, IV, XII ... XV

Compound	hRf values	Eluent
	68	n Heptane
	66	n Heptane
	59	n Heptane
	21	Toluene
	20	Toluene
	16	Toluene

* Medical and Pharmaceutical Institute, 3100 Cluj-Napoca, Romania

** University of Cluj-Napoca, Faculty of Chemistry, 3400 Cluj-Napoca, Romania

As can be observed the presence of the functional groups determine a decrease of the R_f values.

The following correlations are focused on the interaction compound-stationary phase. Thus the more basic character of the aminogroup than that of nitro one, cause the stronger retention of III by comparison with II. The acylation of the amine leading to the very polar amido group strengthened the adsorption to the stationary phase (see e.g. III and IV). The same is valuable when the amine III is compared with the sulfonamide VIII.

It is interesting to observe that the furoyl-aminoderivative V has a lower R_f as the benzoyl amino one (IV) what suggests the participation of the heterocyclic oxygen in the interaction compound-stationary phase. The data reported by Franc [3] at the paper chromatography of the furoic acid supports this assumption. The difference between the 2-furoylaminofluorene (V) and 2-(5'-bromofurly) aminofluorene (VI) may be ascribed to a steric effect of the bromine atom which hindered the suited approach of the molecule-likely of the heterocyclic oxygen-to the silicagel surface. Such an explanation was proposed in a similar case [4].

The thioamide VII has a higher R_f as the amide IV owing to the lower polarity of the thioamido group.

In the sulfonamides series (VIII...XI) the insertion, in the para position of the phenyl residue, of the nitro- amino- or acetylaminogroups decrease the R_f in the expected order. The difference between the amino- (X) and p-acetylaminoderivative (XI) become visible only if a mixture of toluene and ethanol (100:5) was used as eluent.

The fluorene (I) can be considered as a derivative either of diphenylmethane (XII) or of biphenyl (XIII). For this reason we considered of interest to compare the chromatographic behaviour of these three compounds (I, XII and XIII) as well as of their corresponding benzoyl amino-derivatives (IV, XIV and XV).

The data listed in table 2 show a very small difference between the supposed parent compounds XII and XIII, respectively XIV and XV. The ring closure passing from XII or XIII to I and from XIV and XV to IV bring about a decrease of the R_f, id est an increase of the ability of in this way built up compounds I and IV, to become adsorbed.

The chromatography of compounds I [5], XII [6] and XIII [7] was reported earlier but in another conditions and context.

Syntheses of the compounds. The compounds II [8], III [1], IV [1], V [1], VII [1], VIII [2], IX [2], X [2], XI [9], XIV [10] and XV [11] were prepared after literature data.

2-/(5'-bromofuroylamino(2')/fluorene (VI). To a solution of 0.9 g 2-aminofluorene (III) in 15 ml pyridine a solution of 1 g 5-bromo-2-furoyl chloride (XVI) in 15 ml pyridine was added. The mixture was warmed on the steam bath for 30 min. and then poured into 350 ml water acidulated with 20 ml concentrated hydrochloric acid. The precipitate was filtered, washed with water and dried. After recrystallization from 30 ml glacial acetic acid and then from 20 ml DMFA, 0.7 g (41%) pure product were obtained. Brown crystals, m.p. 235 °C C₁₈H₁₂NO₂Br (354.02).

Calcd. N 3.95 Found N 4.5

R E F E R E N C E S

1. V. Fărcăşan, F. Paiu, I. Olteanu, H. Demian, *Stud. Univ. Babeş-Bolyai, Chem.*, **30**, 5 (1985).
2. V. Fărcăşan, I. Olteanu, I. Mester, V. Chiorean, *Stud. Univ. Babeş-Bolyai, Chem.*, **30**, 4 (1985).
3. J. Franc, *J. Chromatog.*, **3**, 317 (1960).
4. V. Fărcăşan, I. Balázs, F. Paiu, *Stud. Univ. Babeş-Bolyai, Chem.*, **2**, 75 (1967).
5. Cayana, M. Rosa, *Riv. Merceol.*, **19**, 113 (1980).
6. W. V. Saeger, E. O. Thompson, *Environ Sci. Technol.*, **14**, 705 (1980).
7. A. Rajzman, H. Heller, *Pestic. Sci.*, **3**, 457 (1972).
8. W. E. Kuhn, "Synthèses organiques" Coll. vol. II, 424 (1949).
9. J. C. Somaglino, *Rev. Fac. Cienc. quim.*, **16**, 227 (1941).
10. A. W. Hofmann, *Liebigs Ann. Chem.*, **132**, 166 (1864).
11. O. Fischer, H. Schmidt, *Ber. dtsch. chem. Ges.*, **27**, 2786 (1894).

PARTICULARITES DE L'AGITATION DES SYSTEMES GAZ-LIQUIDE APPLICATIONS DANS LA CONSTRUCTION DES BIORÉACTEURS

GHEORGHE D. PASAT*, CĂLIN I. ANGHEL** GHEORGHE MENCINICOPUSCHI*** et VIOLETA
D. ANGHEL****

Manuscrit reçu le 30 Janvier 1987

Specific features of mixing for gas-liquid systems. Bendings for designing of biochemical reactors. A study based on experiments and on literature for stir absorbed power evaluation on biosynthesis receptacle is presented. The study serves for fundamental base as a theoretical foundation for practical relations necessary on designing chemical and biochemical reactors fitted with turbine stirrer.

1. Généralités. Au stade actuel de l'utilisation des processus physico-chimique on remarque un développement exponentiel des technologies qu'impliquent l'agitation. Cette évolution impose la diversification des types de réacteurs (Fig. 1) et des dispositifs d'agitation (Fig. 2).

Au cours des dernières années on remarque dans ce domaine là, tant dans notre pays qu'au niveau mondial, deux tendances.

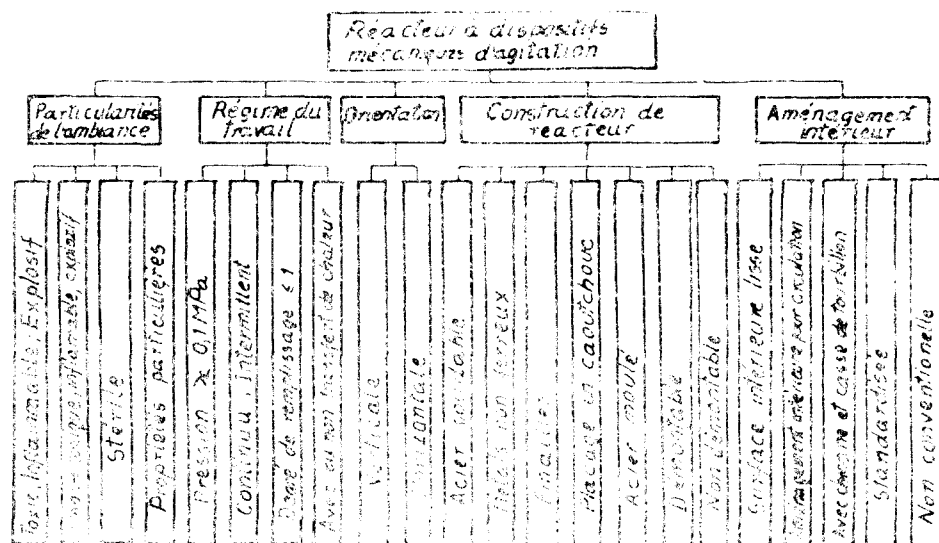


Fig. 1.

³ L'Institute Politehnique de Bucarest, Département d'Ustige Chimique, 7000 Bucarest Roumanie

**** Université de Cluj-Napoca, Faculté de Chimie, 3700 Cluj-Napoca, Roumanie**

*****) Institut de Chimie Alimentaire de Bucarest, 7400 Bucarest, Roumanie**

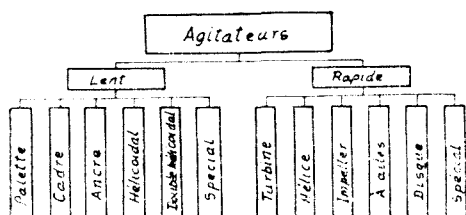


Fig. 2.

jets techniques et, implicitement, des investissements.

La deuxième tendance, spécifique aux entreprises et aux firmes spécialisées dans la réalisation des projets techniques et dans la réalisation des réacteurs à dispositifs d'agitation s'est matérialisée dans la construction de quelques appareils spécialisés qui peuvent travailler dans les conditions spécifiques à efficacité maximale, permettant ainsi l'amortissement rapide de l'investissement. Cette tendance, se manifeste particulièrement dans la réalisation des réacteurs destinés aux processus de biosynthèse, les bioréacteurs.

En présentant les types les plus nouveaux de bioréacteurs, Schügerl /13/, affirme que la tendance de spécialisation demandée par le type de processus de biosynthèse sera amplifiée.

2. L'agitation des systèmes gaz-liquide. L'agitation des systèmes gaz-liquide comprend des applications multiples dans les processus d'absorption comme les bioprocessus aérobies, par exemple, l'épuration de l'eau, l'hydrogénéation catalytique des huiles végétales, l'oxydation des hydrocarbures etc.

Pour l'agitation des systèmes gaz-liquide, les aspects suivants sont essentiels :

- la dispersion du gaz, respectivement le degré de distribution des bulles de gaz
- la durée de séjour du gaz dans le récipient
- la dispersion et la coalescence des bulles de gaz
- le spectre hydrodynamique de l'écoulement induit par l'agitateur
- la puissance requise de l'agitation
- le transfert de la matière à l'interface gaz-liquide.

La distribution des bulles de gaz dans le domaine liquide peut être appréciée par le diamètre moyen des bulles, d_s , nommé aussi, diamètre Sauter /16, 17/ :

$$d_s = \frac{\sum_i^N d_{si}^3}{\sum_i^N d_{si}^2} \quad (1)$$

Le diamètre des bulles et leur dispersion est fonction de la région où se produit la bulle /18/ et de la géométrie du réacteur /17, 19-21/.

En étudiant la dispersion du gaz dans les réacteurs équipés avec des chicanes et distributeurs circulaires de gaz, Shah définit le diamètre Sauter par la relation suivante :

$$d_s = C \cdot Q^m (\eta g / \gamma_L)^{0.25} \sigma^{0.6} (P/V)^{-0.5} \rho_L^{-0.2} \quad (2)$$

La première tendance consiste dans une solution fonctionnelle-constructive avec un niveau élevé d'universalité, dans les conditions d'une bonne efficience, ce que conduit à la réalisation de quelques réacteurs chimiques et/ou biochimiques multifonctionnels. Cette tendance se reflète dans la standardisation des réacteurs à dispositifs d'agitation /1-12/, ce que permet la diminution des coûts des projets techniques et, implicitement, des investissements.

Le terme $\sigma^{0,6}(P/V)^{-0,4}\rho_L^{-0,2}$, est le résultat de l'hypothèse que le numéro de Weber (We) est constant dans les conditions de la turbulence isotropique.

Nagata /20/, Brujin /23/ si van't Riet /24/ ont démontré que pour réaliser la dispersion uniforme du gaz este nécessaire d'atteindre un nombre de tours critique de l'agitateur, n_L ;

$$n_L = \left[A + B \left(\frac{d}{D} \right) \right] \cdot \frac{(\sigma/\rho_L)^{1/4}}{d} \quad (3)$$

$A = 1,22$; $B = 1,25$ — dans le cas des turbines standard (Rushton).
 $A = 2,25$; $B = 0,68$ — dans le cas des agitateurs à ailes.

Pour dimensionner les réacteur équipés à dispositifs mécaniques d'agitation et dans les conditions de l'aérage du système liquide, s'impose de connaître l'aire de l'interface gaz-liquide, a . Après une vaste documentation et selon ses progrès expérimentations, Wiedmann /29/, évalue l'aire de l'interface, a , comme :

$$a = \frac{6f\zeta}{d_s} \quad (4)$$

Le facteur de correction, f , introduit dans la relation (4) l'influence de la géométrie de la bulle de gaz sur l'aire de l'interface.

Dans les conditions particulières de l'agitation des systèmes gaz-liquide ne doit pas négliger le phénomène „d'agglomération du gaz” /17, 23, 25/ dans les régions des éléments du dispositif d'agitation. Autour des palettes de la turbine se forment des cavités de gaz. Van't Riet considère qu'en fonction de la vitesse périphérique de l'agitateur y existe trois types de cavités (Fig. 3) : tourbillonnaire, d'adhérence et totale, chacune de trois ayant une influence dans le fonctionnement du dispositif d'agitation /27/.

La présence du gaz dispersé dans le liquide modifie le spectre d'écoulement induit par l'agitateur et a des effets sur la puissance requise de l'agitation et sur la géométrie de l'agitateur.

On peut donc adapter les relations mathématiques bien établies dans le cas de l'agitation des liquides, pour les conditions spécifiques aux systèmes gaz-liquide. Les facteurs qu'intervient dans le processus d'agitation des systèmes gaz-liquide changent leurs valeurs (Tension de cisaillement, densité, tensions superficielles).

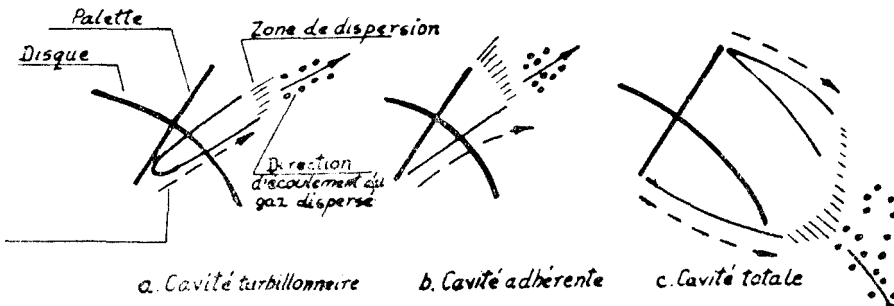


Fig. 3. Modèles de cavité.

La littérature indique les relations /14, 15/ que permettent de déterminer la puissance requise du dispositif d'agitation dans les conditions de l'aérage du système liquide. La puissance requise est dépendante des dimensions géométriques du réacteur et des caractéristiques du milieu réactif.

Dans le présent ouvrage les auteurs se proposent de clarifier le problème de l'influence du débit de gaz sur la puissance requise du dispositif d'agitation, dans les conditions de la modification de la géométrie du dispositif d'agitation. C'est pourquoi on a sélectionné un vaste matériel bibliographique et on a organisé un programme d'expérimentation propre. On propose des relations mathématiques spécifiques à la réalisation des projets techniques pour les réacteurs chimiques et biochimiques dotés à dispositifs mécaniques d'agitation, type turbine standard.

3. Le programme d'expérimentation et la méthode de travail.

Le plan général d'expérimentation tient compte que les processus caractérisés par irréversibilité ont un seul sens possible d'évolution, spécifique aux milieux de biosynthèse. Les plans expérimentaux ont une seule séquence possible — la variable (les variables) se modifie graduellement d'une valeur limite, inférieure d'habitude, à l'autre valeur limite.

Le procédé classique d'expérimentation par l'étude de la variation ordonnée-successive des variables, spécifique aux processus déterminés par plusieurs variables, consiste dans la détermination, par des expérimentations — test, de l'influence des variables indépendantes sur la fonction étudiée.

De ce qui précède, on a établi deux groupes des variables :

- variables majeures : le nombre de tours de l'agitateur, n , le débit d'air, q ;
- variables mineures : le diamètre de l'agitateur, d , les caractéristiques physiques englobant aussi la rhéologie du milieu, ρ et η , le nombre d'agitateurs, N , le diamètre du récipient, D etc.

L'utilisation de l'analyse dimensionnelle et de la normation fait possible de réduire le nombre des variables :

- majeures : le critère de Reynolds, Re et le débit rapporté de gaz, Nq
- mineures : rapports des dimensions géométriques

$$\left(\frac{1}{D}, \frac{H}{D}, \frac{h_1}{D} \text{ etc} \right)$$

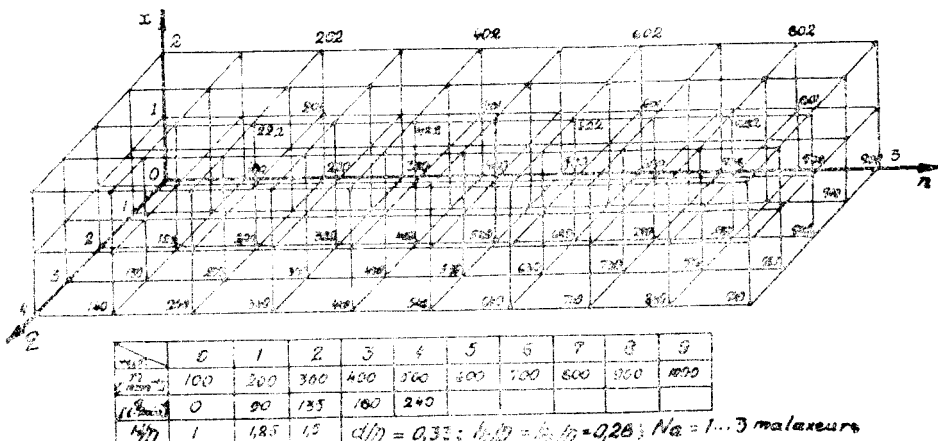


Fig. 4. Planification de l'expérimentation.

A la suite, on a adopté le plan expérimental classique-partial [27], (fig. 4) avec les observations suivantes :

a. Les variables $\frac{h_1}{D}$, $\frac{h_2}{D}$ et N_Q doit être mises en corrélation avec la variable $\frac{H}{D}$.

b. Les limites de variation, des variables sont établis en fonction de : caractéristiques géométriques recommandées dans la littérature de spécialité :

$$\left(\frac{h_1}{D}, \frac{h_2}{D}, \frac{d}{D} \right),$$

caractéristiques du stand expérimental ($100 \leq n \leq 1000$ rot/min; $\frac{H}{D} = 1 \dots 1,5$; $D = 0,24$ m), caractéristiques des appareils à mesurer ($q = 0 \dots 240$ l/min).

c. On a réalisé le plan expérimental aléatoirement pour l'eau et les solutions de Na-CMC et ordonné — successivement pour le milieu de biosynthèse.

Pour déterminer la puissance requise de l'agitateur, le dispositif a fonctionné sans charge et pour fonder statistique les résultats expérimentaux, on a effectué des séries de cinq déterminations pour les mêmes valeurs des paramètres, pour des données caractéristiques bien différentes.

4. Résultats expérimentaux. En suivant le plan expérimental et la méthode de travail présentés jusqu'ici, on a déterminé la puissance requise de l'agitateur en fonction des paramètres hidrodynamiques précisés.

Les données expérimentales sont illustrées par des graphiques utiles à la réalisation des projets techniques des réacteur chimiques et biochimiques équipés à dispositifs mécaniques d'agitation. On mette en évidence l'influence combinée du débit de gaz et des autre paramètres hydrodynamiques sur la puissance requise de l'agitation.

a. *La puissance requise rapportée.* Cette influence se manifeste par l'abaissement brusque de la puissance rapportée ($\Delta P_g / \Delta P_0$) requise par l'agitation, dans les conditions de l'augmentation du débit rapporté de gaz. N_Q . On remarque que pour $N_Q < 175 \cdot 10^{-3}$, $\Delta P / \Delta P_0$ se situe autour des valeurs $0,2 \dots 0,3$ (fig. 5). Ce abaissement est l'effet de la présence du gaz dans le milieu réactif qui abaisse la résistance hydrodynamique opposée par le milieu contre l'avancement de l'aile de l'agitateur. (c'est parce que la viscosité apparente abaisse). Une autre cause de ce abaissement est la naissance et l'extinction des cavités de gaz autour des ailes de l'agitateur. L'augmentation du débit de gaz dispersé par la turbine est suivie par l'extinction des cavités, donc, la distance traversée par l'aile, dans le milieu liquide à grande viscozité, abaisse. On peut dire que la résistance hydrodynamique peut être appréciée comme la moyenne des résistances qui s'opposent à l'avancement dans deux milieux bien différents — liquide et gaz. Dans ces conditions on remarque des discontinuités dans le fonctionnement du dispositif d'agitation qui souffre le changement de son propre état de vibration.

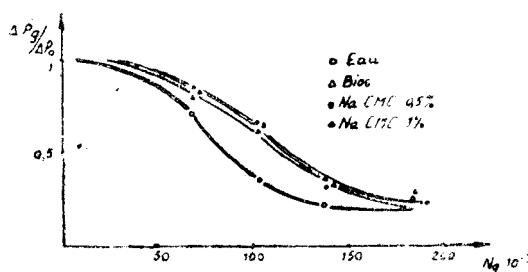


Fig. 5. Dépendance de puissance rapportée.

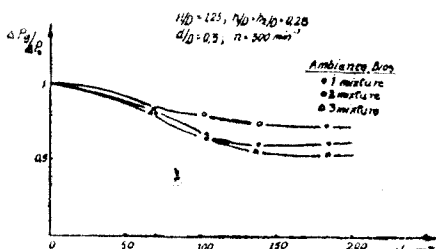


Fig. 6. Dépendance de puissance rapportée.

et l'apparition de certaines vibrations dans la suite des phénomènes de dispersion et de coalescence.

Pour des valeurs $T/D > 1$, on recommande d'utiliser plusieurs agitateurs identiques. On a déterminé le rapport $\Delta P_g/\Delta P_0$ dans le cas de $N_a = 1 \dots 3$ agitateurs. Quand on utilise deux agitateurs, $N_a = 2$, les valeurs $\Delta P_g/\Delta P_0$ sont plus grandes que pour les autres deux valeurs du N_a [22], (fig. 6) Les différences $\Delta P_g/\Delta P_0$ obtenues sont tant mieux évidentes que le débit de gaz est plus grand. L'augmentation du rapport $\Delta P_g/\Delta P_0$, quand on utilise deux agitateurs, peut être expliquée par ce que le placement du distributeur de gaz se réalise presque tout entière par le distributeur, pendant que l'agiteur supérieur contribue seulement à l'agitation de la phase liquide. Ce phénomène est dû au spectre d'écoulement caractéristique à la turbine (absorption axiale, ascendante et/ou descendante et refoulement radial) parce que l'agiteur inférieur disperse le gaz à une surface assez grande par rapport de l'axe du dispositif d'agitation et c'est pourquoi l'absorption axiale du gaz par l'agiteur supérieur est presque impossible.

Les expériences ont démontré que l'emplacement d'un autre agiteur (le troisième) conduit à l'abaissement des valeurs du rapport $\Delta P_g/\Delta P_0$. L'abaissement du rapport $\Delta P_g/\Delta P_0$ est le résultat de l'autoaspiration du gaz qui se trouve au-dessus de la surface libre du milieu soumis à l'agitation par la turbine supérieure. Le phénomène d'autoaspiration est favorisé par l'apparition de certains microtourbillons centraux qui se forment à cause de la distance relativement réduite qui existe entre l'agiteur supérieur et la surface libre, même dans les conditions de l'utilisation des chicanes [27].

b. *La puissance spécifique requise de l'agitation.* On peut déterminer la puissance spécifique requise de l'agitation en rapportant la puissance requise de l'agitation au volume total du milieu soumis à l'agitation :

$$\Delta p_g = \frac{\Delta P_g}{V}, \text{ /Kw} \cdot \text{m}^{-3} \quad (5)$$

La quasitotalité des résultats expérimentaux démontrent que pendant que le débit de gaz augmente, pour le même volume de liquide, la puissance spécifique, Δp_g , abaisse, (fig. 7).

On remarque que pour des débits grands de gaz, la puissance spécifique, Δp_g , a une tendance d'abaissement et l'hauteur relative, H/D , du milieu réactif, abaisse aussi.

Dans les expérimentations effectuées sur le milieu de biosynthèse (bios), on a observé que l'augmentation du débit de gaz produit l'écoulement du milieu accompagné de l'augmentation de la puissance requise de l'agitation, dans les conditions de l'augmentation du volume „apparent” soumis à l'agitation. Pour limiter la tendance d'écoulement, on a ajouté des agents antimoussants. Dès ce moment, on a observé l'abaissement de la puissance requise à valeurs antérieures de l'écoulement dans le fonctionnement du dispositif d'agitation et de coalescence.

On a conclu qu'en utilisant des volumes grands du système gaz-liquide, dans les conditions d'une véhiculation des grandes quantités de gaz, la puissance spécifique, ΔP_g , a des valeurs très réduites.

5. Conclusions. L'évaluation de l'influence du débit de gaz sur la puissance requise de l'agitation implique des expérimentations d'une grande complexité.

Pour la réalisation des projets techniques on construit des modèles de laboratoire et dans les conditions expérimentales et respectant les conditions de la similitude géométrique, on construit des diagrammes $\Delta P_g/\Delta P_0 = f(q)$ ou $\Delta P_g = f(q)$. À la suite, on transpose le modèle de laboratoire et les résultats à échelle industrielle.

On remarque que dans les conditions de sécurité maximale (substances misibles, toxique ou explosives), pour la réalisation du projet technique du dispositif d'agitation, on néglige le débit de gaz et on emploient les relations mathématiques établies pour l'agitation des systèmes liquides.

Notations :

a	— aire de l'interface, m^2
A, B	— constantes (rel. 3)
C	— constante (rel. 2)
d	— diamètre de l'agitateur, m
D	— diamètre du récipient, m
d_s	— diamètre Sauter
f	— facteur de correction
h_1	— hauteur d'emplacement de l'agitateur, m
h_2	— écartement des agitateurs, m
H	— hauteur du milieu réactif, m
m	— indice (rel. 2)
n	— nombre de tours de l'agitateur, $\text{rot} \cdot \text{min}^{-1}$
n_L	— nombre de tours critique (rel. 3), $\text{rot} \cdot \text{min}^{-1}$
N_a	— nombre d'agitateurs
P	— puissance requise de l'agitateur, Kw
ρ_g	— puissance spécifique requise de l'agitateur, $\text{Kw} \cdot \text{m}^{-3}$
V	— volume du milieu réactif, m^3
η	— viscosité dynamique, $\text{Pa} \cdot \text{s}$
φ	— densité, $\text{Kg} \cdot \text{m}^{-3}$
T	— tension interfaciale, $\text{N} \cdot \text{m}^{-2}$
q	— débit du gaz, m^3
E_u	— nombre d'Euler
N_Q	— critère du débit de gaz
Re	— nombre de Reynolds
We	— nombre de Weber

Indices :

L	— liquide
g	— gaz

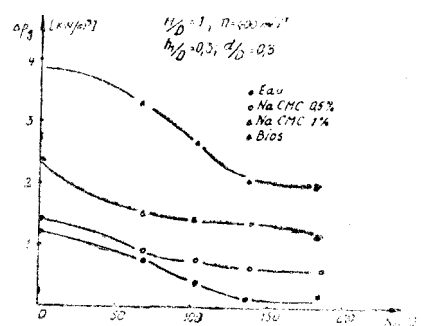


Fig. 7. Dépendance de puissance volumétrique.

B I B L I O G R A P H I E

1. Z. A. Vasil'ev, V. G. Ušakov, "Apparatufl dlia peremešivania jidkikh Sred", Mašinostroenie, Leningrad, 1979.
2. * * * — STAS 5454-76. Amestecătoare verticale. Clasificare — tipizare.
3. * * * — STAS 10.591-76. Brațe pentru amestecătoare verticale.
4. * * * — STAS 10.592-76. Elice pentru amestecătoare verticale.
5. * * * — STAS 10.593-76. Ancoră simplă pentru amestecătoare verticale.
6. * * * — MICH—IITPIC—NID 7816-80. Dispozitive de amestecare. Impellere și spârgătoare de virtej.
7. * * * GOST 26-01-1422-75. Apparatufl germetichniie s mehaniceskim peremesivaiojim ustroistvom s ecranirovannim electropirodom. Objje tchniceskie uclovicia.
8. * * * GOST 26-01-1244-75. Apparatufl s mehaniceskimi ustroistvami, verticalinie, etalnje. Objje tchniceskie uclovicia.
9. * * * — GOST 20.680-75. Apparatufl s mehaniceskimi peremešivaiojim ustroistvami, verticalnje. Tipi i osnovnie parametrii.
10. * * * — TGL 22.102 — Chemieansrüstungen. Rührwerkanschluss für Seitentrieb.
11. * * * — TGL 22.101 — Chemieansrüstungen. Rührmaschinen senkrecht mit Behälter aus Stahl. HauptKennwerte.
12. * * * — DIN 28.130 — Rührbehälter mit Rührwerk. Beuthvertrieb, 1972.
13. K. Schägerl, *Chem. Ing. Tech.*, **52**, 951 (1980).
14. Gh. Mencinicopski, M. Bâldea, Al IV-lea simpozion de microbiologie industrială, Galați, 177 (1984).
15. Gh. D. Pasat, Gh. Mencinicopski, M. Bâldea, Al V-lea Simpozion de microbiologie industrială, Iași, 833 (1985).
16. J. B. Joshi, A. B. Prandt, M. M. Sharma, *Chem. Eng. Sci.*, **37**, 813 (1982).
17. M. Bruxelmane, *Rev. Ferm. Ind. Alim.*, **18**, 35 (1985).
18. H. T. Luong, B. Voleski, *Amer. Inst. Chem. Eng., J.*, **25**, 893; (1979).
19. S. Sicardi, R. Conti, Cr. Boldi, L. Franzino, *Chem. Ing. Tech.*, **53**, 67 (1981).
20. S. Nagata, "Mixing. Principles and applications", J. Wiley and Sons, New York, 1975.
21. H. L. Young, L. Sydney, "Annual Reports on Fermentation Processes", Academic Press, New York, **6**, 101 (1983).
22. J. H. Shah, *Amer. Inst. Chem. Eng., J.*, **28**, 853; (1982).
23. W. Brujin, K. van't Riet, J. M. Smith, *Trans. Inst. Chem. Eng.*, **52**, 101 (1978).
24. K. van't Riet, J. M. Smith, *Chem. Eng. Sci.*, **28**, 13 (1973).
25. J. A. Wiedmann, A. Steiff, P. Weinsbach, *Germ. Chem. Eng.*, **4**, 125 (1981).
26. H. O. Möchel, *Chem. Tech.*, **33**, 344 (1983).
27. Gh. D. Pasat, Teză de doctorat, Institutul Politehnic, București, 1986.

THE BIOLOGICAL ACTIVITY OF SOME SCHIFF'S BASES OF 4-AMINO-BIPHENYL AND 2-PHENYL-4-(p-AMINOPHENYL) THIAZOLE

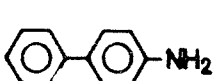
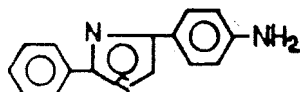
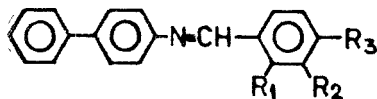
RADU DUMITRU POP, ADRIANA DONEA*, VASILE CHIOREAN and VALER FĂRCĂŞAN*

Received: February 4, 1987

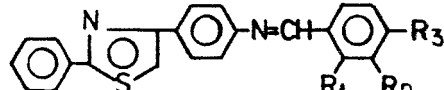
The antimicrobial activity of two series of Schiff's bases, derivatives of biphenyl, III, and of 2,4-diphenylthiazole, IV, against four bacteria strains were studied by the diffusion test procedure. The Hansch method was used for chemical structure — antibacterial action quantitative correlation.

In previous papers [1, 2] we reported the synthesis of some Schiff's bases of 4-aminobiphenyl (I) and 2-phenyl-4(p-aminophenyl) thiazole (II), namely compounds III_{a,c...f,h...j} and IV_{a,c...f,h...j}.

In the present work we describe the preparation of compounds III_{b,z} and IV_{b,g}.

*I**II*III *a...f*

<i>R</i> ₁	<i>R</i> ₂	<i>R</i> ₃
<i>a</i> : H	H	H
<i>b</i> : NO ₂	H	H
<i>c</i> : H	NO ₂	H
<i>d</i> : H	H	NO ₂
<i>e</i> : NO ₂	H	NO ₂

IV *a...j*

<i>R</i> ₁	<i>R</i> ₂	<i>R</i> ₃	<i>R</i> ₁	<i>R</i> ₂	<i>R</i> ₃
<i>f</i> : H	H	H	H	H	Cl
<i>g</i> : H	H	H	H	H	OH
<i>h</i> : H	H	H	H	H	OCH ₃
<i>i</i> : H	H	H	H	H	N(CH ₃) ₂
<i>j</i> : H	H	H	H	H	CH ₃

Taking into account the multiple biological activity of aromatic Schiff's bases reported as antimicrobials (e.g. [3]), pesticidals (e. g. [4]), fungicidals (e. g. [5]), citostatics (e. g. [6]), tuberculostatics (e. g. [7]) or oestrogenes (e. g. [8]) as well that of some compounds with biphenilic skeleton (e.g. [9...12]), we considered of interest to test the biological behaviour of the compounds III and that of the analogous one IV, where a thiazole ring is inserted between the two phenyl rings.

* University of Cluj-Napoca, Faculty of Chemistry, 3400 Cluj-Napoca, Romania

The microbiostatic activity of these compounds was examined on four bacteria strains: *Staphylococcus aureus* (var. Oxford) (S.a), *Bacillus subtilis* (B.s.), *Escherichia coli* (E.c.) and *Pseudomonas aeruginosa* (P.a.) using the diffusion test.

The results are listed in Table 1.

Table 1
Microbiostatic activity of compounds III_{a...j} and IV_{a...j}

Compound (Molecular weight)	Diameter of the area of complete inhibition in mm determined by 100 µg substance (calculated for 1 µmol)			
	S.c.	B.s.	E.c.	P.a.
<i>Derivatives of biphenyl</i>				
III _a [(257.3)]	12 (30.9)	17 (43.8)	22 (36.6)	20 (51.5)
III _b (302.3)	12 (36.3)	10 (30.2)	22 (66.5)	22 (66.5)
III _c (302.3)	12 (36.3)	—	22 (66.5)	22 (66.5)
III _d (302.3)	12 (36.3)	10 (30.2)	22 (66.5)	16 (48.4)
III _e (347.3)	—	10 (34.7)	21 (72.9)	16 (55.6)
III _f (291.8)	—	16 (46.7)	12 (35.0)	18 (52.5)
III _g (273.3)	14 (38.3)	—	20 (54.7)	—
III _h (287.3)	14 (40.2)	—	—	12 (34.5)
III _i (300.4)	12 (36.1)	12 (36.1)	12 (36.1)	20 (60.1)
III _j (271.3)	—	10 (27.1)	18 (48.8)	18 (48.8)
<i>Derivatives of 2,4-diphenylthiazole</i>				
IV _a (340.4)	16 (54.5)	12 (40.8)	15 (51.1)	17 (57.9)
IV _b (385.4)	10 (38.6)	13 (50.1)	14 (54.0)	12 (46.3)
IV _c (385.4)	14 (54.0)	10 (38.6)	14 (54.0)	12 (46.3)
IV _d (385.4)	14 (54.0)	—	18 (69.4)	20 (77.1)
IV _e (402.4)	16 (64.4)	10 (40.2)	16 (64.4)	18 (72.4)
IV _f (374.9)	14 (52.5)	10 (37.5)	17 (63.7)	16 (60.0)
IV _g (372.4)	14 (52.1)	17 (63.3)	18 (67.0)	12 (44.7)
IV _h (370.5)	14 (51.9)	—	20 (74.1)	—
IV _i (383.5)	12 (46.0)	—	15 (57.5)	—
IV _j (354.5)	—	—	16 (56.7)	—

The compound was considered "inactive" when the zone of inhibition determined by 100 µg was smaller than 10 mm.

The highest activity was observed by the compound IV_d against P.a. For three of the tested bacteria the most marked inhibition was displayed by derivatives of 2,4-diphenylthiazole, namely IV_e for S.a., IV_g for B.s. and IV_d P.a. Only in the case of E.c. a derivative of biphenyl, III_e, showed the best activity.

The largest spectrum was remarked by the compounds IV, six of them were active against all the tested bacteria.

Thus the insertion of the thiazole systems between the two phenyl rings seems to be favourable for the antibacterial properties.

Some of the tested compounds exhibit a good microbiostatic activity and so are suited for a more detailed study of their biological behaviours.

In the two series of Schiff's bases in order to quantitatively correlate the chemical structure to the bacteriostatic activity, we considered the biphenyl respectively the 2,4-diphenylthiazole as support and the benzylideneamino group as the pharmacophore one. The Hansch equations [13] were used and the antimicrobial activity was expressed as the logarithm of the inverted molare concentration necessary to produce a total inhibition area of 1 mm diameter.

In the biphenyl series, III, good correlations were obtained for the test on E.c., as ensure the data listed in Table 2.

The best statistical indexes were observed if the two parameters were introduced in the relation which express the parabolic function of π and the lineare one of σ (eq. 5). Equation 2 point out the importance of the electronic factor for the antimicrobial activity and suggests a specific compound — biological receptor interaction. The improvement of the correlation obtained if the hydrophobicity constant π was also introduced in calculation (eq. 3), point out the importance of the ability to penetrate the bacterial cell wall for the antibacterial effect. The same equation reveals the favourable effects brought about by the substituents with electron with drawing and hydrophylic character.

For S.a., B.s. or P.a. no significat correlations were observed.

In the 2,4 -diphenylthiazole series, IV, the best results were acquired for the test on B.s. See Table 3.

The values of the statistical indexes in the case of the liniar dependence of the inhibition function of π (Eq. 6) shows the importance of the hydrophobic factor for the microbiostatic activity. The electronic factor do not be neglected (eq. 7). The use of boths parameters, π and σ , lead to good statistical indexes (eq. 8). The best correlation was obtained with the parabolic equation 9. No improvement was afforded if σ was introduced in the parabolic equaltion (Eq. 10).

From these data may be concluded that for the antimicrobial effects the hydrophylic — hydrophobic character of the compounds, controling the accumulation of these one in the cell, is important.

By the other tested bacteria (P.a., S.a. and E.c.) no satisfactory correlations were obtained.

Experimental. Schiff's bases. To a solution of 0,001 moles 4-aminobiphenyl (I) or 2-phenyl-4-(p-aminophenyl)-thiazole (II) in 5–10 ml ethanol a solution of 0,001 moles o-nitrobenzaldehyde or p-hidroxybenzaldehyde in 5–15 ml ethanol was added. The mixture was refluxed for one hour and after cooling the precipitate was filtered, dried and recrystallized. Additional data were given in Table 4.

Biological test. For the diffusion test the agar was used. The medium was inoculated and 0.1 ml from a solution of 1 mg/ml of the compound in DMFA were introduced into the wells punched in the gel. As controle 0.1 ml DMFA were used. After 24 hours incubation at 37°C the diameter of the complete inhibition area was measured.

Table 2

The Hansch equations (Compounds IV_{a...g, i, j} test on E.c.)

Equation		n	r	F	E _v %
$\log 1/C = -0.1527\pi + 7.7449$	(1)	9	0.469	$F_{1,7} = 10.845$	10.82
$\log 1/C = 0.1554\sigma + 7.7064$	(2)	9	0.705	$F_{1,7} = 2.964$	42.58
$\log 1/C = -0.1913\pi + 0.1248\sigma + 7.7231$	(3)	9	0.914	$F_{2,6} = 8.422$	77.95
$\log 1/C = -0.2861\pi^2 - 0.1206\pi + 7.7826$	(4)	9	0.623	$F_{2,6} = 1.055$	18.34
$\log 1/C = -0.1245\pi^2 - 0.1746\pi + 0.1621\sigma + 7.7410$	(5)	9	0.929	$F_{3,5} = 6.307$	78.11

n = number of measurements; r = the correlation coefficient
 F = F-test of significance; E_v% = the coefficient of variation

Table 3

The Hansch equations (Compounds III_{a...c, e...g} test on B.s.)

Equation		n	r	F	E _v %
$\log 1/C = -0.1651\pi + 7.6466$	(6)	6	0.892	$F_{1,4} = 5.86$	74.52
$\log 1/C = -0.1098\sigma + 7.6755$	(7)	6	0.640	$F_{1,4} = 1.04$	26.19
$\log 1/C = -0.1403\pi - 0.0505\sigma + 7.6597$	(8)	6	0.930	$F_{2,3} = 4.237$	77.46
$\log 1/C = 0.1494\pi^2 - 0.1825\pi + 7.6235$	(9)	6	0.977	$F_{2,3} = 13.94$	92.45
$\log 1/C = 0.1562\pi^2 - 0.1858\pi + 0.0051\sigma + 7.6211$	(10)	6	0.977	$F_{2,3} = 5.253$	88.77

Table 4

Schiff's bases III_{b, g} and IV_{b, g}

Compound	Solvent used for recrystalliza- tion	Melting point °C (colour)	Formula (Molecular weight)	Analysis N%	
				Calculated	Found
III _b	Methanol	109 - 110 (mustard)	C ₁₉ H ₁₄ N ₂ O ₃ (302.3)	9.27	8.9
III _g	Acetone	247 - 8 (orange)	C ₁₉ H ₁₅ NO (273.3)	5.12	5.4
IV _b	Ethanol	165 - 6 (lemon-yellow)	C ₂₂ H ₁₅ N ₃ O ₂ S (385.4)	10.9	11.1
IV _g	Xylene	204 - 5 (yellow)	C ₂₂ H ₁₆ N ₂ OS (372.4)	7.52	7.8

REFERENCES

1. V. Fărcăsan, A. Donea, *Stud. Univ. Babeş-Bolyai, Chem.*, **25**(1), 42 (1979).
2. V. Fărcăsan, A. Donea, *Stud. Univ. Babeş-Bolyai, Chem.*, **26**(1), 76 (1980).
3. A. E. Lipkin, I. S. Chichkanova, T. A. Degtyareva, *Khim. Farm. Zhur.*, **4**, 18 (1970).
4. I. P. Vladimirtsev, V. V. Stopkhan, S. S. Khripko, T. I. Cherepenko, V. M. Cherkasov, *Fiziol. Aktiv. Veshchestva*, **1969**, 191.
5. *Lilly Industries Ltd.*, Brit., 1, 328, 549 (1970).
6. E. M. Hodnett, P. D. Mooney, *J. Med. Chem.*, **13**, 786 (1970).
7. J. R. Merchant, D. S. Chothia, *J. Med. Chem.*, **13**, 335 (1970).
8. H. H. Keasling, F. W. Schueler, *J. Am. Pharm. Assoc.*, **39**, 87 (1950).
9. A. L. Walpole, M. H. C. Williams, P. C. Roberts, *Brit. J. Ind. Med.*, **9**, 255 (1952).
10. A. Furst, B. I. Freedlander, *Wasmann J. Biol.*, **11**, 267 (1953).
11. K. Kraft, *Pharmazie*, **5**, 257 (1959).
12. E. Chierici, *Ann. Chim. farm.*, **1938**, 48.
13. I. Simiti, I. Schwartz, „Structura chimică. Activitatea biologică”, Ed. Dacia, 1974, p. 118.

ADSORBED FILMS AT THE BENZENE/WATER INTERFACE

EMIL CHIFU*, JÁNOS ZSAKÓ*, MARIA TOMOAIA-COTIȘEL*, MARIUS SĂLĂJAN*,
IOAN DEMETER-VODNÁR* and CSABA VÁRHELYI*

Received: March 5, 1987

Interfacial tension was measured at the benzene/water interface as function of surfactant concentration in benzene. Two surfactants were studied, viz. astaxanthin (3,3'-dihydroxy-4,4'-dioxo- β -carotene) and the non electrolyte complex $[\text{Co}(\text{DH})_2\text{I}(\gamma\text{-picoline})]$. Interfacial pressure *vs.* mean molecular area curves are constructed and limiting molecular area, surface compressional modulus and Gibbs free energy of adsorption values are derived. Area necessities of both surfactants are calculated on the basis of a molecular model. The behaviour of the adsorbed surfactant monolayers is discussed in terms of molecular structures, intermolecular interactions and penetration of benzene molecules between the oil phase parts of the surfactant molecules.

Introduction. The properties of fluid interfaces and the behaviour of substances with surface activity adsorbed at liquid/liquid interfaces are intensively studied because of their importance in many fields of practical interest, such as extraction and mass transfer, some electrolysis processes, generation of foams and emulsions, detection of surfactant traces etc, [1], and because of their importance in theoretical domains like modelling of processes occurring in bio-interfaces [2].

In the present paper the behaviour of adsorbed films of two surfactants (S), viz. of astaxanthin and of the complex $[\text{Co}(\text{DH})_2\text{I}(\gamma\text{-picoline})]$, was studied at the benzene/water (B/W) interface, by means of interfacial tension measurements at constant temperature. Both surfactants are soluble in the oil phase and insoluble in water.

Experimental. Materials used were of high purity: benzene, commercial product of p.a. purity (Reactivul, Bucharest); astaxanthin (AX; 3,3'-dihydroxy-4,4'-dioxo- β -carotene) was a commercial product (Hoffmann-La Roche) of all-*trans* configuration. The non-electrolyte type iodo-bis-dimethylglyoximino- γ -picolino-Co(III) complex (ID; $[\text{Co}(\text{DH})_2\text{I}(\gamma\text{-pic.})]$) was obtained as described earlier [3]. Purity of the complex was assured by recrystallization and checked by means of chemical analysis. As aqueous phase twice distilled water was used.

Interfacial tension measurements were performed by pendant drop technique. The apparatus used was similar to those described in the literature [4], allowing the reproducibility of interfacial tension measurements within $\pm 0.1 \text{ mN/m}$.

Temperature was maintained at $20 \pm 0.1^\circ\text{C}$.

Results and Discussion. In Fig. 1, interfacial tension (σ) *vs.* time (t) curves are given for benzene solutions containing AX in different concentrations and being in contact with pure water. As seen, in the first minutes, and especially at high concentrations of the carotenoid, a pronounced decrease of the inter-

* University of Cluj-Napoca, Faculty of Chemical Technology, 3400 Cluj-Napoca, Romania

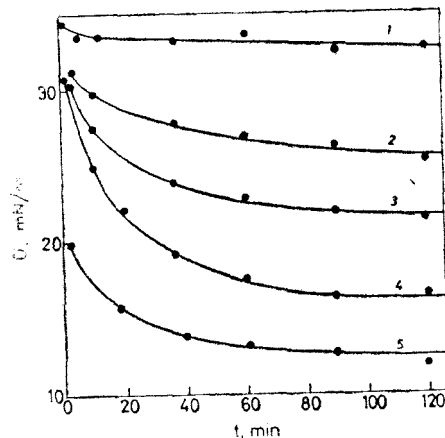


Fig. 1. Time evolution of σ in the system benzene-AX/water at different concentrations in AX. $C \times 10^4$, mole/l: 1-0; 2-0.99; 3-1.48; 4-2.59; 5-5.21.

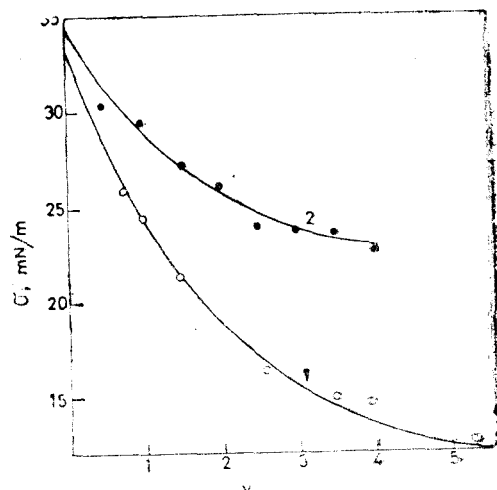


Fig. 2. Equilibrium surface tension σ vs. concentration curves. 1-AX; $y = [AX] \times 10^4$, mole/l; 2-ID, $y = [ID] \times 10^3$, mole/l. Full line: calculated by means of Eq. (1).

facial tension is observed, due to the adsorption of AX molecules at the interface. The adsorption equilibrium is reached in about two hours. A similar picture is obtained also with ID.

The limiting values of σ obtained for high t values and at different S concentrations, have been taken for the equilibrium interfacial tension (σ), allowing us to construct σ vs. $[S]$ or vs. x curves, where $[S]$ and x stand for the molar concentration and for the molar fraction of S.

The experimental σ vs. $[S]$ curves obtained are given in Fig. 2, for both surfactants studied. These curves were simulated by the following polynomial:

$$\sigma = a_1 x^4 + a_2 x^3 + a_3 x^2 + a_4 x + a_5 \quad (1)$$

The constant coefficients a_i were derived using a curve fitting method and their values are given in Tab. 1. In Fig. 2 the full line curves are calculated by means of Eq. (1) and by using a_i values presented in Tab. 1. As seen, the calculated curves describe well the experimental ones.

Table 1

Coefficients a_i of Eq.(1) derived from the experimental σ vs. x data

S	$a_1 \times 10^{-16}$	$-a_2 \times 10^{-12}$	$a_3 \times 10^{-9}$	$-a_4 \times 10^{-5}$	a_5
AX	172.4	340.5	28.21	11.95	32.97
ID	0.08741	0.7784	0.3148	0.8515	34.40

Further, interfacial pressure (π) vs. mean molecular area (A) curves were constructed. The interfacial pressure can be defined as:

$$\pi = \sigma_0 - \sigma \quad (2)$$

where σ_0 and σ stand for the equilibrium interfacial tension at zero adsorption, i.e. zero concentration of S in the oil phase, and at a certain non zero concentration of S, respectively. The π values being calculated by means of Eq. (1) one obtains:

$$\pi = -a_1x^4 - a_2x^3 - a_3x^2 - a_4x + (\sigma_0 - a_5) \quad (3)$$

The corresponding A value can be obtained by using the Gibbs equation written in the following form:

$$A = -\frac{kT}{x} \left(\frac{\partial x}{\partial \sigma} \right)_T \quad (4)$$

where k is the Boltzmann constant. The derivative $(\partial x/\partial \sigma)_T$ can be calculated on the basis of Eq. (1) leading to the relation:

$$A = -\frac{kT}{4a_1x^4 + 3a_2x^3 + 2a_3x^2 + a_4x} \quad (5)$$

By calculating the mean molecular area of the surfactant adsorbed at the benzene/water interface as function of x , as well as the corresponding π values by using Eqs. (5) and (3), respectively, the isotherms given in Fig. 3 could be constructed. Extrapolation to $\pi = 0$ of the linear portion of the isotherms, observed at high interfacial pressures, allowed us to derive limiting molecular area (A_0) values. The A_0 values derived are presented in Tab. 2. The same table contains also the A_0 value of AX derived earlier [5] from the compression isotherm recorded at the air/water (A/W) interface. A_0 values, as well as the collapse areas (A_c) for spread film, can be well correlated with geometric characteristics of the S molecules. Accordingly to our rotating rigid plate model of carotenoid molecules [6], these are anchored with their polar headgroup into the aqueous phase and at low A values their hydrocarbon chain adopts an orientation perpendicular to the interface. By considering the cross section of the

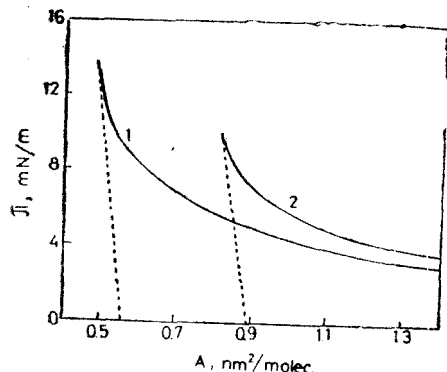


Table 2
Interfacial characteristics of surfactant monolayers

S	Interface	A_0 nm ² /molec.	$-\Delta G^\circ$ kJ/mole	C_{S0}^1 mN/m
AX	B/W	0.56 ± 0.02	34.0 ± 0.2	103
	A/W	0.46 ± 0.01	-	99
ID	B/W	0.89 ± 0.03	27.6 ± 0.2	119

Fig. 3. π vs. A isotherms of the adsorbed interfacial films. 1—AX; 2—ID.

molecule, parallel with the interface, to be characterized by two linear dimensions, perpendicular to each other, denoted by a and b ($a > b$), the area necessity of the tetragonally close packed rotating molecules will be $A_4 = a^2$ and that of the non-rotating close packed molecules $A_p = ab$. Our calculations and experimental results showed that $A_0 \approx A_4$ and $A_c \approx A_p$ [6]. The same model calculations gave for AX the values given in Tab. 3. This table contains also

Table 3
Geometric characteristics of surfactant molecules

S	a , nm	b , nm	c_B , nm	A_4 , nm ²	A_p , nm ²
AX	0.65	0.45	2.5	0.42	0.29
ID	0.90	0.66	0.67	0.81	0.59

the length of the hydrocarbon chain, thought to be perpendicular to the B/W interface, which remains in the B phase. This is denoted by c_B . In the case of ID, spectral data obtained with bis dimethyl glyoximino Co(III) complexes [7, 8], plead for the geometric configuration given in Fig.4 *a* for the equatorial

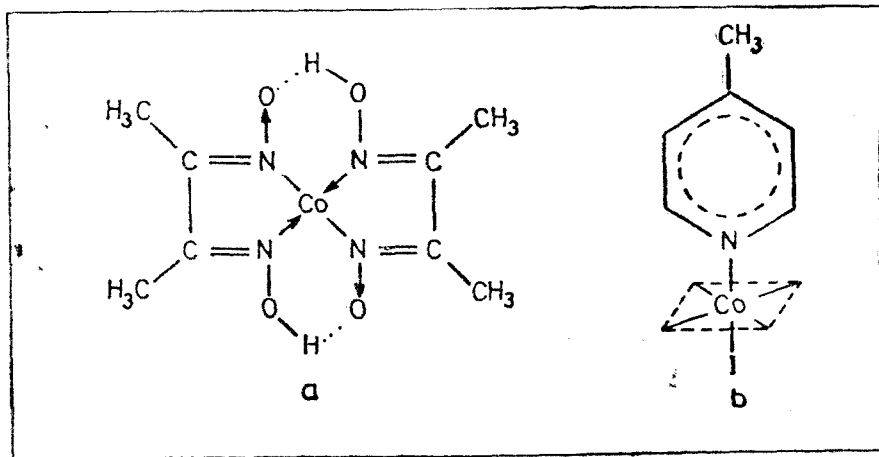


Fig. 4. Structure of ID.

a — equatorial plane; *b* — axial ligands. The dashed line square indicates the equatorial plane.

plane of the complexes. Fig. 4*b* shows the axial ligands. By presuming ID to be anchored into the W phase by means of its only hydrophilic ligand, i.e. of I, the equatorial plane of the complex will lay on the interface and the γ -picoline ligand penetrates into the B phase. Geometric characteristics obtained on the base of this hypothesis, are given in Tab. 3. By comparing the A_4 values (Tab. 3) with the experimentally obtained A_0 ones (Tab. 2), one can see that A_0

obtained at the A/W interface is very near to the A_4 value calculated, but A_0 derived for the B/W interface is much higher. This effect might be assigned to the penetration of B molecules into the interfacial adsorbed monolayer or at least between the hydrocarbon chains of AX, diminishing the intermolecular attracting forces. A similar but lower effect is observed also with ID, its A_0 value exceeding A_4 .

Table 2 contains also the Gibbs free energy of adsorption, ΔG° , representing the variation of the standard chemical potential in the adsorption process, which can be given as [9]:

$$\Delta G^\circ = -RT \ln \left(\frac{\pi}{x} \right)_0 \left(\frac{x_s}{\pi_s} \right) \quad (6)$$

where $(\pi/x)_0$ stands for the slope of π vs. x curve in its initial portion ($x \rightarrow 0$). x_s and π_s correspond to the standard state. By taking $x_s = 1$ and $\pi_s = 1$ mN/m, Eq. (6) gives:

$$\Delta G^\circ = -RT \ln \left(\frac{\pi}{x} \right)_0 \quad (7)$$

in which π is to be expressed in mN/m. Since in isothermal conditions one obtains:

$$\left(\frac{\pi}{x} \right)_0 = -\lim_{x \rightarrow 0} \frac{d\sigma}{dx}$$

By taking into account Eq. (1), Eq. (7) becomes:

$$\Delta G^\circ = -RT \ln (-a_4) \quad (8)$$

ΔG° values given in Tab. 2 have been calculated by means of Eq. (8) by using a_4 values presented in Tab. 1.

As seen, $(-\Delta G^\circ)$ values are rather high, indicating a strong adsorption of the surfactants at the B/W interface, due presumably to the penetration of the polar groups into the W phase. In the case of AX the ΔG° value is near to those reported for other carotenoids [10].

As an example let us consider izozeaxanthin (iZX) and canthaxanthin (CX) [10] as well as AX, investigated in the present paper. All these carotenoids have two identical polar headgroups at the two extremities of a hydrocarbon chain with a conjugated π -bond system. The molecules can be thought to be anchored into the W phase with one of their polar headgroups, the other one remaining in the B phase. Since in the case of iZX having an OH group in its polar headgroups, $\Delta G^\circ = -33.3$ kJ/mole has been obtained, with CX, having a CO group, $\Delta G^\circ = -33.0$ kJ/mole was derived [10]. The $\Delta G^\circ = -34.0$ kJ/mole found in the present paper for AX, which contains both an OH group and a CO one, seems to be perfectly reasonable. ΔG° must characterize mainly the interaction of the polar headgroup with the aqueous phase, i.e. it must be determined by the energy of hydration. It is obvious that $(-\Delta G^\circ)$ increases in the order CX < iZX < AX, and the same order of increasing hydration energy can be expected indeed. $(-\Delta G^\circ)$ of ID is lower than that of AX, which is reasonable due to the lower polarity of the I^- ligand as compared to the polarity of

the OH and CO groups of AX, which leads to lower hydration energy. The interaction of the S molecules with the aqueous subphase is shown to be weaker with ID as compared to AX, also by the more expanded character of the monolayers of the former as compared to the latter. In Fig. 3, the π vs. A curve of ID is far above the isotherm of AX, although the concentration values are tenfold higher in the case of the former, as compared to the latter.

From the π vs. A curves of the adsorbed surfactant monolayer surface compressional moduli were derived. The surface compressional modulus (C_s^{-1}) is defined as :

$$C_s^{-1} = -A \left(\frac{\partial \pi}{\partial A} \right)_T \quad (9)$$

Combination of Eqs. (4) and (9) leads to the relation :

$$C_s^{-1} = - \frac{x \left(\frac{\partial \sigma}{\partial x} \right)_T^2}{\left(\frac{\partial \sigma}{\partial x} \right)_T + x \left(\frac{\partial^2 \sigma}{\partial x^2} \right)_T} \quad (10)$$

Frequently, condensed monolayers are characterized by means of the C_{so}^{-1} value defined as :

$$C_{so}^{-1} = -A_0 \left(\frac{\partial \pi}{\partial A} \right)_0 = +A_0 \frac{\pi_M}{A_0 - A_m} \quad (11)$$

where π_M and A_m stand for the maximum π value, and for the minimum A value, experimentally attained, respectively. In the case of monolayers spread at the A/W interface, these magnitudes represent the collapse characteristics, π_c and A_c , respectively.

The C_{so}^{-1} values derived from the π vs. A curves given in Fig. 3., are presented in Tab. 2, together with the corresponding value obtained for AX at the A/W interface. As seen, this limiting value of C_s^{-1} for high π values does not differ essentially from each other at the B/W and A/W interfaces in the case of AX. With ID, it is a little higher as compared to AX, indicating the monolayer of the former to be less compressible as compared to the latter. The C_s^{-1} values obtained are near to the lower limit (≈ 100 mN/m), admitted for the condensed liquid state of monolayers [11].

In order to obtain a clear image on the compressibility of the monolayers studied and in the whole π range investigated, C_s^{-1} vs. π curves were constructed, by using Eq. (9). The $(\partial \pi / \partial A)_T$ values were derived graphically from the π vs. A curves. Results are presented in Fig. 5.

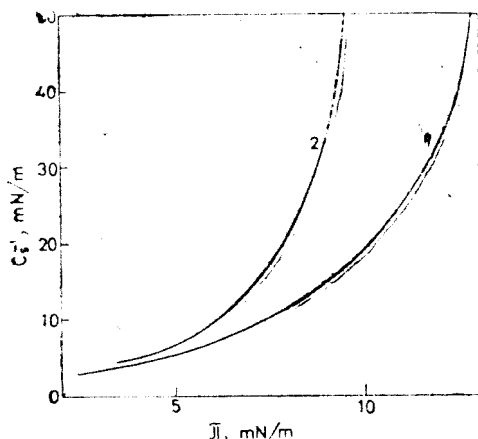


Fig. 5. Surface compressional modulus of the surfactants, as function of $\pi \cdot 1 - \text{AX}$; 2-ID.

former to be less compressible as compared to the AX one. This difference in the behaviour of the surfactants studied might be due to the different character of their oil phase hydrophobic chain. In the case of ID this chain is a short one, but with AX it is much longer (see c_B values given in Tab. 3). On the other hand, by taking into account the molecular structures, it is obvious that the penetration of benzene molecules does not affect essentially the intermolecular forces acting between ID molecules, but the same phenomenon may play an important role in diminishing the intermolecular attraction between AX molecules. Therefore, in the case of ID, at high π values the atoms of the equatorial plane of neighbouring molecules arriving near to each other, C_s^{-1} increases very rapidly with increasing π . With AX, with increasing π the benzene molecules situated between adjacent surfactant molecules are gradually expelled, entailing a lower slope of the C_s^{-1} vs. π curve. Inspection of Fig. 5 shows the shape of the curves to be consistent with this theoretical expectation. The comparison of the experimental A_0 , and of the theoretical A_0 values given in Tabs. 2 and 3, shows the above picture to be consistent also with the A_0 values obtained. As seen $A_0 = 1.33 A_4$ in the case of AX, but only $A_0 = 1.1 A_4$ with ID for the same interface B/W. One may presume the relatively high A_0 value of AX to be due exactly to the penetration of B molecules between the hydrocarbon chains of the surfactant molecules, the adsorbed film being more expanded than the spread one.

We mention that an attempt was made to obtain C_s^{-1} vs. π curves by using Eq. (10) and the regression polynomial (1) leading to the following expression:

$$C_s^{-1} = -x \frac{(4a_1x^3 + 3a_2x^2 + 2a_3x + a_4)^2}{16a_1x^3 + 9a_2x^2 + 4a_3x + a_4} \quad (12)$$

These calculations gave reliable results only for low π values, e.g. with AX up to about 9 mN/m. At higher π values Eq. (12) gives negative values. This is not surprising since the regression polynomial cannot be expected to have the same second order derivative as the experimental curve has. Therefore, graphical derivation was needed to obtain the C_s^{-1} vs. π curves. As seen, at all π values C_s^{-1} of ID is higher than that of AX, indicating the monolayer of the

REFERENCES

- P. C. Hiemenz, "Principles of Colloid and Surface Chemistry", Marcel Dekker, Inc., New York, 1986; K. Motomura, *J. Colloid Interface Sci.*, **64**, 348 (1978); R. Averyard and J. Chapman, *Can. J. Chem.*, **53**, 916 (1975).

2. M. Dupeyrat, E. Nakache, *Bioelectrochem. Bioenerg.*, **5**, 134 (1978); A. Sanfeld, A. Steinchen, *Biophys. Chem.*, **3**, 99 (1975).
3. Cs. Várhelyi, B. Böhm, *Stud. Univ. Babeş-Bolyai Chem.*, **9**(1), 55 (1964).
4. J. M. Andreas, E. A. Hauser, W. B. Tucker, *J. Phys. Chem.*, **42**, 1001 (1938); C. E. Stauffer, *J. Phys. Chem.*, **69**(6), 1933 (1965).
5. E. Chifu, J. Zsakó, M. Tomoaiia-Cotisell, M. Sălăjan, I. Albu, *J. Colloid Interface Sci.*, **112**, 241 (1986).
6. J. Zsakó, E. Chifu, M. Tomoaiia-Cotisell, *Gazz. Chim. Ital.*, **109**, 663 (1979).
7. A. Nakahara, *Bull. Chem. Soc. Japan*, **28**, 473 (1955).
8. R. Blinc, D. Hadzi, *J. Chem. Soc.*, **1958**, 4536; *Spectrochim. Acta*, **16**, 853 (1960).
9. R. Aveyard, B. Vincent, *Progr. in Surface Sci.*, **8**, 59 (1977); R. Aveyard in "Surfactants", Ed. Th. F. Tadros, Acad. Press, London, 1984 p. 160.
10. M. Tomoaiia-Cotisell, *Ph. D. Thesis*, Univ. Cluj-Napoca, 1979; M. Tomoaiia-Cotisell, E. Chifu, *Rev. Chim. (Bucharest)*, **32**(11), 1063 (1981).
11. J. T. Davies, E. K. Rideal, "Interfacial Phenomena", Acad. Press, New York, London, 1963 p. 265.

RECENZII

Paul C. Hiemenz, „Principles of Colloid and Surface Chemistry”, 2nd ed., Marcel Dekker, Inc. New York and Basel, 1986, 815 pp.

Paul C. Hiemenz is Professor at California State Polytechnic University in Pomona. The first edition of this book was published in 1977.

Although in prefacing the first issue of his textbook the author dedicated it primarily to students, we think it can successfully be consulted also by specialists from most various fields of contemporary science and technology, such as: chemical industry, environmental science, science of materials and soils, geology, petroleum science and industry, food production, biochemistry and molecular biology, etc. The more so as colloid and surface chemistry have not secured a proper status yet among other disciplines in many of the higher education curricula.

The second edition of the book contains the following chapters: (1) Colloid and surface chemistry: their scope and variables, (2) Sedimentation and diffusion and their equilibrium, (3) Solution thermodynamics: osmotic and Donnan equilibria, (4) The viscosity of dilute dispersions, (5) Light scattering, (6) Surface tension and contact angle: application to pure substances, (7) Adsorption from solution, (8) Colloidal structure in surfactant solutions, (9) Physical adsorption at the gas-solid interface, (10) Metal surfaces: microscopy, spectroscopy, and diffractometry, (11) Van der Waals attraction and flocculation, (12) The electrical double layer, and (13) Electrophoresis and other electrokinetic phenomena. We mention that the topics discussed in (8) and (10) are developed under separate chapters only in this new, second edition of the book.

Professor Hiemenz is also the author of a separate work entitled: "Polymer Chemistry: The Basic Concepts", Marcel Dekker, New York, 1984. Nevertheless, he makes incursions in the physical chemistry of macromolecules in the present edition of his "Principles of Colloid and Surface Chemistry", too. In his view, colloid chemistry is the science of large molecules and of finely subdivided multiphase systems, the latter being micro- and ultramicroheterogeneous systems in our nomenclature.

Still, the author underlines the fact that colloid chemistry and surface chemistry meet only in systems containing more than one phase. He also emphasizes, from the beginning, the importance of the concept of stability in colloid

chemistry, as well as the clear-cut distinction between macromolecular colloids and multiphase dispersions.

Beside "classic" problems such as transport phenomena in colloidal systems (sedimentation and diffusion), viscosity of dispersions, Rayleigh and Debye light scattering, adsorption on various interfaces and their applications (detergency, flotation etc.), a series of present-day subjects are to be noticed in the reviewed book: interpretation of surface tension from the point of view of intermolecular forces (Girifalco-Good-Fowkes equation); micellar catalysis; micro-emulsions and their applications (such as oil tertiary recovery), etc.

In the present edition a separate chapter is destined to metallic surfaces and due modern methodologies such as: Scanning Electron Microscopy, Auger Electron Spectroscopy, Low-Energy Electron Diffraction, Field Ionization Microscopy.

Of special importance for the instruction of future specialists are chapters 11 and 12, in which basic problems relating to stability and coagulation (flocculation) of colloid systems are treated. The DLVO (Derjaguin, Landau, Verwey, Overbeek) theory is also discussed, and the theory of DLJ (Dzyaloshinskii, Lifshitz, Pitaevskii) is referred to.

Moreover, Professor Hiemenz is well known by his research work on the role of van der Waals forces in colloid chemistry, with particular emphasis on flocculation phenomena.

Professor Hiemenz's excellent book, useful to beginners as well as to specialists, represents a pleading for the prominent place this interdisciplinary – namely colloid and surface chemistry – must occupy among the different high school compartments such as: chemistry, chemical engineering, biochemistry, petroleum science, geology, and so on.

EMIL CHIFU

Liviu Oniciu et al, **La corrosion des métaux. Aspects fondamentaux et protection anticorrosive**, Ed. scientifique et encyclopédique, Bucharest, 1986.

Alors qu'aujourd'hui on estime que presque un tiers de la production mondiale annuelle d'acier est perdu à cause de la corrosion, nous considérons

qu'il n'est plus nécessaire à mettre en évidence l'importance et l'actualité de la connaissance des mécanismes des processus de corrosion ou des méthodes de protection anticorrosive. Dans ce contexte, le livre du professeur Oniciu et ses collaborateurs, détient une place à part parmi les autres ouvrages de même sujet, par son contenu orienté fortement vers la présentation des aspects théoriques fondamentaux du phénomène de corrosion et de la protection anticorrosive.

L'ouvrage compte cinq chapitres chacun étant suivi d'une bibliographie sélective. Dans le premier chapitre est présentée, tout d'abord, l'ampleur des pertes dues à la corrosion en utilisant des données récentes et convaincantes. Un bref aperçu historique offre ensuite aux auteurs la possibilité d'évidencier les plus importants résultats théoriques et pratiques. A la fois ils ont aussi la possibilité de passer en revue les directions actuelles de la recherche dans le domaine de la corrosion et de la protection anticorrosive.

Le deuxième chapitre est entièrement dédié à la présentation du processus de corrosion chimique. La thermodynamique et la cinétique de la formation des couches d'oxydes sur les métaux purs et sur les alliages sont traitées d'une manière brève mais profonde. Une attention particulière est accordée à l'oxydation des métaux en exemplifiant en détail à l'aide du processus d'oxydation du fer.

Le troisième chapitre occupe une place privilégiée dans l'ouvrage par son étendue — presque 30% du total — et surtout par la densité de l'information contenue. Ainsi, au début, sont présentées les bases de la thermodynamique et de la cinétique électrochimique moderne, de même que les techniques d'investigation des processus d'électrode. Il faut noter l'effort constant des auteurs pour présenter toutes les informations pour qu'elles soient le plus utiles possible à ceux qui font de la recherche dans ce domaine, de la corrosion et de la protection anticorrosive. On peut donner comme exemple la présentation des diagrammes Pourbaix et Edeleanu—Evans. Ensuite, sont examinés les différents types de processus catiodynamique qui accompagnent de règle le processus de corrosion : la décharge des ions d'hydrogène rencontrée dans la corrosion en solutions acides, la réduction de l'oxygène présente dans la corrosion en solutions neutres et basiques et la réduction d'autres systèmes redox comme $\text{Fe}^{2+}/\text{Fe}^{3+}$, nitrite, hydrazine, sulfite, etc. Dans tous les cas examinés les auteurs insistent sur la mise en évidence des paramètres déterminants dans le fonctionnement de chacun des systèmes examinés. Dernièrement, sont exposés les types de corrosion rencontrés le plus souvent dans la pratique : la corrosion par macropiles galvaniques, la corrosion par piles de concentration — à oxygène ou à un ion métallique —, la corrosion

par piles électrolytiques, la corrosion par piles formées des défauts de la couche d'oxyde passivant et la corrosion par micropiles galvaniques.

Le phénomène de passivation des métaux et des alliages ainsi que la théorie générale de la passivation sont traités dans le quatrième chapitre. Il est insisté sur les paramètres physico-chimiques qui contrôlent l'installation de la passivation et aussi sur les possibilités d'utilisation pratique de cette modalité de ralentissement de la corrosion.

Le dernier chapitre, le plus développé — il représente presque la moitié de l'ouvrage —, est consacré entièrement aux principes de la protection anticorrosive et du génie de la protection anticorrosive. Les différentes modalités connues pour la prévention ou seulement pour la diminution de la corrosion sont examinées, par exemple : le choix des meilleures solutions constructives, l'utilisation des inhibiteurs de corrosion, la déposition des couches protectrices, la protection électrochimiques, etc. Les problèmes spécifiques de la lutte anticorrosive dans une série de secteurs économiques de grande importance (l'industrie pétrolière, pétrochimique, de synthèse organique, thermoénergétique, etc.) ainsi que dans d'autres situations différentes ayant comme facteur commun le milieu corrosif identique (la corrosion dans l'atmosphère, dans l'eau de mer) sont également présentes. La grande diversité, le caractère interdisciplinaire, la précision du détail qui caractérisent les informations contenues dans ce chapitre nous permettent d'affirmer que cette partie de l'ouvrage représente la pièce maîtresse du livre.

Par la concision et la clarté du style, par la présentation systématique du matériel, par l'utilisation équilibrée des exemples les plus adéquates le livre reste accessible malgré son niveau scientifique bien élevé. La lecture de ce livre offre à tous les intéressés dans l'étude de la corrosion et de la protection anticorrosive une riche information (413 citations bibliographiques) accompagnée d'un très bon matériel illustratif (240 figures et 66 tableaux).

CĂTĂLIN POPESCU

Liviu Literat, Transport Phenomena and Specific Equipment in Chemical Industry. Transport Process, Edited by University of Cluj-Napoca, 1985, 174 pp.

The series of lectures written by prof. Liviu Literat comprises the first part of the curriculum taught at the Faculty of Chemical Technology, Cluj-Napoca, and deals with the main problems of the transport phenomena theory.

Adopting the generalizing point of view according to which the transfer of momentum, heat and mass represents particular cases of the general concept of property transport, the author approaches from this position the entire field of transport and transfer phenomena. Thus, in the course of the six chapters, the general features of the property transport are presented, the main transport mechanisms are described and the equations of the transport phenomena are deduced, stressing the analogies stemming from the transport mechanisms for momentum, heat and mass transfer. The general transport equations derived from the property balance were particularized for the cases of momentum, heat and mass transfer, with special emphases on their common basis and on the correlations between the physical and mathematical models describing them.

Much attention has been given to the fluids flowing, by establishing the continuity equations of the momentum and of the energy balance, necessary for understanding the heat and mass transfer by convective mechanism, and the analogies between them.

The third chapter is devoted to the modelling of transport phenomena, especially to the experimental modelling. Elements of similitude theory are reviewed and the general methods for establishing the similitude criteria and the criterial equations are presented. For space economy sake, the illustration of the methods for determining the similitude criteria was made distinctly for hydrodynamic, thermal and mass similitude. The chapter ends with a synthetic overview on similitude in momentum, heat and mass transport, stating that the similitude criteria represent property fluxes of identical or different type, transport by either molecular or convective mechanisms.

In the fourth chapter, a discussion is given of the property transport through a limit layer. The structure of the limit layer in laminar and turbulent flow is analyzed, the equations of the limit layer are deduced, and its thickness is estimated.

Along with the description of the hydrodynamic limit layer, the thermal and the diffusive limit layers are referred too, and the analogy between them and the influence of the limit layer on the interphase property transfer are underlined.

The next chapter deals with some analogies with are specific for the transport phenomena. Thus, the analogies in momentum, heat and mass transfer are described (the Reynolds, Prandtl, Karman, Chilton-Colburn analogies) underscoring their importance in the evaluation of partial coefficients of convective transport. The final part of this chapter is reserved for a presentation of some analogic experimental methods applied to chemical engineering (the electrothermal, thermohydrodynamic and electrooptical analogy).

The last chapter brings to conclusion the problems of property transport by reviewing the procedures aiming at intensifying the transport phenomena. The routes towards the intensification are suggested by using as criteria the consequences of the problems dealt with in previous chapters.

A concise treatment is given of the transfer intensification by hydrodynamic methods (statical turbulence promoters), the intensification by using oscillations, by means of electromagnetic fields and surface phenomena.

The course is characterized by a pregnant note of originality which is unique in our specialty literature, by its way of stating and solving the problems of the property transport theory, attempting to crystallize a systemic, unitary point of view on this matter.

I suggest that priority should be given to the apparition of the subsequent parts of this course, taking into account its utility for introducing a new and valuable conception in the teaching of "Transport Phenomena and Specific Equipment in Chemical Industry" discipline.

It is my opinion that by the appearance of this first part of the course "Transport Phenomena and Specific Equipment in Chemical Industry" in Cluj-Napoca, an important step is made towards an improved instruction of the students in chemical engineering in our country.

ZENO GROPSIAN

L. Kékedy: **Metallic and Ion-selective Electrochemical Sensors** (Sensori electrochimici metalici și ionselectivi) București, Editura Academiei R. S. România, 1987, 232 pp.

The book is divided into 8 chapters: General problems concerning analytical sensors (1), Electrode materials, their physico-chemical properties and usefulness (2), Amperometric (Galvanic) sensors and experimental technique using them (3), Metallic electrodes as potentiometric sensors (4), Metallic sensors in limited diffusion field (Thin layer electrochemistry) (5), Semiintegral electroanalysis (6), New (non-conventional) polarographic methods (7) and Ion selective sensors (8).

A very good illustration (122 figures and 9 tables), a modern and generous list of references (418 articles and monographs) and a remarkable original contribution of the author, make the book a valuable guide in the field electroanalytical chemistry.

The theoretical and experimental aspects are treated at high level, corresponding to the

high school requirements, and the original contributions are well underlined.

A special mention for the chapter 3, the backbone of the book, and for the chapter 8, having a great importance in the analysis of chemical and biochemical technologies.

As concerning the other six chapter, the attention is retained by the numerous details and recommendations to follow in experimental analytical applications, by the lucid apprecia-

tions of the pricisions and the restrictions of the described methodes.

The book represents the first Roumanian source of information in the field of electrochemical sensors, and illustrates the importance of the applied electrochemistry in practical activity. It is a valuable source of information for researchers, engineers and students in chemistry and chemical technology.

L. ONICIU

CRONICĂ

Participări la manifestări științifice internaționale

- La al 7-lea Simpozion Internațional de „Strucțura, Funcția și Metabolismul Lipidelor din Plante”, organizat la Universitatea Davis California (SUA) în perioada 27 iulie – 1 august 1986, lucrarea „*Molecular Associations in Lipid-carotenoid Monolayers*”, de M. Tomoaiă-Cotîșel, I. Zsakó, E. Chifu și P. J. Quinn, a fost prezentată de Dr. P. J. Quinn de la Universitatea din Londra – King's College.
- La al 7-lea Congres Internațional de „Foto-sintează”, organizat la Universitatea Brown Providence, Rhode Island (SUA) în perioada 10–15 august 1986, lucrarea „*Collapse Mechanism of Some Carotenoid Monomolecular Films – Membrane Model*” de M. Tomoaiă-Cotîșel, I. Zsakó, E. Chifu, D. A. Cadenhead și H. E. Ries, Jr., a fost prezentată de Dr. D. A. Cadenhead de la Universitatea Buffalo.
- La al 6-lea Simpozion Internațional de „Surfațanti în soluție” organizat la New Delhi (India) în perioada 18–22 august 1986 Prof. Dr. Emil Chifu a trimis conferință plenară: „*Discussion of Compression Isotherms of Some Carotenoid Monolayers on the Basis of HMO Calculations*”. Prof. Emil Chifu a făcut parte din Comitetul Internațional de organizare al Simpozionului.

Vizite în străinătate

Lector Dr. Maria Tomoaiă-Cotîșel a făcut o vizită la Universitatea din Londra – King's College, în cadrul cooperării româno-britanice pe tema „Studiul filmelor superficiale cu aplicații în biochimia fizică a membranelor naturale” în perioada 16 august – 7 septembrie 1986. Cu acest prilej a efectuat cercetări în colaborare cu grupul de specialiști condus de Dr. P. J. Quinn.

Vizite din străinătate

● Dr. D. Driucenko și Dr. V. Salimov de la Institutul de Cercetări Cosmice al Academiei de Științe a URSS – Moscova a vizitat în perioada 14–17 februarie 1986 laboratoarele grupului de cercetare în domeniul Chimiei coloizilor și suprafeteelor de la Facultatea de tehnologie chimică – condus de Prof. Dr. Emil Chifu. Cu acest prilej au fost purtate discuții în cadrul colaborării la programul „Intercosmos”.

● La același grup de cercetare a efectuat o vizită de lucru și Dr. Peter J. Quinn în perioada 26 octombrie – 1 noiembrie 1986. Vizita a avut loc în cadrul cooperării româno-britanice cu tema: „*Studiul filmelor superficiale cu aplicații în biochimia fizică a membranelor naturale*”. Cu această ocazie Dr. P. J. Quinn a expus conferința „*Mecanismul și cindica transițiilor de fază în fosfolipide*” în cadrul Seminarului științific de chimie fizică în zina de 29 octombrie 1986.

Organizări de manifestări științifice în cadrul Universității

Al II-lea Simpozion de „*Chimia Coloizilor și Suprafeteelor*” s-a desfășurat în perioada 8–10 septembrie 1986 la Facultatea de Tehnologie Chimică – în cadrul Catedrei de chimie fizică, organică și tehnologică, sub egida M.I.Ch., ICECHIM – Centrul de Chimie fizică, CNST, MEI și a Universității din Cluj-Napoca. Președintii Comitetului de organizare au fost: Director General chimist Maria Ionescu – Institutul Central de Chimie, Prof. Dr. Emil Chifu, șef de catedră – Universitatea din Cluj-Napoca, Prof. Dr. Doe. Constantin Luca, director – ICECHIM – Centrul de Chimie fizică și Prof. Dr. Gheorghe Mărcuț, director – Institutul de Chimie Cluj-Napoca. După cunținutul Recto- rului Universității din Cluj-Napoca, Prof. Dr. Aurel Negruțiu, au fost susținute următoarele conferințe plenare: „*Chimia coloizilor și suprafeteelor*” – Ministrul Secretar de Stat Mihail Florescu, membru corespondent al Academiei RSR; „*Chimie supramoleculară și cataliză supramoleculară*” – Prof. Dr. Doe. Constantin Luca; „*Unele probleme de actualitate în chimia interfețelor lichide*” – Prof. Dr. Emil Chifu; „*Membrane de sinteză în procese de separare*” – Dr. Gheorghe Rădulescu; „*Interacția polimerilor cu substanțe tensioactive*” – Dr. George Popescu și Mircea Marinescu.

Lucrările s-au desfășurat în patru secțiuni: fenomene interfaciale, sisteme disperse, membraane biologice și de sinteză, sisteme coloidale în procese tehnologice. Au fost prezentate 155 de comunicări elaborate de 332 de autori.

Publicări de tratate, cărți și cursuri universitare

Encyclopedie de chimie, vol. 2, C–CH și vol. 3, CI – , elaborată sub coordonarea Acad. dr.

ing. Elena Ceausescu, colectivul de redactie: E. Ciorănescu-Nenitescu, ... E. Chifu, V. Fărcăsan, I. Haiduc, S. Mager, Gh. Marcu, L. Oniciu, Editura Științifică și Encyclopedică, București, 1986.

L. Oniciu, S. Ivășan, M. Apostolescu, E. Schmidt, Coroziunea metalelor, Editura Științifică și Encyclopedică, București, 1986.

L. Literat, Fenomene de transfer și utilizare în industria chimică. Procese de transport, Iași Univ. Cluj-Napoca, 1986.

Luerări științifice apărute în reviste de specialitate din țară și străinătate

E. Chifu, C. I. Gheorghiu, I. Stau, Some Remarks Concerning the Marangoni Flow on an Inclined Plane, *VI. Internationale Tagung über Grenzflächenaktive Stoffe*, pp. 211–217, Bad Sauer (DDR), April 22–27, 1985.

E. Chifu, I. Albu, C. I. Gheorghiu, E. Gavrilă, M. Sălăjan, M. Tomoiaia-Cotîșel, Marangoni Flow – Induced by Temperature Gradients – Against Gravity Forces, *Rev. Roumaine Chim.*, **31**, 105 (1986).

E. Chifu, J. Zsakó, M. Tomoiaia-Cotîșel, M. Sălăjan, I. Albu, Xanthophyll Films. IV. Interaction of Zeaxanthin with Electrolytes at the Air/Water Interface, *J. Colloid Interface Sci.*, **112**, 241 (1986).

I. Haiduc, C. Silvestru, Trichlorodiphenylantimony (V), in *Inorganic Synthesis*, vol. 24, Edited by S. Kirschner, J. Wiley & Sons, 1986, p. 194.

F. Dogar, L. Silaghi-Dumitrescu, R. Greco, I. Haiduc, Amine Adducts of Nickel (II) Diphenyldithiophosphinate with Substituted Ethylenediamines, *Rev. Roumaine Chim.*, **31**, 79 (1986).

L. Silaghi-Dumitrescu, I. A. Ayila-Diaz, I. Haiduc, Dimethyl- and Diphenyldithioarsinates of some Main Group Metals, *Rev. Roumaine Chim.*, **31**, 335 (1986).

I. Haiduc, M. Curtui, I. Haiduc, Solvent Extraction of Uranium(VI) with Di-2 ethylhexyl-dithiophosphoric Acid from Aqueous Nitrate, Chloride, Sulfate and Phosphate Media, *J. Radioanal. Nuclear Chem. Articles*, **99**, 257 (1986).

C. Silvestru, L. Silaghi-Dumitrescu, I. Haiduc, M. J. Begley, M. Nunn, D. B. Sowerby, Synthesis of Diphenylantimony(III) Dialkyldithio- and Diaryldithiophosphinates and arsinites; Crystal Structures of $\text{Ph}_2\text{SbS}_2\text{MPh}_3$ ($\text{M}=\text{P}, \text{As}$), *J. Chem. Soc., Dalton Trans.*, **1986**, 1031.

P. Clare, D. E. Sowerby, I. Haiduc, The Crystal Structure of Bis (N-pentafluorophenyl) tetraphenylcyclodisilazane-tetrabenzenec, $(\text{Ph}_2\text{SiNC}_6\text{F}_5)_2\text{C}_4\text{H}_6$, *J. Organometal. Chem.*, **310**, 161 (1986).

I. Haiduc, I. Silaghi-Dumitrescu, Inorganic (carbon-free) Chelate Rings, *Coord. Chem. Revs.*, **74**, 127 (1986).

M. Begley, D. B. Sowerby, D. M. Wesolek, C. Silvestru, I. Haiduc, Diphenylantimony(III) Diphenylphosphinate and Diphenylthiophosphinate; Synthesis, Spectra and Crystal Structure, *J. Organomet. Chem.*, **313**, 281 (1986).

I. Literat, D. Vasilescu, Masă ceramică superaluminoasă ca liant mulitic și porozitate controlată, suport de catalizator, *Materiale de Construcții*, **16**, 47 (1986).

I. Literat, N. Farbăș, Cercetarea microfazelor din sistemele silicatice tehnice cu ajutorul microondei electronice cu ecalibrator, *Materiale de Construcții*, **16**, 140 (1986).

S. Mager, V. Fărcăsan, I. Cristea, I. Pannea, I. Hopirtean, F. Jugrestan, F. Paiu, A. Horváth, Contribuții la asimilarea unor antidiabetici cu nucleu pirimidinic, în *Progresă de cercetare biochimică*, Edit. Acad. RSR, Cluj-Napoca, 1986, p. 65.

G. Marcu, A. Hantz, M. Somay, C. S. Várhelyi, F. Tolea, Study on some Cobalt(II) Dioxygen Chelate Adducts with Tertiary Phosphines, *Rev. Roumaine Chim.*, **31**, 227 (1986). G. Marcu, Al. Botar, A. Naumescu, Contributions to the Study of Cobalt(II) Dioxygen Complexes, *Rev. Roumaine Chim.*, **31**, 981 (1986). G. Marcu, V. Andreica, A. Tibad, M. Trif, Colorarea în roz-roșu rubiniu a geamului contactat în prealabil cu o topitură de staniu, *Materiale de Construcții*, **16**, 60 (1986).

L. Oniciu, P. Ilea, G. Trantabăț, Procedeu de obținere a rodiului metalic, *Rev. Chim. (București)*, **37**, 770 (1986).

L. Oniciu, V. A. Topan, I. Mureșan, D. Gherțoiu, Coroziunea electrocatalizatorilor în pilule de combustie cu hidrazină, *Ibidem.*, **37**, 153 (1986).

L. Oniciu, B. M. Rus, D. Constantin, F. Ciomoș, Electrozi de zinc pentru acumulatoare alcăline, *Ibidem.*, **37**, 44 (1986).

L. Oniciu, D. A. Löwy, I. A. Silberg, O. H. Oprea, C. R. Florea, Cationic Membrane Reference Electrode, *Extended Abstracts of 37th Meeting of the International Society of Electrochemistry*, Vilnius, USSR, 24–31 august, 1986, 2, p. 379.

L. Oniciu, D. A. Löwy, I. A. Silberg, D. F. Anghel, Potentiometric Determination of Cationic Surfactants Used in Adiponitrile Electrosynthesis, *Analisis*, **14**, 456 (1986).

L. Oniciu, I. Mitrache, A. Mureșan, I. Marian, I. A. Silberg, Thermal Modification of Semiconductor (Electrolyte couple under Illumination, Extended Abstracts of 37th Meeting of the International Society of Electrochemistry, Vilnius, USSR, 24–31 august, 1986, 3, p. 306.

L. Oniciu, V. A. Topan, A. Mureșan, D. Gherțoiu, A. Pântea, Some Fundamental Aspects of Lead Electrowinning, *Ibidem.*, **1986**, 4, p. 345.

I. Silaghi-Dumitrescu, I. Haiduc,

Why are Cyclosilazane Rings more Stable than Cyclodisiloxanes? A qualitative Molecular Orbital Approach to the Bonding in Cyclodisilazanes and Cyclodisiloxanes, *Inorg. Chim. Acta*, **112**, 159 (1986).

I. Silaghi-Dumitrescu, I. Haiduc, The Bonding in Dialkyldithiophosphinato Metal Complexes. A Molecular Orbital Study of Bis-(dimethylidithiophosphinato)nickel(II), *Rev. Roumaine Chim.*, **31**, 955 (1986).

M. Tomoiaia-Cotisel, I. Zsakó, M. Sălăjan, E. Chifu, Interaction of Unimolecular Films of some Carotenoids with Electrolytes at the Air/Water Interface, *Water and Ions in Biological Systems*, pp. 371–381 A. Pullmann, V. Vasilescu and L. Packer, eds., Union of Societies for Medical Sciences, Bucharest, 1985.

D. Pázmány, A. Silvestru, E. Grünwald, C.s. Várhegyi, Utilizarea cumarinei extrase din plante ca agent de luciu în băile de nichelare, *Industria ușoară (București)*, **33**, 129 (1986). C.s. Várhegyi, I. Gănescu, A. Hantz, I. Papa, Neue Reinekesalzähnliche Verbindungen mit Diisobutyl-phenylphosphin und Diphenyl-ethylphosphin, *Rev. Roumaine Chim.*, **31**, 291 (1986).

J. Zsakó, J. Demeter-Vodnár, I. Báldea, C.s. Várhegyi, Kinetics and Mechanism of Substitution Reactions of Complexes, LVIII. $\text{Hg}^{(II)}$ assisted Aquation of *cis*-Co(en)₂Br(gamma-picoline)²⁺, *Rev. Roumaine Chim.*, **31**, 443 (1986). J. Zsakó, G. Liptay, C.s. Várhegyi, Kinetic Analysis of Thermogravimetric Data, XXV. Derivatographic Study of Some $\text{Co}(\text{NCS})_4(\text{amine})_2$ Type Complexes, *J. Thermal Anal.*, **31**, 1027 (1986).

J. Zsakó, M. Tomoiaia-Cotisel, A. Moicanu, E. Chifu, Insoluble Mixed Monolayers II. Protolytic Equilibria and the Influence of the pH on the Collapse Pressure, *J. Colloid Interface Sci.*, **110**, 317 (1986).

Brevete

S. Mager, A. Benkő, I. Hopărtean, M. Rusu, Gr. Perint, Procedeu de obținere a este-

rului p-toluensulfonic al p-nitro-acetofenon-oximei *Brevet R.S.R.* nr. 89 672 din 1985.

G.h. Marcu, C. Porumb, V. Andreica, A. Tibad, M. Trif, Procedeu de obținere a sticelor intens colorate în albastru egiptean și turquiz, *Brevet R.S.R.* nr. 90 043 din 1986.

G.h. Marcu, C. Porumb, V. Andreica, M. Trif, Procedeu de obținere a sticlei intens colorate în verde smarald (rubin verde smarald), *Brevet R.S.R.*, nr. 90 044 din 1986.

G.h. Marcu, Al. Potar, A. Pătruț, Procedeu de preparare a heteropolianionilor de mangan, *Brevet R.S.R.* nr. 90 021 din 1986.

Al. Botar, M. Rusu, A. Naumescu, D. Itu, G.h. Marcu, Procedeu de preparare a heteropolianionilor de tipul CoL , *Brevet R.S.R.*, nr. 90 022 din 1986.

Suștineri de teze de doctorat

Măruțoiu Constantin, *Cromatografia pe strat subțire cu gradient programat de temperatură, utilizarea la controlul poluării mediului*, conducător științific prof. dr. doc. Candin Liteanu (7 februarie 1986).

Cosma Viorica, *Cercetări privind elaborarea și aplicațiile analitice ale unor electrozi-membrană ion-selectivi solizi. Electrozi Cu^{2+} și Cd^{2+} -selectivi*, conducător științific prof. dr. doc. Candin Liteanu (22 martie 1986).

Soecaciu Carmen, *Contribuții la chimia di-tiofosfaților organo-stanici*, conducător științific prof. dr. Ionel Haiduc (18 octombrie 1986). Kolick Herman, *Contribuții la studiul reacțiilor fotochimice ale azoxiderivaților aromatici*, conducător științific prof. dr. doc. Maria Ionescu (8 octombrie 1986).

Oprea Gabriela-Maria, *Studiul unor noi reactivi de flotație și cu acțiune chelativantă*, conducător științific prof. dr. Emil Chifu (10 decembrie 1986).



INTreprinderea POLIGRAFICĂ CLUJ,
Municipiul Cluj-Napoca, Cd. nr. 428/1987

In cel de al XXXII-lea an (1987) *Studia Universitatis Babeş—Bolyai* apare în specialitățile:

matematică

fizică

chimie

geologie-geografie

biologie

filosofie

științe economice

științe juridice

istorie

filologie

In the XXXII-nd year (1987) of its publication, *Studia Universitatis Babeş—Bolyai* is issued as follows:

mathematics

physics

chemistry

geology-geography

biology

philosophy

economic sciences

juridical sciences

history

philology

Dans sa XXXII-e année (1987), *Studia Universitatis Babeş—Bolyai* paraît dans les spécialités:

mathématiques

physique

chimie

géologie-géographie

biologie

philosophie

sciences-économiques

sciences juridiques

histoire

philologie

43 870

Abonamentele se fac la oficiile poștale, prin factorii poștali și prin difuzorii de presă, iar pentru străinătate prin „ROMPRESFILATELIA”, sectorul export-import presă, P. O. Box 12—201, telex. 10376 prsfir, București, Calea Griviței nr. 64—66.